Joana Patrícia Martins Moreira

Promising caspases modulators with flavonoid scaffold

Dissertation presented to the Faculdade de Farmácia da Universidade do Porto, to obtain the degree of Master in Pharmaceutical Chemistry

Work developed under the scientific supervision of Professor Honorina Maria de Matos Cidade and Professor Lucília Helena Ataíde Saraiva.

July 2015

This work was developed in the Centro de Química Medicinal da Universidade do Porto-CEQUIMED-UP, Laboratório de Química Orgânica e Farmacêutica, Departamento de Ciências Químicas, Faculdade de Farmácia da Universidade do Porto, and Laboratório de Microbiologia, Departamento de Ciências Biológicas, Faculdade de Farmácia da Universidade do Porto. This research was partially supported by the Strategic Funding UID/Multi/04423/2013 through national funds provided by FCT – Foundation for Science and Technology and European Regional Development Fund (ERDF), in the framework of the programme PT2020 and the Project Pest-OE/SAU/UI4040/2014 (FCT) and REQUIMTE-Pest-C/EQB/LA0006/2013.

Some results presented in this dissertation are part of the following scientific poster communications:

4. **Moreira J.***, Salazar S., Pinto M., Leão M., Saraiva L., Cidade H. Baicalein derivatives with caspase modulatory activity. 10th Yes Meeting - Young European Scientist Meeting, Porto, Portugal, 17-20 September 2015 (submitted).

3. **Moreira J.***, Pinto M., Saraiva L., Cidade H. Synthesis of alkylated derivatives of chrysin with caspase modulatory activity. 8th IJUP - Encontro Investigaçao Jovem da Universidade do Porto, Porto, Portugal, 13-15 May 2015 (P-423).

2. Mokra E.*, **Moreira J.**, Pinto M., Saraiva L., Cidade H. Synthesis of alkylated derivatives of 3,7-dihydroxyflavone with potential antitumor activity. 8th IJUP - Encontro Investigação Jovem da Universidade do Porto, Porto, Portugal, 13-15 May 2015 (P-422).

1. **Moreira J.***, Pinto M., Saraiva L., Cidade H. Synthesis of caspases modulators with flavonic scaffold. XX Encontro Luso-Galego de Química, Porto, Portugal, 26-28 November 2014 (P-377).

* Presenting author

Acknowledgements

É um prazer agradecer a todos aqueles que fizeram com que esta tese fosse possível, não só para o apoio científico, mas também pela sua amizade. No entanto, gostaria de expressar a minha mais profunda gratidão particularmente à:

Professora Doutora Honorina Maria de Matos Cidade, orientadora desta tese, pelos valiosos ensinamentos, espirito crítico notável, todo o incentivo e amizade demonstrados ao longo do trabalho. Um especial obrigada por toda a disponibilidade e, sobretudo, por ter despertado em mim “este bichinho” pela investigação.

Professora Doutora Lucília Helena Ataíde Saraiva, co-orientadora desta tese, pela orientação científica e revisão crítica desta tese, pelos ensinamentos e pela sua prontidão de auxílio.

Professora Madalena Maria de Magalhães Pinto, responsável do Laboratório de Química Orgânica e Farmacêutica, por toda a simpatia e disponibilidade. Por todas as conversas reconfortantes nos momentos menos bons.

Doutora Andreia Palmeira, pela colaboração e ensinamentos no estudo de Docking, por toda a disponibilidade e apoio. O seu contributo foi essencial para o enriquecimento deste trabalho.

Dra Sara Cravo, pelos conhecimentos transmitidos, colaboração científica e, sobretudo, por toda a ajuda prestada na síntese em micro-ondas, assim como no desenvolvimento do trabalho em HPLC. Os seus conhecimentos e apoio foram sem dúvida um fator importante para o trabalho.

Gisela Adriano pelo suporte técnico.

À minha querida Eva Mokrá, pela ajuda em algumas das sínteses, pelo empenho, pelo interesse, pela amizade e sobretudo pela experiência de um auxílio mútuo.

Sofia Salazar, pela realização dos estudos de avaliação da atividade moduladora de caspases.

Todos os docentes e colegas deste laboratório, em particular ao Pedro Brandrão pelo auxílio nos primeiros tempos no laboratório, à Ana Oliveira, Ana Rita Neves, Inês Cruz e Leticia Carraro por todo o apoio, conversas e debates de “tudo e de nada”.

Aos meus amigos de sempre e aos que não são de sempre mas serão para sempre e à família Castro, por compreenderem as ausências, pelo carinho, preocupação e apoio.

Aos meus queridos pais, pelo apoio, carinho e, sobretudo, compreensão. Às minhas irmãs, de sangue e coração, e cunhados, que mesmo longe tentam estar sempre perto. Aos quatro rebentos desta família, Miguel, Margarida, Rodrigo e Leonardo e à minha afilhada Constança, que trazem alegria à minha vida.

Por fim, a ti Simão Castro, pelo cuidado constante, pelo amor, carinho e compreensão.

"*Se tiver o hábito de fazer as coisas com alegria, raramente encontrará situações difíceis"*
Baden Powell

Abstract

The apoptosis is a highly regulated programmed cell death that is important for maintaining the integrity and homeostasis of multicellular organisms. Conversely, deregulation of apoptosis, resulting in either less or excessive cell death, is associated with several pathologies including cancer. The intracellular machinery responsible for apoptosis is dependent on a family of proteases that have a cystein at their active site and cleave their target proteins at specific aspartic acids, called caspases. Thus, modulators of these proteins may represent a promising therapeutic strategy against apoptosis-related diseases.

Flavonoids represent an interesting class of naturally occurring compounds that have been attracting attention of the scientific community because of their wide range of biological properties, being the antitumor activity one of the most studied. The antitumor activity of flavonoids is associated, at least in part, to their ability to induce apoptosis by affecting the expression or activity of a wide variety of molecules involved in apoptosis pathways. Additionally, this class of secondary metabolites has shown to be activators of caspases.

In order to improve the antitumor effects and to study the influence of alkylation of the flavonoid scaffolds on this activity, we have proposed to develop alkylated flavonoids with enhanced antitumor activity. Accordingly, in this work we described the synthesis of twenty-six alkylated derivatives (eighteen flavones and eight flavonols) of three natural flavonoids (baicalein, 3,7-dihydroxyflavone and chrysin). On the basis of our current state of knowledge sixteen from these twenty-six alkylated flavonoids are described for the first time.

The synthesis of alkylated flavonoids was carried out by reacting the building blocks with alkylating agents, in alkaline medium using microwave-assisted organic synthesis (MAOS). Previously, the suitable amount of alkylating agent to obtain the intended alkylated derivatives was determined by a HPLC-DAD study.

The structure elucidation of the synthesized compounds was established on the basis of IR and NMR techniques.

The ability of three synthesized alkylated flavonoids (**Biso1**, **Brop1** and **Bali1**) to modulate procaspases-3 and -7 activity was evaluated using yeast-based assays. Results

showed that the monoalkylated derivatives of baicalein **Biso1**, **Brop1** and **Bali1** behaved as procaspase-7 activators, being **Biso1** the most potent compound.

An *in silico* docking study was performed using procaspases-3, -6, and -7 as targets, and **Biso1**, **Brop1** and **Bali1** as potential ligands. In accordance with the results of the biological assays, docking studies suggested that **Biso1** was the most active procaspases activator.

In summary, the results of this study demonstrate the possibility of obtaining new potential procaspase activators through the alkylation of flavonoids derivatives.

Keywords: Cancer, Caspase Activators, Flavonoids, Alkylation

Resumo

A apoptose é um processo de morte celular programada altamente controlado, que é importante para a manutenção da integridade e homeostasia dos organismos multicelulares. A desregulação da apoptose, resultando numa deficiência ou exacerbação da morte celular, está associada a diversas patologias, incluindo o cancro. A maquinaria intracelular responsável pela apoptose é dependente de uma família de proteases que têm um resíduo de cisteína no seu local ativo e clivam as proteínas alvo em resíduos de ácido aspártico, denominadas caspases. Assim, os moduladores destas proteínas pode representar uma estratégia terapêutica promissora contra doenças relacionadas com apoptose.

Os flavonóides representam uma classe de compostos que tem atraído a atenção da comunidade científica devido à sua ampla gama de propriedades biológicas, sendo a atividade antitumoral uma das mais estudadas. A atividade antitumoral de flavonóides está associada, pelo menos em parte, à sua capacidade para induzir apoptose afetando a expressão ou a atividade de uma ampla variedade de moléculas envolvidas em vias de apoptose. Além disso, estes metabolitos secundários têm mostrado ser ativadores de caspases.

Com o intuito de melhorar os efeitos antitumorais e estudar a influência da alquilação dos scaffolds flavonóides nesta atividade, propusemo-nos a sintetizar flavonóides alquilados com actividade antitumoral melhorada. Assim, neste trabalho descrevemos a síntese de vinte e seis derivados alquilados (dezoito flavonas e oito flavonóis) de três flavonóides naturais (baicaleína, 3,7-dihydroxyflavone e crisina). Com base no nosso conhecimento atual desasseis destes vinte e seis flavonóides alquilados são descrito pela primeira vez.

A síntese de flavonóides alquilados foi realizada fazendo reagir os blocos construtores com agentes alquilantes, em meio alcalino, utilizando síntese orgânica assistida por microondas (MAOS). Previamente, foi elaborado um estudo utilizando o HPLC-DAD para determinar a quantidade adequada de reagente alquilante para obter os derivados alquilados.

A elucidação estrutural dos compostos sintetizados foi estabelecida com base em técnicas de espetrofotometria de infravermelho e ressonância magnética nuclear.

Para três flavonóides alquilados sintetizados (**Biso1**, **Brop1** e **Bali1**) foi avaliada a capacidade para modular a actividade das procaspases-3 e -7, utilizando ensaios baseados em levedura. Os resultados mostraram que os derivados da baicaleína **Biso1**, **Brop1** e **Bali1** se comportaram como ativadores da procaspase-7, sendo o **Biso1** o composto mais potente.

Um estudo *in silico* de docking foi realizado utilizando as procaspases-3, -6, -7 como alvos, e os derivados **Biso1**, **Brop1** e **Bali1** como potenciais ligandos. Em concordância com os resultados obtidos nos ensaios biológicos, os estudos de docking sugeriram que o derivado **Biso1** foi ativador mais potente das procaspases.

Em resumo, os resultados deste estudo demonstram a possibilidade de serem obtidos potenciais moduladores da actividade de caspase com base na alquilação do scaffold flavonoide.

Palavras-chave: Cancro, Ativadores de Caspases, Flavonóides, Alquilação

Table of Contents

List of Figures

List of Tables

Abbreviations and Symbols

^{13}C NMR	NMR Carbon nuclear magnetic resonance
^{1}H NMR	NMR proton nuclear magnetic resonance
ANS	Anthocyanidin synthase
Apaf-1	Apoptotic protease-activating factor-1
ASK-1	Apoptosis signal regulating kinase 1
Bad	Bcl-2-associated death promoter
BAK	Bcl-2 antagonist/ Killer
BAX	Bcl-2 associated X protein
BcL-2	B cell lymphoma 2
BcL-XL	B cell lymphoma –extra large
BH3-only	Bcl-2 homology domain 3 only
Bid	BH3-interacting domain death agonist
BIR	Baculoviral IAP repeats
Brs	Broad singlet
CARD	Caspases-recruitment domain
CDKs	Cyclin-dependent kinases
CEQUIMED-UP	Centro de Química Medicinal da Universidade do Porto
c.f.u.	Colony-forming units
CHI	Chalcones isomerase
CHS	Chalcones synthase
Ciimar	Interdisciplinary Centre of Marine and Environmental Research
Cit c	Cytochrome c
CrmA	Cytokine response modifier
C4H	Cinnamic acid 4-hydroxylase
DED	Death effector domain
d	doublet
dd	double doublet
DD	Death domain
DFR	Dihydroflanonol-4-reductase
DISC	Death-induced signaling complexes
DMSO	dimethylformamide
DR	Death receptor
DR3	Death receptor 3
EGFRs	Epidermal growth factor receptors
ERK	Extracellular-regulated kinase
EtOAc	Ethyl acetate
FADD	Fas-associated death domain

FHT	Flavanone 3β-hydroxylase
FLS	Flavonol synthase
FNS I	Flavone synthase I
GI_{50}	Concentration of compound that inhibited 50% of the net cell growth
HMBC	Heteronuclear multiple bond correlation
HPLC	High performance liquid chromatography
HPLC-DAD	High performance liquid chromatography with Diode Array Detector
HSQC	Heteronuclear single quantum coherence
HTS	High-throughput screening
IAP	Inhibitor apoptosis protein
IC_{50}	Concentration of compound that causes 50% growth inhibition
IMAs	Isatin Michael acceptors
IR	Infrared spectroscopy
J	coupling constant
JNK	C-Jun N-terminal kinase
Ki	Values of inhibition constant
LRR	Leucine-rich repeats
m	multiplet
MAOS	Microwave-assisted organc synthesis
MARK	Mitogen-activated protein kinases
Mcl-1	Anti-apoptotic BCL-2 protein
Me_2CO	Acetone
MOMP	Mitochondrial outer membrane permeabilization
MW	Microwave
PAC-1	Procaspase-activating compound -1
PAL	Phenylalanine ammonia lyase
PARP	Poly (ADP-ribose) polymerase
PDGFRs	Platelet derived growth factor receptors
PKs	Protein-Kinases
PYP	Pyrin domains
q	Quadruplet
ROS	Reactive oxygen species
Rt	Retention time
s	singlet
SAR	Structure-activity relationship
t	triplet
TLC	Thin layer chromatography
TNF	Tumor necrosis factor
TNFR	Tumor necrosis factor receptor
TNFR1	Tumor necrosis factor receptor-1

TRAIL-R1	TNF-related apoptosis-inducing ligand receptor-1
TRAIL-R2	TNF-related apoptosis-inducing ligand receptor-2
VEGFRs	Vascular endothelial growth factor receptors
XIAP	X chromosome-linked inhibitor of apoptosis protein
WHO	World Health Organization
4CL	4-Coumarate: Coenzyme A ligase
$\Delta\Psi m$	Variation of the membrane potential
δ	chemical shift
δc	Carbon chemical shift
δ_H	Proton chemical shift
υ	Wavenumver (cm^{-1})

Chapter 1:

Outline and Aims of the Dissertation

1.1. Outline of the dissertation

The dissertation is organized in six chapters.

Charter 1- Outline and Aims of the Dissertation

The first chapter establishes the aims of the work focusing also on the organization of the dissertation, giving a brief description of what will be referred in each chapter.

Chapter 2- Introduction

The second chapter deals with the theoretical background that supports the developed work and so is sub-divided into two subchapters. The first subchapter is focused review about caspases, namely, their structure and classification, modulation of caspases activity and pharmacological regulators. A brief review concerning flavonoids, including chemistry and the biological activities described for this group of compounds particularly their antitumor activity is described in the second subchapter.

Chapter 3– Results and Discussion

The third chapter focus on the results and discussion of the developed research work, being sub-divided into five subchapters, which deal with the discussion of the results obtained concerning the synthesis, optimization of reactions conditions, determination of the peck purity, biological activity and docking studies.

Chapter 4 – Conclusions

The fourth chapter focus on the main conclusions and future work.

Chapter 5 - Experimental Procedures

The fifth chapter refer the synthetic procedures adopted for the synthesis of the derivatives of baicalein, 3,7-dihydroxyflavone and chrisin, as well as describe about the optimization of reactions conditions. A reference to the procedure used for the evaluation of peck purity, biological activity and docking studies is also presented in this chapter.

Chapter 6 – References

Herein is presented a list of the references used in this dissertation.

Chapter 7 – Appendixes

The seventh chapter includes a table with the structure of all synthesized compounds.

1.2. Aims of the dissertation

As a result of the search for new bioactive compounds with antitumor activity by CEQUIMED-UP and UCIBIO/REQUIMTE, the prenylflavonoids **FP2** (**1**) and **FP11** (**2**) (**Figure 1**) have been identified as procaspase-7 activators.

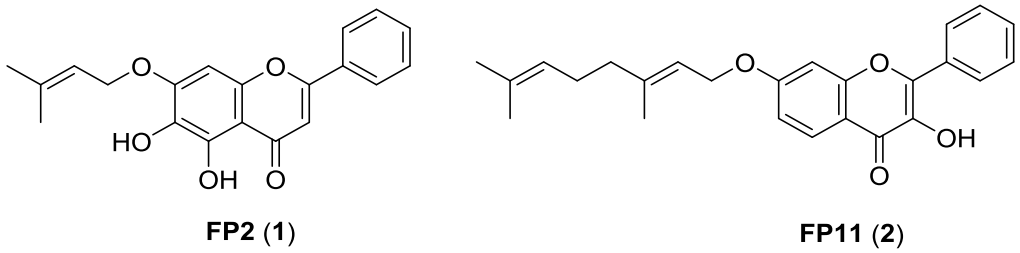

FP2 (**1**) **FP11** (**2**)

Figure 1: Chemical structures of prenylflavonoids identified as procaspase-7 activators.

The main purpose of this dissertation was to obtain more potent procaspase activators, using **FP2** (**1**) and **FP11** (**2**) as models by molecular modification of natural flavonoids.

Other aims of this research work were:

- to apply non-classic methodologies for the synthesis of flavonoids, namely MAOS;
- to draw some SAR considerations;
- to evaluate the effect of the synthesized flavonoids on the executioner procaspases activity using yeast-cell based models;
- to perform doking studies of bioactive compounds with their targeted procaspases-3, 6 and 7.

Chapter 2:

Introduction

2.1. Caspases

2.1.1. Structure and classification

Caspases form a cysteine protease/peptidases family that uses the cysteine residue as catalytic nucleophile. They share a high specificity to break target proteins in sites after aspartic acid residues. The name "caspase" is derived from this characteristic molecular function: cysteine-aspartic-acid-proteases.[1]

The caspases family consists in fifteen different proteins, being eleven expressed in human cells (caspases-1 to -10 and -14).[2] They are grouped into two families: the inflammatory and apoptotic. However, these proteins are usually classified into three subfamilies because apoptotic caspases are subclassified according to their mechanism of action.[3] Thus, according with their physiologic function, substrate specificity and sequencing similarities, they are grouped into three subfamilies: inflammatory (Group I), initiator of apoptosis (Group II) and effector/executioner of apoptosis (Group III) caspases.[2]

The inflammatory caspases are involved in the inflammatory response of the cytokines activation, while the initiator and effector/executioner caspases are involved in the apoptotic cascade.[4] The initiator caspases are the first to be activated in a particular death pathway and are the first step for the executioner caspases activation.[1]

All the caspases can be found in cells in their inactive form, as zymogen (procaspase) precursor. The initiator caspases are present in the cell as zymogen monomers and the executioner caspases exist as inactive zymogen dimers.[4] These procaspases are simple strand proteins, with a variable size N-terminal prodomain, a central large subunit, with the cysteine residue active site, and a C-terminal small subunit (p10; ~10 KDa). The catalytic domain includes the large subunit (p20; ~20 KDa) and the small subunit, which has essential residues for caspases activity (**Figure 2**).[2]

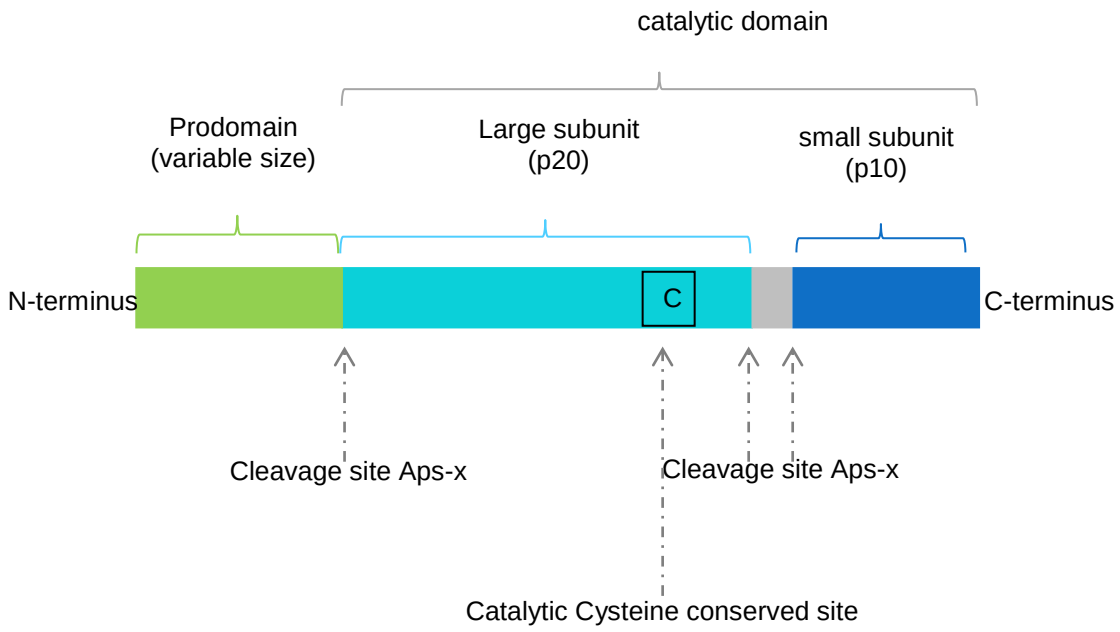

Figure 2: A schematic representation of structural features of human procaspases (C represent the active site residue).

The Group I, including procaspases-1, -4 and -5, presents a large N-terminal prodomain that has a caspases–recruitment domain (CARD), crucial for the formation of protein complex that lead to caspases activation (**Figure 3**). The Group II, including procaspases-2, -8, -9 and -10, has a large N-terminal prodomian (>90 amino acids), containing a CARD (procaspases -2 and -9) or a death effector domain (DED; procaspases-8 and -10) that is important in protein–protein interactions with other adaptive proteins (**Figure 3**). The Group III, including the effector procaspases-3, -6 and -7, has only a short prodomain of 20-30 amino acids (**Figure 3**).[2]

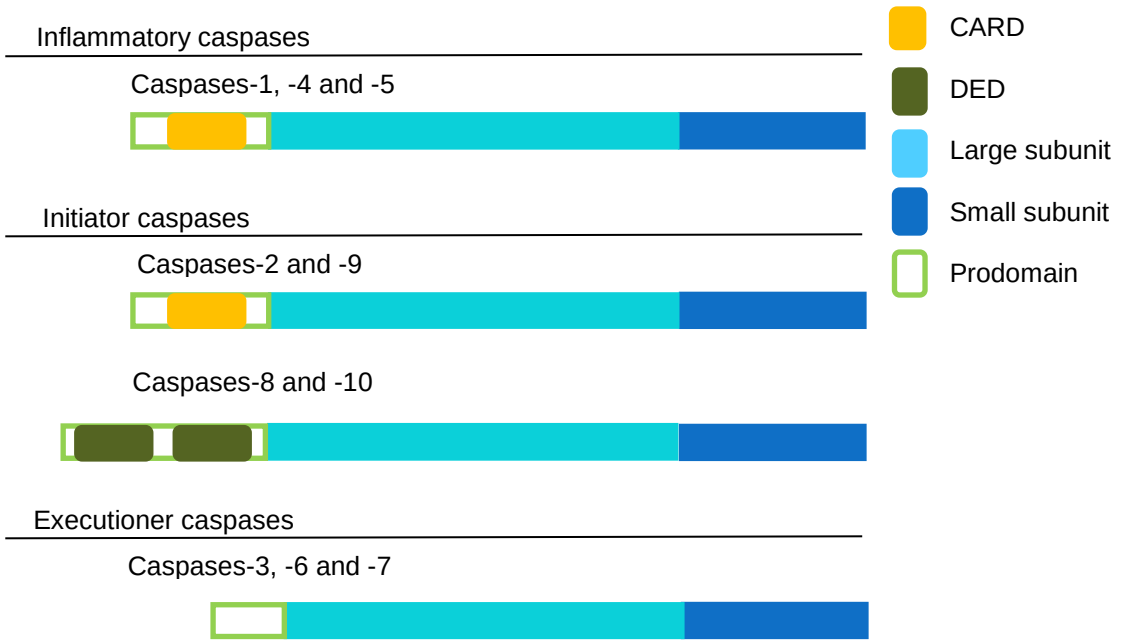

Figure 3: Schematic representation of the domain organization of human procaspases from different subfamilies.

2.1.2. Caspases activation

Biochemical and structural analysis revealed an underlying conservation of the caspases activation process. Additionally, the stabilization process of the proenzyme latent state is also conserved.[1,5]

The activation of initiator caspases is mediated by dimerization, through "induced proximity", when adaptor proteins interact with the prodomains. However, interdomain cleavage, promoted by initiator caspases, is involved in the activation of executioner caspases.[5,6]

Studies revealed that active initiator caspases are dimers with identical catalytic units, where each catalytic unit has one active site. The subunits are derived of only one molecular precursor (procaspase) through an internal cleavage in subunits marked sites. In fact, it has been demonstrated that this cleavage is neither necessary nor sufficient for the initiator and inflammatory caspases activation.[4] It is required a dimerization of the zymogen monomers to assume an active conformation. The dimerization process occurs in a multiprotein activation complex that recruits procaspase through the N-terminal recruitment domain (**Figure 4**).[1]

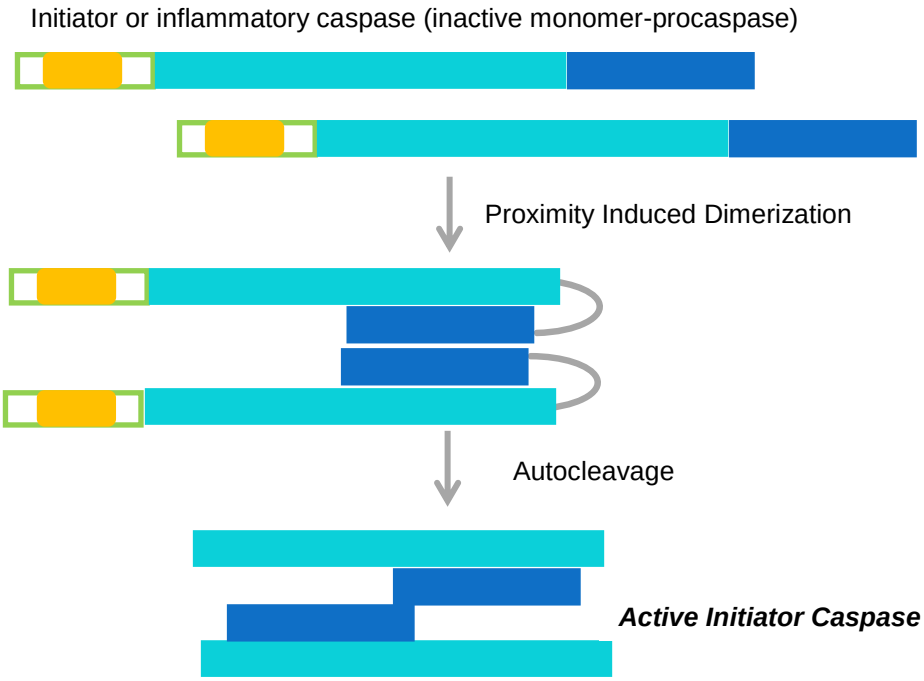

Figure 4: Mechanisms of initiator caspases activation. Dark Blue indicates small subunit, clear blue indicates large subunit, green represent prodomain that contains CARD represented by the yellow color.

Concerning executioner caspases, their precursor procaspases are found in the cytosol in the inactive dimer form.[4] These are activated through limited proteolysis inside the interdomain linker, by initiator caspases or occasionally by other proteases in specific circumstances (**Figure 5**).[1]

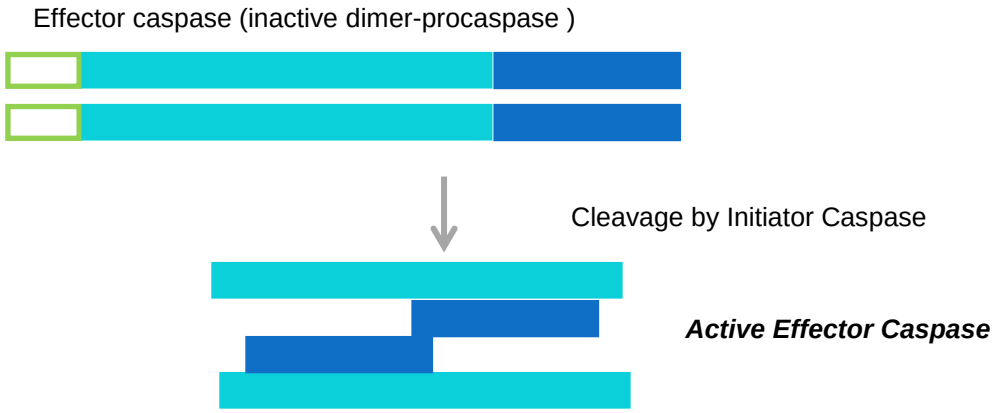

Figure 5: Mechanisms of effector caspases activation. Dark Blue indicates small subunit, clear blue indicates large subunit and the prodomain is represented in green.

Studies of X-ray crystalline structure of some caspases have suggested that caspases are present in the dimers form, with two large and two small subunits, like heterodimers ($p20_2$-$p10_2$) (**Figure 6**).[5,7] Each heterodimer subunits are formed from hydrophobic interactions that bend into a compact cylinder, dominated by a central strand of six β-sheets. The heterodimers interact through a twelve β-sheets which are surrounded by five α-helices, distributed in the opposite side of the β-sheets formed site. This unique protease structure is almost caspase exclusive. On the caspases heterodimers, two of these cylinders align in a head-tail configuration getting the two active sites on opposite sides.[5]

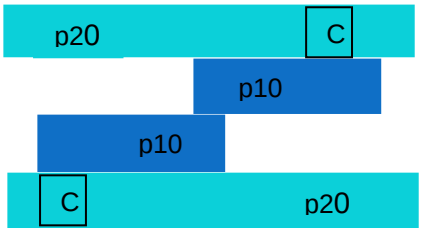

Figure 6: A schematic representation of active caspases structure (C represent the active site residues). Dark Blue indicates small subunit and clear blue indicate large subunit.

Regarding the activation of inflammatory caspases-1 and -5, it occurs in a complex named inflammasome (**Figure 7**). The inflammasome includes procaspases-1 and -5, which contains CARD, as well as the NALP-1 protein. This complex formation results in the processing and activation of IL-1β and IL-18 cytokines that has a central role in the immunity response to microbial pathogens.[5]

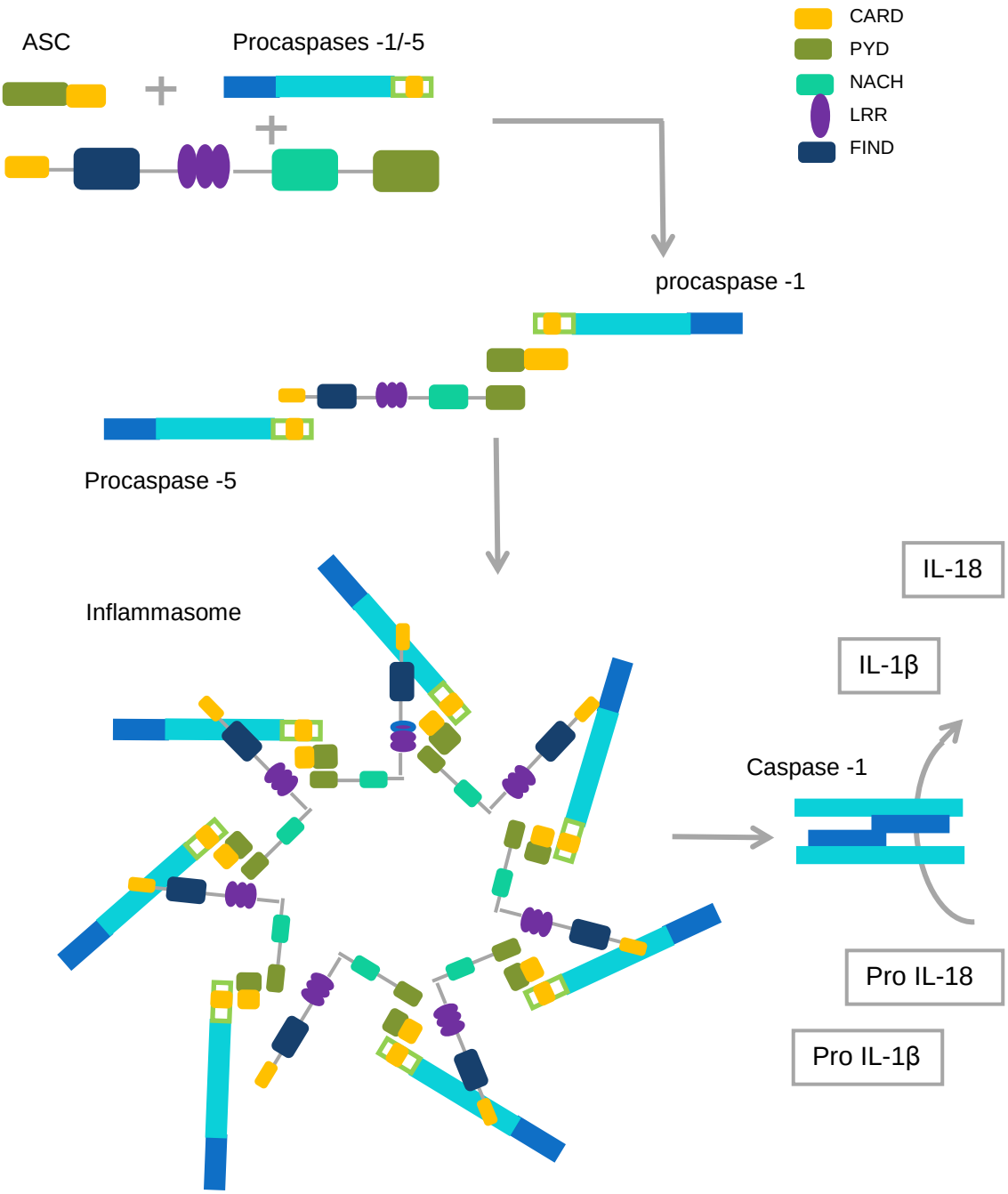

Figure 7: Mechanisms of inflammatory caspases activation. The inflammasome is formed with proteins (such as NALP-1 protein) and procasases-1 and -5. The NLR family is characterized by the presence of a central nucleotide-binding and oligomerization (NACHT) domain, which is commonly flanked by C-terminal leucine-rich repeats (LRRs) and N-terminal caspase recruitment (CARD) or pyrin (PYD) domains. Procaspase-1 binds to CARD in ASC that which in turn have PYD that is responsible for recruitment with PYD of NLRL-1, and procaspase-5 binds to the CARD. Active caspases are released and allows activation of pro IL-11β and pro IL-18 in IL-1β and IL-18 cytokines.

2.1.2.1. The caspase pathways

The signal transduction for caspase activation may occur by two main distinct pathways: extrinsic, which is a receptor-mediated pathway, and intrinsic, a mitochondrial-mediated pathway (**Figure 8**). [5]

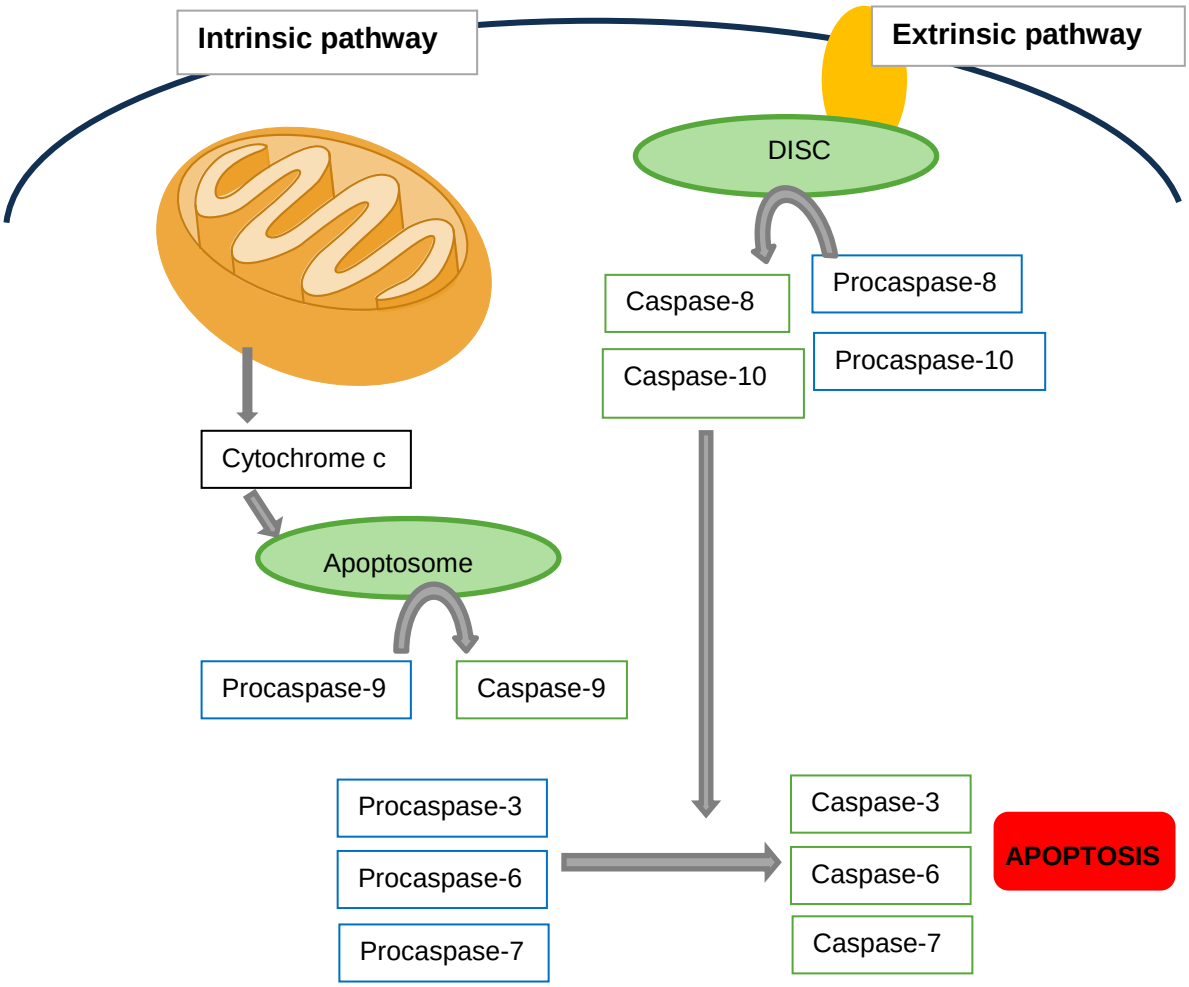

Figure 8: The caspases pathways: extrinsic and intrinsic. The extrinsic pathway, formed DISC enables the activation of caspase-8 and -10, which will activate procaspases-3, -6 and -7. The intrinsic pathway is in apoptosome that allows the activation of procaspase-9, which will also activate procaspases-3, -6 and -7. Thereby apoptosis is activated.

2.1.2.1.1. Extrinsic pathway

The process is initiated by extracellular signals delivered in the form of ligands binding to death receptors (DRs).[3] DRs are the transmembrane proteins containing an extracellular ligand-binding domain and an intracellular death domain (DD), which is required for receptors to recruit downstream apoptotic proteins.[8] They are members of the tumor necrosis factor (TNF) superfamily and include TNF receptor-1 (TNFR1), the FAS (also known as CD95 or APO-1), death receptor 3 (DR3), and TNF-related apoptosis-inducing ligand receptor-1/2 (TRAIL-R1/R2).[3,5] The bounding of TNF and other ligands with the transmembrane death receptors leads to the recruitment of intracellular adaptor proteins (Fas-associated death domain, FADD), which in turn recruit the initiator procaspases-8 and 10, forming death-induced signaling complexes (DISC).[6] It is inside this DISC that the initiator procaspases-8 and -10 are activated through induced proximity dimerization (**Figure 9**).[6]

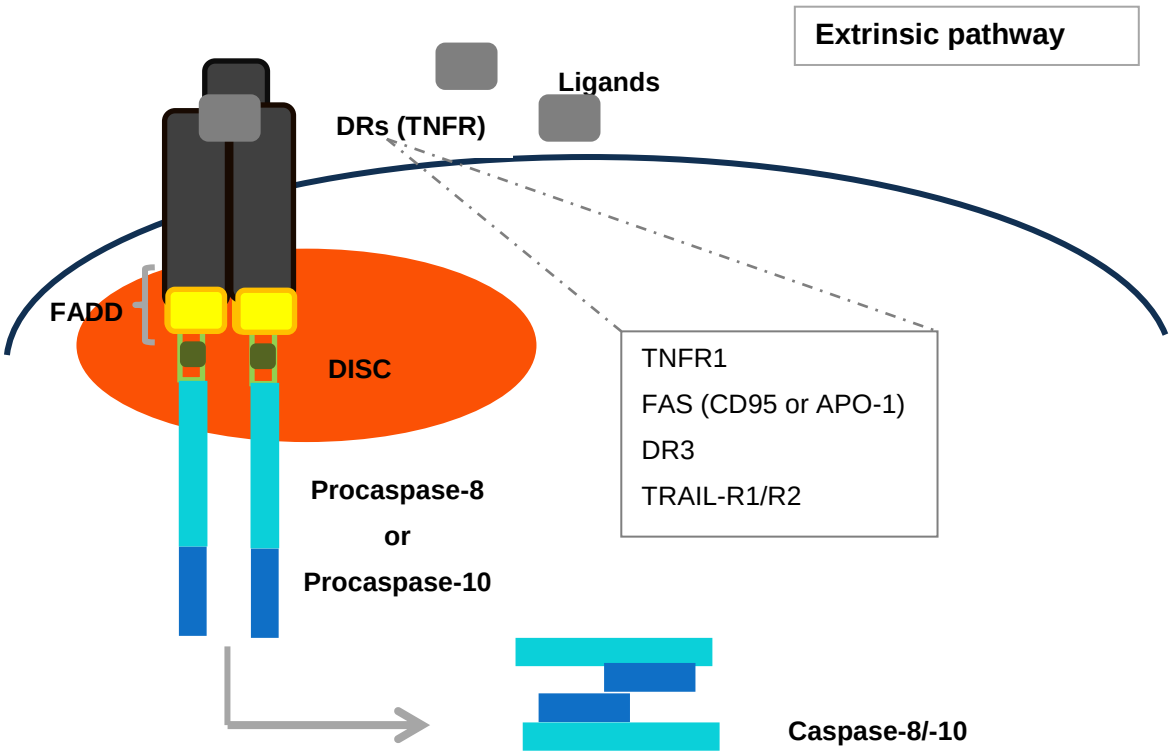

Figure 9 : Activation of the extrinsic pathway.

The DISC molecules interactions are based in homotypic contacts. The DD of the receptor interacts with the DD of the FADD, the DED of the FADD interacts with the DED of the procaspases N-terminal and cell inhibitor proteins.[8]

The procaspase-8 processing includes two cleavages. The first cleavage occurs between the protease domains, where the subunits p43/41 and p10 are formed, remaining both the products bounded to the DISC (p43/41 through DED interactions and p10 by interactions with proteases large domain). The second cleavage occurs between the prodomain and the large subunit. As a result of this cleavage, p43/41 is processed to the p26/p24 prodomain and p18.[5] Therefore, after the dimerization, the N-terminal DED are proteolytically removed and the mature caspase-8 is released to the cytosol, triggering the apoptosis process. The same happens with caspase-10.[1] After this, caspase-8 and 10 subsequently activates the downstream executioner procaspases to induce apoptosis.

2.1.2.1.2. Intrinsic pathway

In the intrinsic pathway, several stimuli like oxidative stress, thermal shock, DNA damage, among others, trigger the release of mitochondria cytochrome *c* to the cytoplasm, because the mitochondrial outer membrane permeabilization (MOMP) is altered.[4]

The MOMP is highly controlled primarily through interactions between pro- and anti-apoptotic members of the BCL-2 protein family. BCL-2 protein family is divided into three groups based on their BCL-2 homology domain organization: anti-apoptotic (e.g. BCL-2 and BCL-XL), pro-apoptocic effectors (e.g. BAX and BAK), and pro-apoptotic BH3-only proteins (e.g. BID).[9] Activation of BAX and BAK is essential for MOMP.[4] The anti-apoptotic BCL-2/Bcl-xL inhibit BAX and BAK and the BH3-only proteins help in the regulation of the balance between the pro- and antiapoptotic proteins (**Figure 10**).[6]

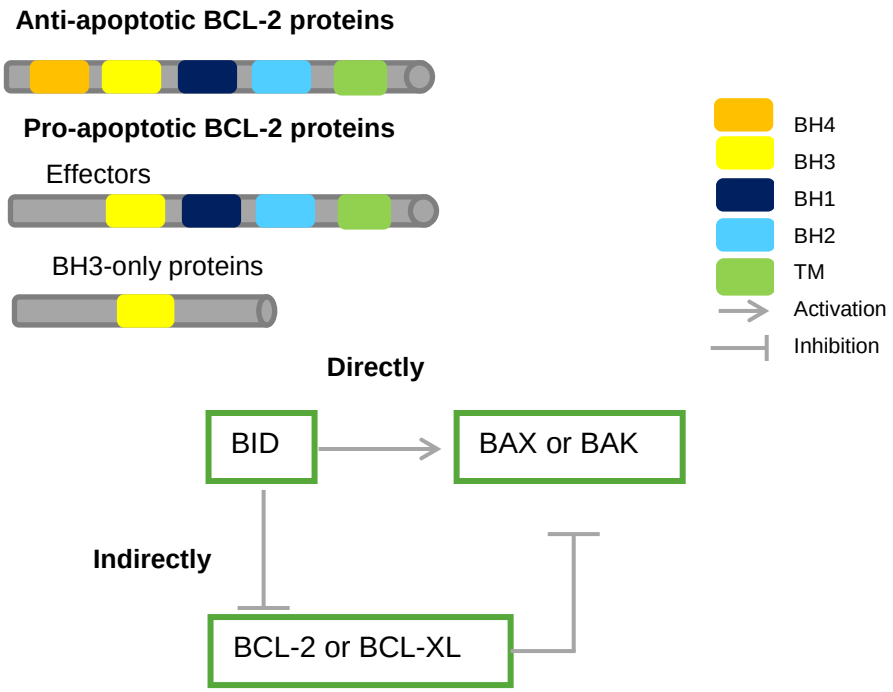

Figure 10: Anti-apoptotic and pro-apoptotic BCL-2 family. This family can be divided according to their BCL-2 homology domain organization: the anti-apoptotic BCL-2 proteins (Bcl-2 and Bcl-xL) and two types of pro-apoptotic BCL-2 proteins, effectors that actually cause MOMP or BH3 only that relay the apoptotic signal to the effectors (BAX and BID, respectively). BID active directly BAX or BAK or indirectly by inhibition Bcl-2 or Bcl-xL, that to be inhibited loses the ability to inhibit BAX or BAK.

After the release of cytochrome *c* (**Figure 11A**), a cytoplasmic complex with high molecular weight, the apoptosome, is formed. It is formed by a central protein known as apoptotic protease-activating factor-1 (Apaf-1) that also contains the CARD domain.[5] In the presence of cytochrome *c* and ATP, Apaf-1 becomes more linear allowing its polymerization.[1] In this phase, the procaspase-9 is recruited to the complex through interactions between Apaf-1 CARD and procaspase-9 CARD, leading to its activation.[6] The caspase-9 then activates downstream executioner procaspases to induce apoptosis (**Figure 11**, **A**).[1,6]

Beyond the cytochrome *c,* a secondary mitochondrial activator of caspases/direct IAP-binding protein (Smac/DIABLO) is released into the cytoplasm. Smac/DIABLO interacts with the antiapoptotic protein X chromosome-linked inhibitor of apoptosis protein (XIAP). Caspases-3, -7 and -9 are inhibited by XIAP. Then, if Smac/DIABLO is released, XIAP is inhibited and caspases stay active (**Figure 11**, **B**).[10]

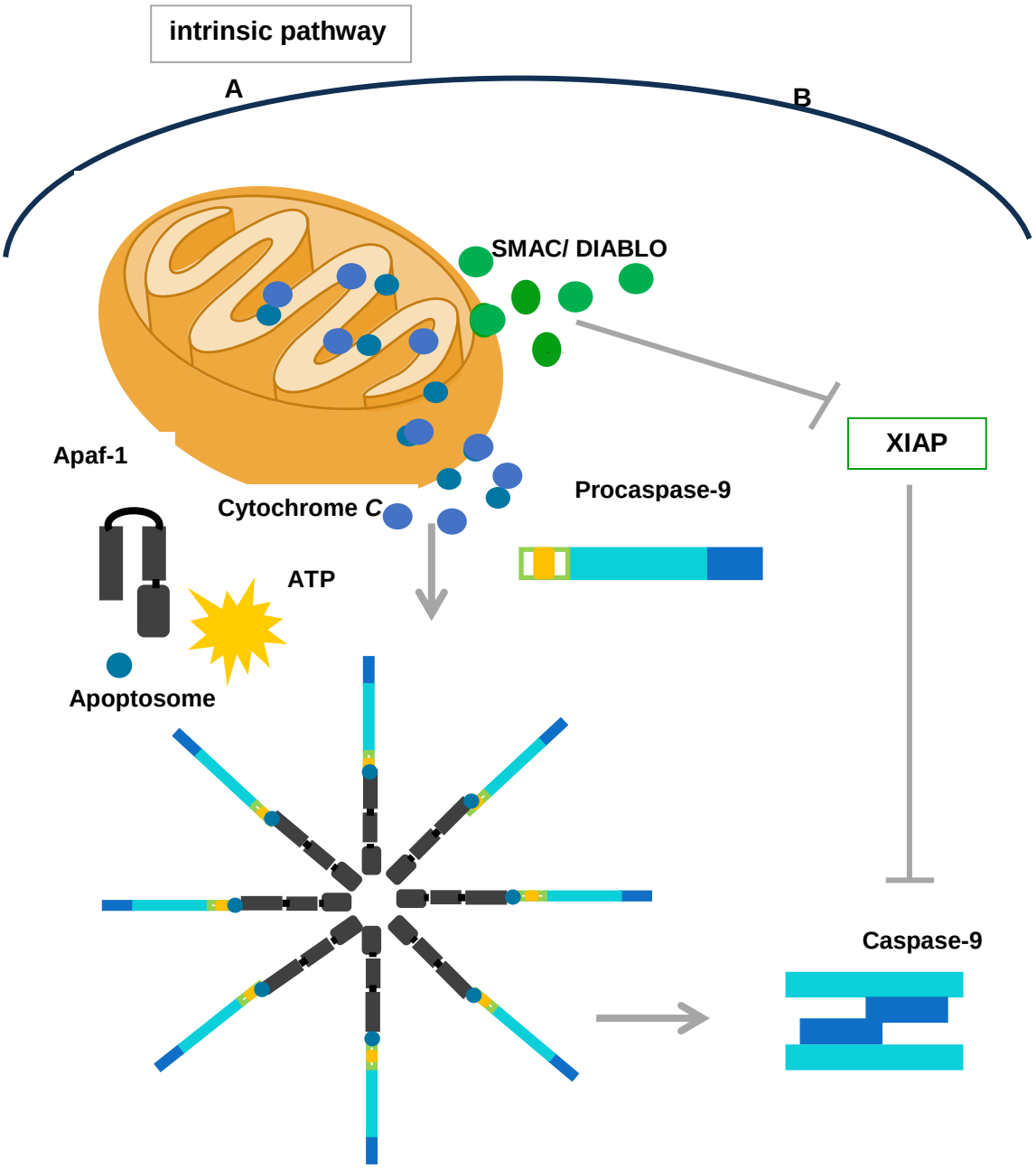

Figure 11: Activation of the intrinsic pathway.

The cascade activation of effector caspases-3, -6 and -7 varies between the intrinsic and extrinsic pathways (**Figure 12**). On the extrinsic pathway, two types of signalization can occur. The first type is characterized by high levels of formed DISC and, consequently, an increase of active caspase-8, which on the other hand, leads to the activation of effector caspases-3 and -7. The second type presents low levels of DISC and, as such, needs an additional amplification circuit that involves the caspase-8 cleavage of BID protein to generate tBit that leads to the release of mitochondrial

cytochrome *c*. Therefore, the apoptosome is formed, procaspase-9 is activated into caspase-9 and the effector caspases-3 and -7 activation initiates the death cascade (**Figure 12**).[5]

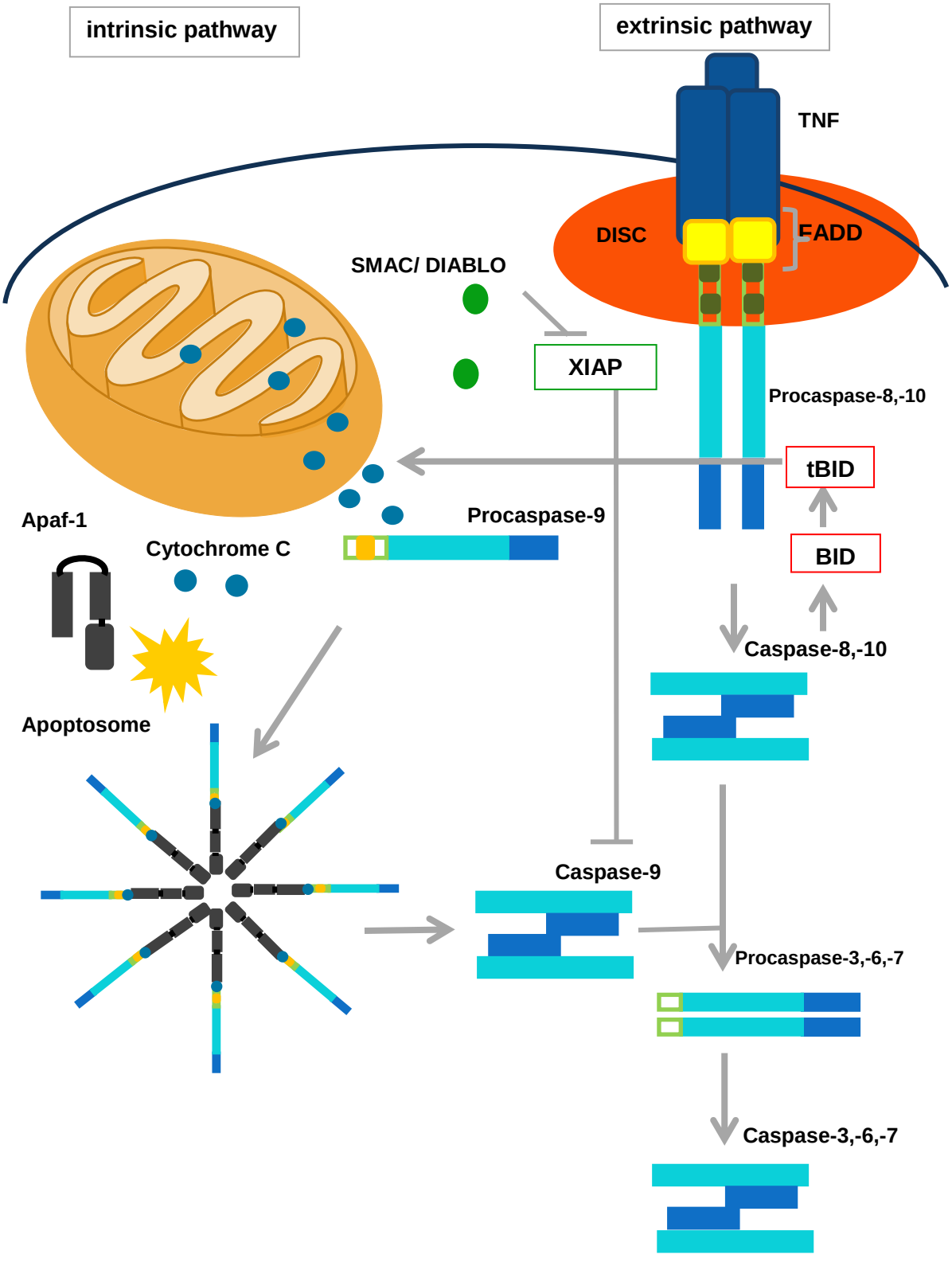

Figure 12: Activation of effector caspases.

2.1.3. Modulation of caspases activity

The activity of caspases can be regulated directly, through activators or inhibitors that directly bond to the caspases active or allosteric sites, or indirectly by the interference with signaling events along the caspases cascade that promotes caspases activation.
To date, although several compounds have proved to interfere with the caspase activity, most of them act on the signaling pathway involved in caspase activation. Only a limited group of compounds have demonstrated to directly interfere with caspases active or allosteric sites. Additionally, the majority of the reported compounds act as inhibitors. In fact, until present, only few activators of caspases have been reported.

2.1.3.1. Active site-directed inhibitors of caspases

The active site-directed inhibitors include peptide-derived inhibitors and non peptidic inhibitors with heterocyclic scaffolds.

2.1.3.1.1. Peptide-derived inhibitors

The development of caspases selective inhibitors was based on substrate specificity. Through combinatory approaches it was possible to identify the ideal substrate as well as different binding requirements for caspase subfamilies. Furthermore, structural analysis of caspase-inhibitor complexes propitiated a better understanding of the binding modes and the caspases subsites geometry.[2]

Many of the caspase inhibitors are peptide derivatives based on the strict requirement for an aspartic acid residue in the P1 position of the tetrapeptide motif recognized in the substrate (**Figure 13**).[11]

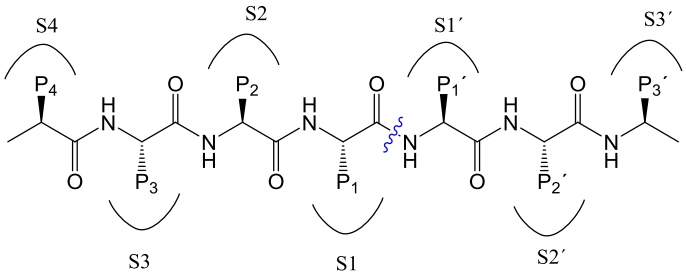

Figure 13: Structure illustrating substrate/inhibitor residues (P) and protease binding sites (S). Prime and non-prime indications distinguish respectively between the C- and N-side of the cleavage site.

The most common strategy to convert substrates to pseudosubstrate inhibitors was based on the Asp ligation at P1 from the peptide sequence to an electrophilic moiety, such as an aldehyde or fluoromethylketone. This moiety covalently interacts with the nucleophilic Cys of the active site and, therefore, inhibits caspases.[2]

Nevertheless, the presence of the electrophilic moiety is not the only structural requirement to activity inhibition.[2] In fact, Le et al. (2006) investigated the replacement of the conventional electrophilic moiety by a much less reactive azidomethylene substituent in a series of azidomethylene-based peptidomimetics, obtaining some potent inhibitors of caspase-1 (**Table 1**).[12]

Table 1: Azidomethylene-based peptidomimetics inhibitors of caspase-1.[12]

Compound		IC_{50}(nM)	Mr
3	Ac-Try-Ala-Asp-H	2±0.4	492
4	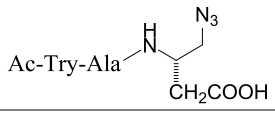	226±32	519
5	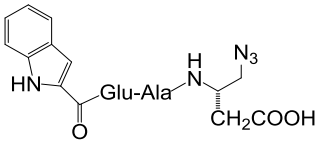	75±10	487
6	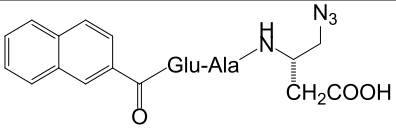	40±5	498
7	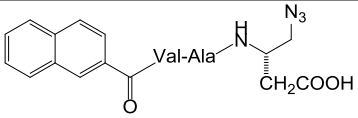	4.6±0.5	468
8	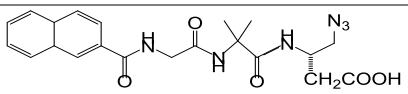	7.9±0.75	496

More recently, Loser et al[13] (2010) reported some non-covalent caspase-1 peptide-derived inhibitors based on the 2-naphthoyl-Val-Ala-Asp sequence. These inhibitors were produced by incorporating a secondary amine (reduced amide) isostere in place of the conventional electrophile (e.g., aldehyde). They showed to be potent, reversible and competitive inhibitors being selective for caspase-1 (e.g., Ki= 47 nM) over caspases-3 and -8, with minimal cytotoxicity (**Table 2**). Unlike most cysteine protease inhibitors, these compounds do not react covalently and indiscriminately with thiols.[13]

Table 2: Benzylamine inhibitors of caspases-1.[13]

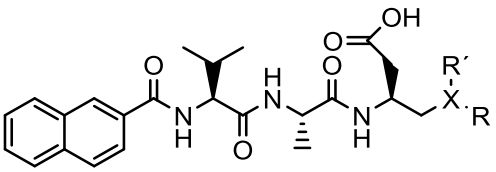

Compound	R	R´	X	Ki (nM)
9	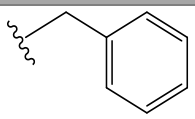	H	N	600±47
10	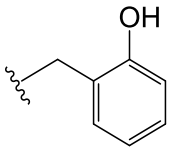	H	N	47±7
11	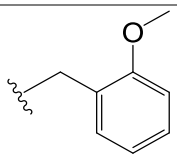	H	N	965±76
12	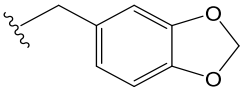	H	N	209±21
13	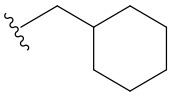	H	N	945±99
14	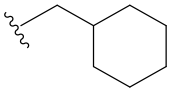	Me	N	128±14

Ki= values of inhibition constant

Docking studies of the most potent compound of this series into the active site of caspase-1 revealed the orientation of benzylamino residue into the S1' pocket and additional hydrogen interactions of the hydroxyl group in the *ortho* position.[13]

Several peptidomimetic caspase inhibitors were developed by pharmaceutical companies and have entered in clinical trials.[2] One example is the broad-spectrum caspase inhibitor IDN-6556 (**15**, **Figure 14**) that is a potent and irreversible inhibitor of Fas-induced apoptosis *in vitro.*[14] IDN-6556 (**15**) entered in clinical trials for treatment of liver diseases and in patients undergoing liver transplantation.[14]

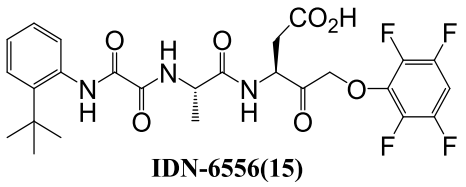

Figure 14 Structure of the active-site inhibitor IDN-6556 (**15**).

In addition to IDN-6556, other inhibitor VX-765 (**16**, **Figure 15**) entered in clinical trials. VX-765 is a second generation reversible peptide-derived inhibitor that has been examined in clinical trials for inflammatory diseases.[15] It is a prodrug that requires esterase cleavage of the 5-ethoxydihydrofuran-2(3H)-one moiety to yield the aldehyde functionality of the drug VRT-043198 (**17**, **Figure 15**). This moiety covalently interacts with the nucleophilic Cys of the active site and, therefore, inhibits caspases.[16]

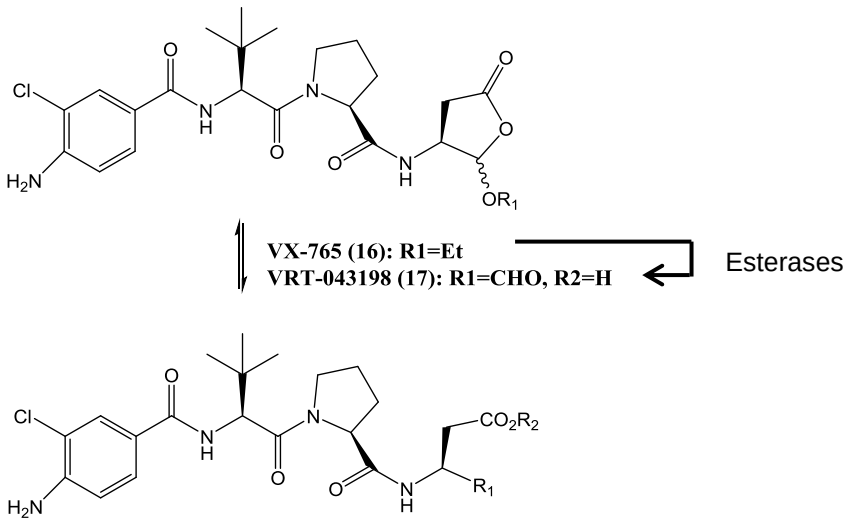

Figure 15: Structure of peptide-derived caspase inhibitors VX-765 (**16**) and VRT-043198 (**17**).

The syntheses of several cyanopropanate-containing small molecules based on the peptidic scaffold of prodrug VX-765 were also accomplished (**Figure 16**). These

compounds were found to be selective and potent inhibitors of caspase-1 (IC_{50} values ≤1 nM).[15]

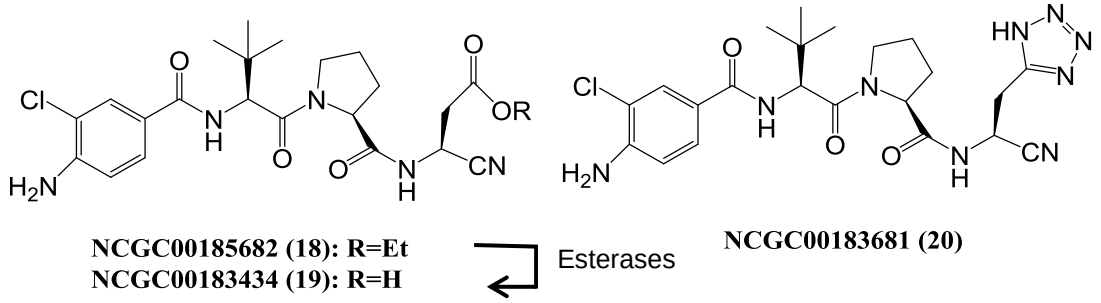

Figure 16: Structure of cyanopropanate-containing small molecules based on peptidic scaffold of VX-765 as inhibitors of caspase-1 (NCGC00185682 (**18**), NCGC00183434 (**19**) and NCGC00183681 (**20**)).

2.1.3.1.2. Natural caspase inhibitors

The first natural caspase inhibitor found was a cytokine response modifier (CrmA), a product of cowpox virus. It was responsible for the effective inhibition of the interleukin-1β activation in chorioallantoic membranes of chicken embryos. The inhibitor interacts with caspase-1 active site, due to the pseudosubstrate Leu – Val – Ala – Asp sequence.[17]

2.1.3.1.3. Nonpeptidic inhibitors

Simultaneously to the development of peptidomimetic caspase inhibitors, other scaffolds were identified through high-throughput screening (HTS) of chemical libraries. 5-Nitroisatin (**21**, **Figure 17**) was first discovered as a nonpeptide caspase-3 inhibitor by using a HTS of the Smith Kline Beechan compound collection.[18] The modification of this compound led to the development of a series of potent isatin analog inhibitors of caspases-3, -7, including compounds **22** and **23** (**Figure 17**).[19] These isatin sulfonamide compounds showed to be potent and selective caspase inhibitors.[19] However, their use may be limited because of the highly reactive nature of their ketone carbonyl groups toward nucleophiles. So, a new class of isatin sulfonamide analog compounds has been achieved called isatin Michael acceptors (IMAs), like compound **24**. This class has comparable potency against caspases-3 and -7, but reduced selectivity over caspases-1, -6 and -8.[20] However, when pyrrolidine was substituted for a thiomorpholinyl residue (compound **25**), an increased caspase-6 inhibition and moderate selectivity over

caspases-3 and -7 was observed, representing a new class of small molecules caspase-6 inhibitors which could serve as lead compounds for the development of a second generation inhibitors.[21]

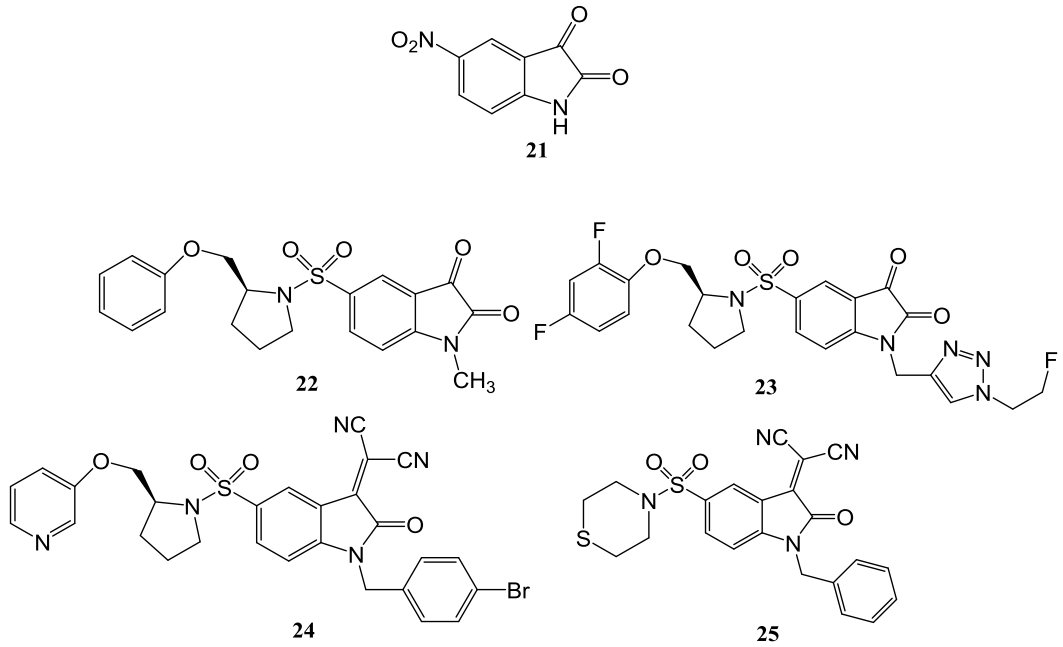

Figure 17: Structures of the isatin sulfonamides caspase inhibitors **21**-**25**.

Another class of caspase inhibitors includes those possessing a 1,4 – benzodioxane scaffold, like compounds **26** and **27** (**Figure 18**). Compound BI-7E7 (**26**) was identified as an inhibitor of caspase-8-mediated peptide cleavage. Optimization of the thiazole ring through docking studies resulted in compound BI-9B12 (**27**) with an improved inhibitory activity on caspases-3, -7 and -8.[22]

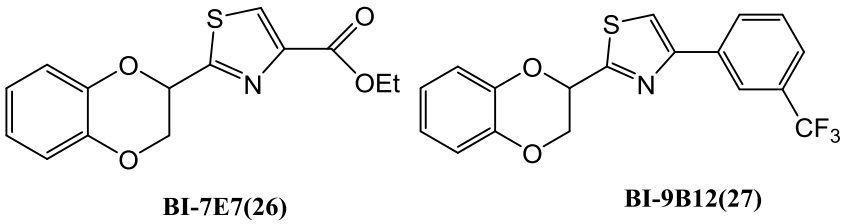

Figure 18: Structures of 1,4- benzodioxane derivatives **26** and **27**.

In 2005, other class of caspase inhibitors was introduced based on the 2,3-dihydro-1H-pyrrolo[3,4-c]quinoline-1,3-dione scaffold (**28**, **Figure 19**).[23] The mechanism of

caspase inhibition of these compounds is mediated by the nucleophilic attack of catalytic cysteine to one of the carbonyl functions at the fused pyrrol ring, leading to the reversible covalent inhibition of the targeted caspases.[2] Many compounds were described based in this scaffold, differing at the substituents R1, R2, and R3. According to Kravchenko et al. (2005), caspase-3 inhibitory activity was highly dependent on substitutions on the core scaffold, especially at the 8-position. The compound **29** (**Figure 19**) with a morpholinesulfonyl moiety at the 8-position and a 1,3,5-trimethyl-1-H-pyrazol-4-yl group at the 2-position was the most potent (IC_{50} = 4 nM).[24]

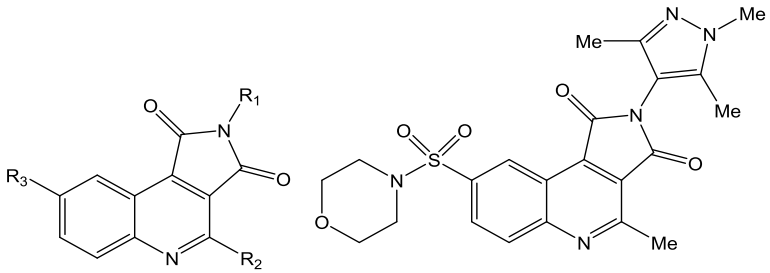

Figure 19: Caspase inhibitors with a pyrrolo[3,4-c]quinoline-1,3-dione scaffold (**28**) and selected caspases-3 inhibitor (**29**).

2.1.3.2. Allosteric inhibitors of caspases

Allostery is a basic principle of control of enzymatic activities based on the interaction of a protein or a small molecule with a site of an enzyme distinct from the active one. Allosteric modulators represent an alternative approach to the design and synthesis of small molecule activators or inhibitors of proteases and are therefore of wide interest for Medicinal Chemistry.[25]

Allosteric regulation involves the understanding of some concepts. The concept of conformational selection proposes that a protein exists in equilibrium of multiple conformations, some of them catalytically active, with others being inactive. With the bond of a preferential molecule, there is conformation stabilization (**Figure 20**). The conformational selection can arise in two ways: or a molecule bonds to the recognized orthosteric site through an endogenous ligand or it bonds to an allosteric site.[2]

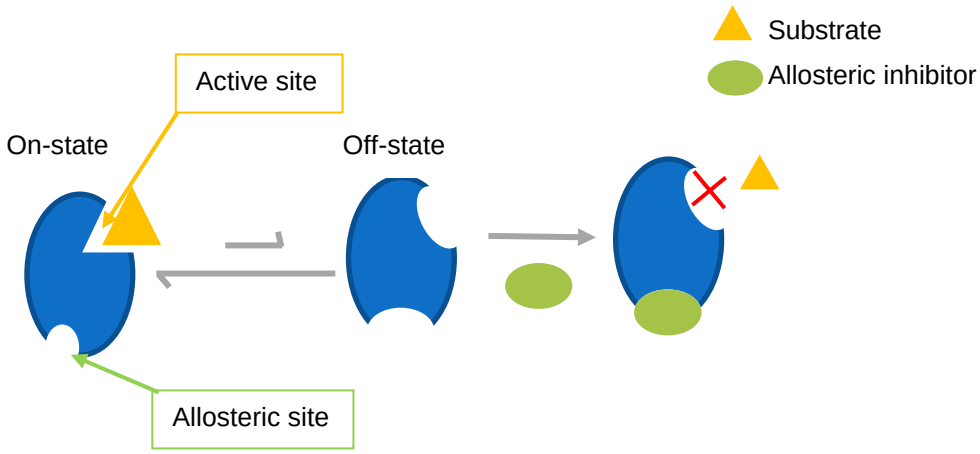

Figure 20: Model of allosteric inhibition. A dynamic protein exists in equilibrium of several low-energy conformations, which are active (on-state) or inactive (off-state). Reversible binding to or irreversible trapping of a distinct conformation shifts this equilibrium, inducing an alteration of enzyme activity.
(Adapted) [25].

Many new allosteric interactions with caspases were revealed by disulfide trapping. A disulfide reversible ligation is formed between cysteine residues at the target protein surface with a small molecule containing sulfhydryl. If a small molecule shows affinity to the protein, the dissulfite is stabilized and a possible modulation of the biological function is measured (**Figure 21**).[26]

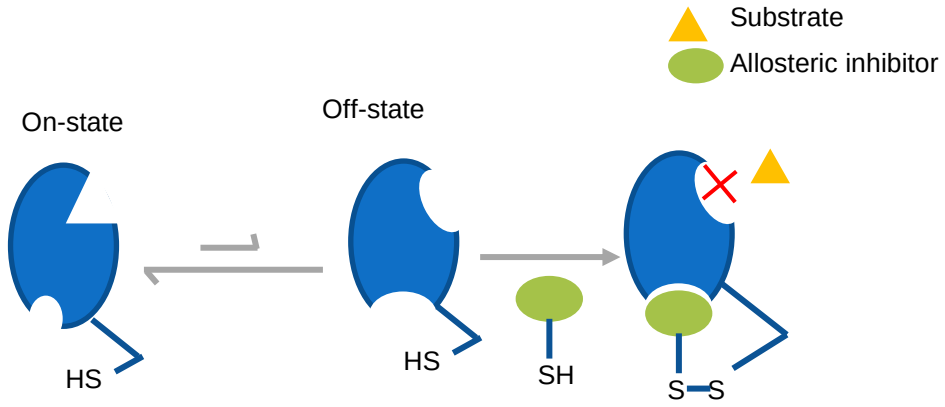

Figure 21: Model of disulfide trapping. A dynamic protein exists in equilibrium of several low-energy conformations, which are active (on-state) or inactive (off-state). Protein has cysteine residues near the allosteric site that interact with small molecule that also contain cysteine residue, preventing the binding of substrate. The caspases is shown as monomer, for simplicity.
(Adapted) [27]

The first successful utilization of disulfide trapping for the caspases allosteric modulation was reported in 2004.[28] The screening of a thiol-containing compound database for caspase-3 binding resulted in the discovery of DICA (**30**, **Figure 22**) and FICA (**31**, **Figure 22**) as new inhibitors of caspase-3. DICA and FICA were found to trap the enzyme in a zymogen-like conformation [29], binding selectively to *Cys264* located in a central cavity at the dimerization interface.[25]

In the caspase-7, different binding modes of DICA and FICA in the allosteric site were demonstrated, but an identical conformational rearrangement in the protease domain was observed. Both compounds induce a switch of active dimerized caspase-7 conformation into a procaspase-7-like conformation by irreversibly trapping the zymogen-like conformation.[25]

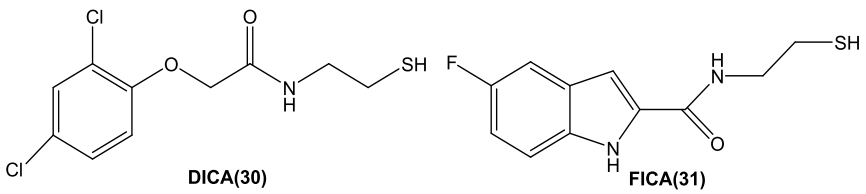

Figure 22: Structures of the allosteric inhibitors of caspases-3 and -7 DICA (**30**) and FICA (**31**).

The disulfide trapping approach was also applied to the discovery of new inflammatory caspase-1 inhibitors. Despite the low rate of homology between caspases-3/7 and caspase-1, small molecule inhibitors could be identified which interfere with a comparable located *Cys331* residue at the dimerization interface. Using this approach, compound **32** (**Figure 23**) was identified as an inhibitor of caspase-1.[27] The identification of functional allosteric sites in C1, C3 and C7 served as source of inspiration for further efforts to identify allosteric modulators of these and other caspases.[29]

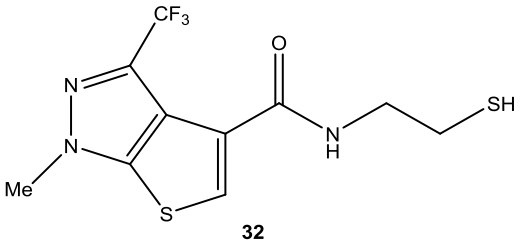

Figure 23: Structure of the caspase-1 allosteric inhibitor, compound **32**.

In addition to the small molecule allosteric inhibitors of caspases, some macromolecular inhibitors are also known. For example, AR-F8 is one of the caspase-2 specific macromolecular ligands that significantly inhibits its activity. For this peptidic inhibitor, a high selectivity for caspase-2 over caspases-3, -7, -8, and -9 was observed. Contrary to compounds **30** and **31,** which caspase inhibition lead to zymogen-like structures, AR-F8 induced only minor conformational changes within caspase-2. The strong inhibitory effect is due to a slight misalignment of the active cysteine site and the disruption of hydrogen-bond interactions between the substrate and the active site.[2]

Another example of macromolecular inhibitors is the endogenous inhibitor XIAP, a member of inhibitor apoptosis proteins (IAPs). IAPs are a cell protein family that includes eight members, being six of them identified in humans. This, in general, are expressed at high levels in the majority of human cancers.[30] XIAP protein is a caspase inhibitor of caspases-3, -7 and -9 that can interact not only with the allosteric site, but also with the active binding site, depending on the caspase. Caspase-3 and -7 are inhibited by prevention of substrate access to the active site whereas caspase-9 is inhibited allosterically.[25] XIAP is composed by three baculoviral IAP repeats (BIR) with distinct binding properties. For caspases-3 and -7, the second BIR domain is the responsible for preventing the substrate bonding. On the other hand, the third BIR domain is responsible for XIAP-mediated inhibition of caspase-9. BIR3 bonds to the N-terminal region of the small subunit of caspase-9.[2,5] IAPs do not bind nor inhibit caspase-8 (extrinsic pathway), however they bind and inhibit procaspase-3 substrate, stopping the cascade and protecting the caspase-8 induced apoptosis. The interaction between XIAP and caspases can be disrupted by several small molecules. One example is the compound **33** (**Figure 24**) that interferes with XIAP's ability to inhibit caspase-3 [31], and compound **34** (**Figure 24**) that interacts with de BIR3 domain of XIAP, avoiding its bond to caspase-9.[32] With this approach, the inhibitory effect of XIAP on caspases activity will be blocked and caspases activity will no longer be inhibited.

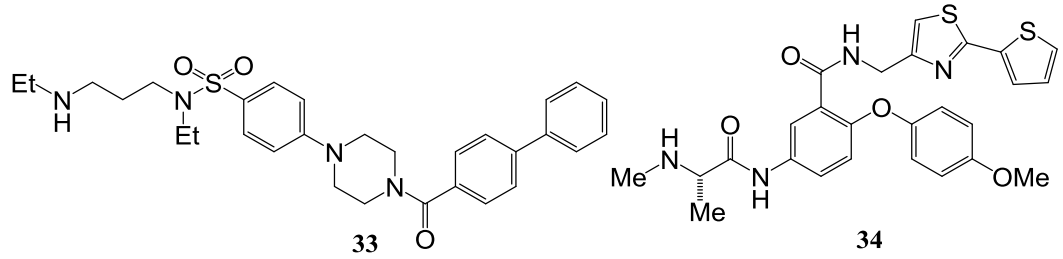

Figure 24: Structures of XIAP inhibitors, compounds **33** e **34**.

2.1.3.3. Small molecule activators of caspases

Activation, instead of inhibition, of caspase activity with synthetic small molecules has been less investigated. Such small molecules can reveal key aspects in the activation of these enzymes and provide a direct effect on important physiological processes. Only in 2006, it was published the first report about caspase activators, when approximately 20,500 structurally diverse small molecules were screened for their ability to activate procaspase-3 *in vitro.*[33] The evaluation of the ability of a group of structural diverse small-molecules to activate procaspase-3 resulted in the identification of the procaspase-3 activator compound, PAC-1 (**35**, **Figure 25**).

Additionally, further PAC-1 derivatives were synthesized and evaluated in order to determine their effects on procaspase-3. Consequently, a PAC-1 analogue (PAC-1B or de-allyl PAC-1, **36**) was identified, with similar potency than PAC-1 (EC_{50} value 0.43 µM, PAC-1B value 0.22 µM).[33]

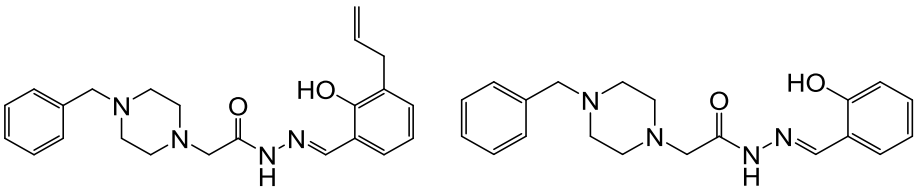

PAC-1(35) **PAC-1B(36)**

Figure 25: Structures of PAC-1 (**35**) and its close analog PAC-1B (**36**).

SAR studies allowed concluding that the presence of the N-benzylpiperazinyl group and the aromatic hydroxyl moieties are crucial for activation and the allyl group is dispensable for the biological activity.[34] Peterson et al. (2009), demonstrated that zinc inhibits the enzymatic activity of procaspase-3 and that PAC-1 strongly activates procaspase-3 in buffers that contain zinc [34]. In fact, it was demonstrated that PAC-1 and zinc form a tight complex with one another, with a dissociation constant of approximately 42 nM.[34] Moreover, the presence of the N-benzylpiperazinyl group and the aromatic hydroxyl moieties in PAC-1 seems to be fundamental for the ability of PAC-1 to bind zinc ions from the active site, allowing the proenzyme to autoactivate itself to caspase-3 (**Figure 26**).[35] Although, PAC-1 was the first compound to be considered as direct

activator of caspases, its direct activating ability was questioned, particularly by Denault et al, who demonstrated that PAC-1 and related compounds were not activating executioner caspases directly, reinforcing the idea that the mechanism of action is due to the zinc chelatio9n.[36]

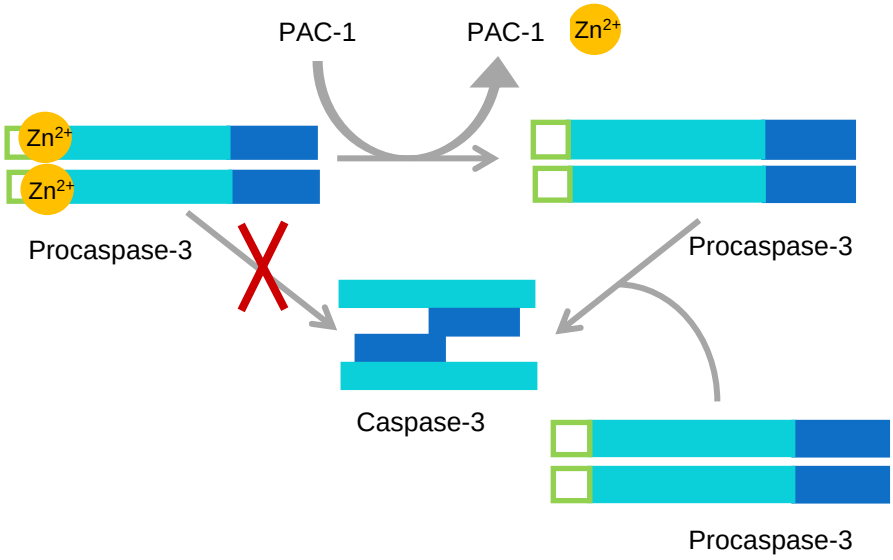

Figure 26: The proposed mechanism for PAC-1-induced activation of procaspase-3 *in vitro*. In the presence of PAC-1, the zinc ion is removed by giving up the caspase-3 activation to function as an enzyme and proteolytically cleave another molecule of procaspase-3. When the zinc ion is not removed, there is an impediment to activation of procaspase-3.
(Adapted) [34]

The relatively short *in vivo* half-live of PAC-1 (2.1 ± 0.3 h in dogs)[37] following i.v. administration is a major challenge for using this compound *in vivo* studies. In this sense, very recently, Roth et al. (2015) designed a series of PAC-1 analogues containing modifications that systematically block sites of metabolic vulnerability. Evaluation of the library of compounds identified four potentially superior candidates (**37**-**40**, **Figure 27**) with comparable anticancer activity in cell culture, enhanced metabolic stability in liver microsomes, and improved tolerability in mice.[37]

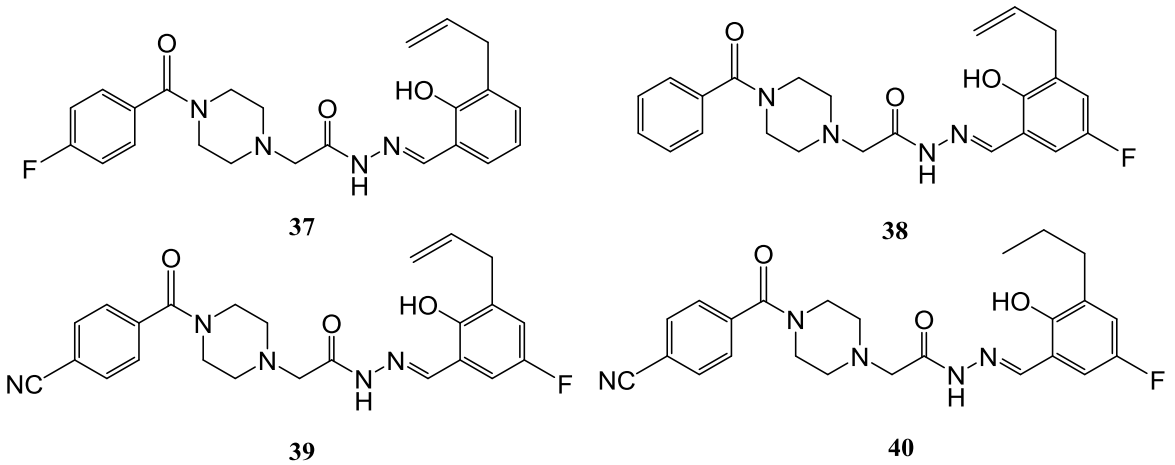

Figure 27: Derivatives of PAC-1 (**37**, **38**, **39** and **40**) with enhanced metabolic stability in liver microsomes, and improved tolerability in mice.

In 2014, several benzothiazole derivatives emerged as procaspase-3 activators, from a series of benzothiazole derivatives bearing the ortho-hydroxy-N-acylhydrazone moiety.[37,38] Among those compounds, benzothiazoles **41**-**43** (**Figure 28**) revealed to be potent inhibitors of human tumor cell lines and more potent than PAC-1 as procaspase-3 activators. SAR studies demonstrated that the phenyl group on the 2-hydroxyphenyl ring was critical for the *in vitro* pharmacological activity.[39] and that the introduction of a lipophilic group at the 4-position of the 2-hydroxy phenyl ring was beneficial to the antitumor activity.[38]

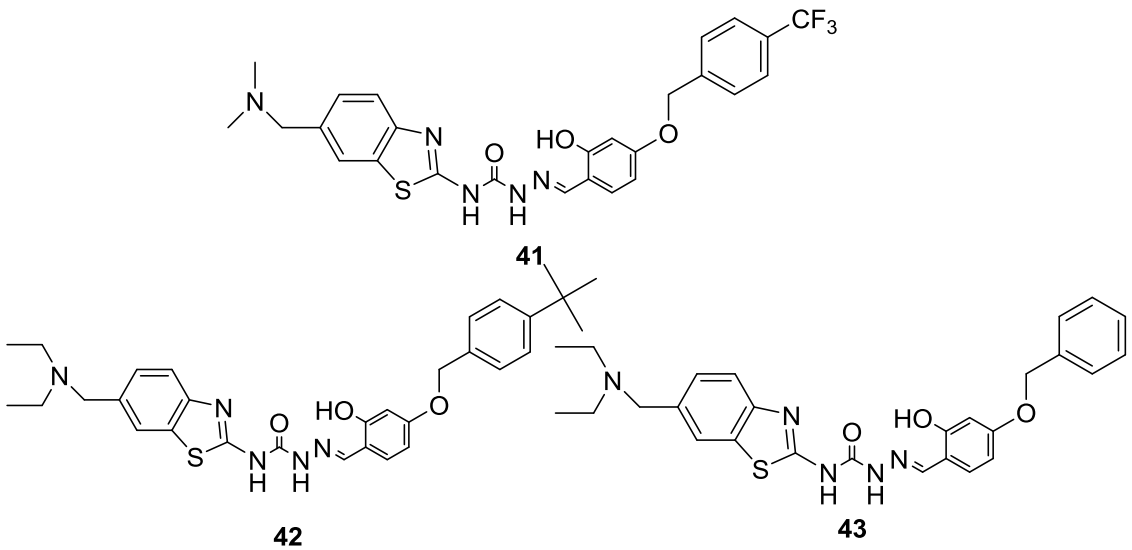

Figure 28: Structures of PAC-1 analogues (**41**, **42** and **43**).

In 2009, a library of approximately 62,000 compounds was tested and several hit compounds revealed the ability to activate procaspase-3.[40] Among these, compound 1541 (**44**, **Figure 29**) was the most potent direct activator of procaspases-3 and -6, but no activity was detected for procaspases-1 and -7. In addition, several 1541 analogs were synthesized and tested.[40] Compound 1541B (**45**, **Figure 29**), possessing a 8-methoxy group instead of a hydroxyl group on the coumarin nucleus, showed a potent activation of procaspase-3, but no activity toward procaspase-6 was detected. Compound 1541C (**46**, **Figure 29**) with an additional bromine atom at position 6 revealed a reduced potency for procaspase-3, but an increased potency for procaspase-6. Furthermore, the deletion of the imidazopyridine *metha* substituent on the phenyl ring (1541D, **47**, **Figure 29**) was associated with the absence of activation of procaspases-3 and -6, suggesting that the presence of this group was crucial for the activity.[40]

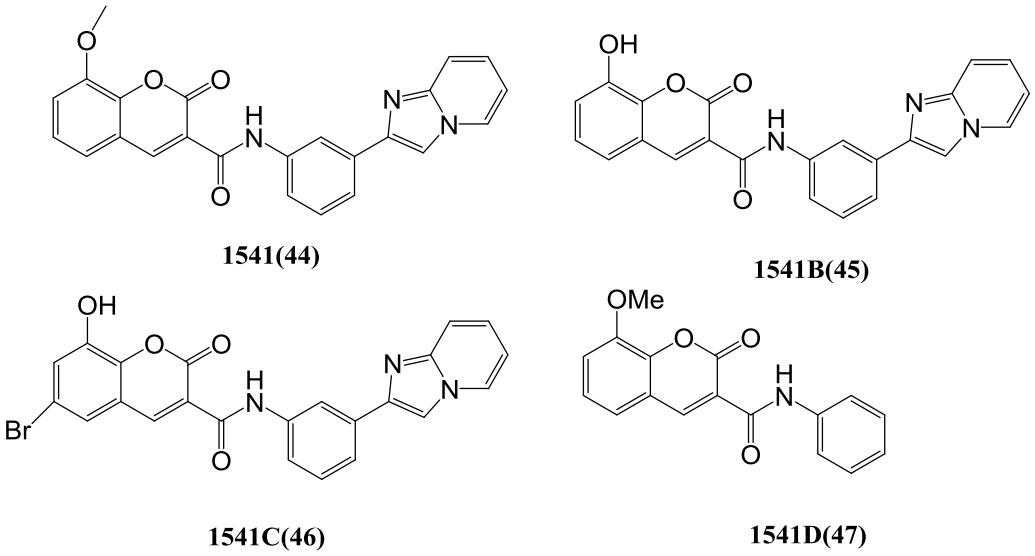

Figure 29: Structures of 1541 (**44**) and its derivatives1541B (**45**), 1541C (**46**) and 1541D (**47**).

Wolan et al. (2009) demonstrated that compound **44,** at low concentrations, activates the procaspase-3 (EC_{50} = 2.4 µM), but at higher concentrations partially inhibits the active enzyme. It was proposed that compound 1541 binds near one active site of the dimeric procaspase and induces the formation of an active conformation, resulting in the subsequent enhancement of the proteolysis at the other active site. Nevertheless, at higher concentrations, compound 1541 binds to both active sites, causing the partial inhibition (**Figure 30**).[2]

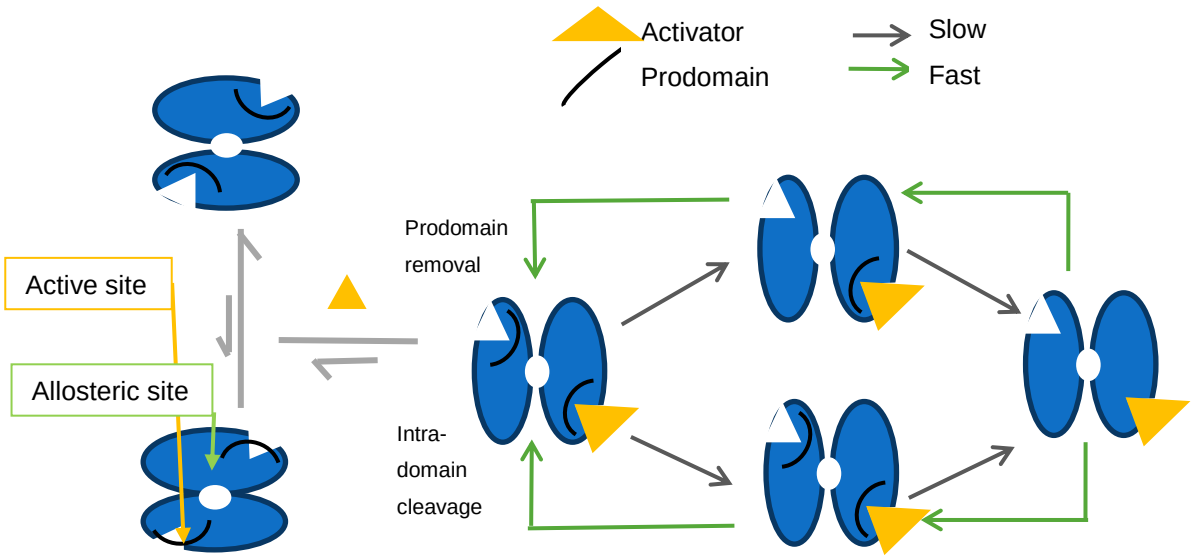

Figure 30: The proposed mechanism of activation-assisted procaspase-3 self-activation. The activator inducing initial slow autoproteolytic activation phase (grey arrows). Thus, increases active caspases, resulting in the subsequent enhancement of the proteolysis at the other active site.

2.2. Flavonoids

The flavonoids are a group of secondary metabolites that exist either as free aglycones or glycosidic conjugates. They are widely found in normal human diet.[41,42], being components of fruit, vegetables, nuts, and plant-derived drinks.[43] To date, some 10,000 different flavonoids have been characterized.[44]

2.2.1 Chemistry

Chemically, flavonoids possess a fifteen-carbon skeleton consisting of two benzene rings (rings A and B) that are linked by a three carbon unity which may or may not form a third ring (ring C). This basic structure occurs in a variety of structural forms including those that could be considered as structurally derivatives of 1,1-, 1,2- and 1,3-diphenylpropane (**Figure 31**). The first group is known as neoflavonoids, while the second group is known as isoflavonoids and the third is commonly known as flavonoids [45]

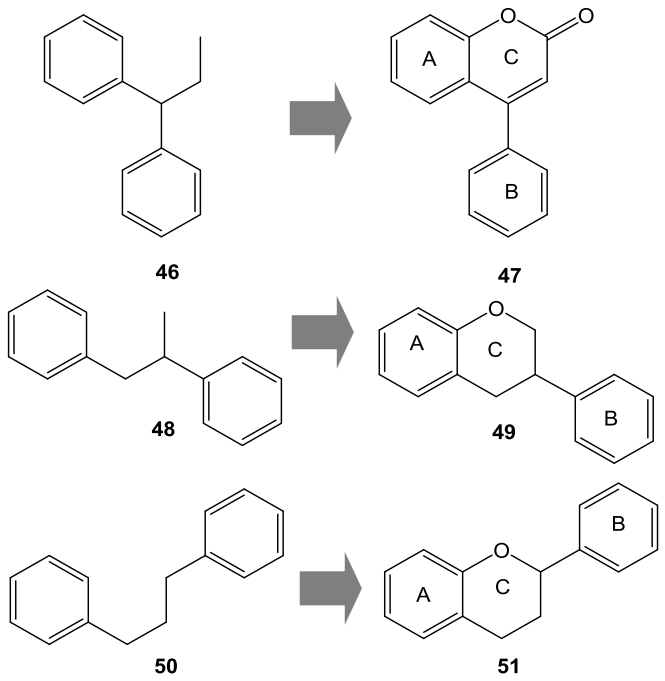

Figure 31: Basic skeletons and numbering pattern of structural derivatives of 1,1-, 1,2- and 1,3-diphenylpropane (**47**, **49** and **51** respectively).

Considering flavonoids group, they can be subdivided into several sub-classes according to the presence (or absence) of a third ring, a double bond between carbon atoms 2 and 3, a carbonyl group on C-4, and hydroxyl groups in the C ring (**Figure 32**).

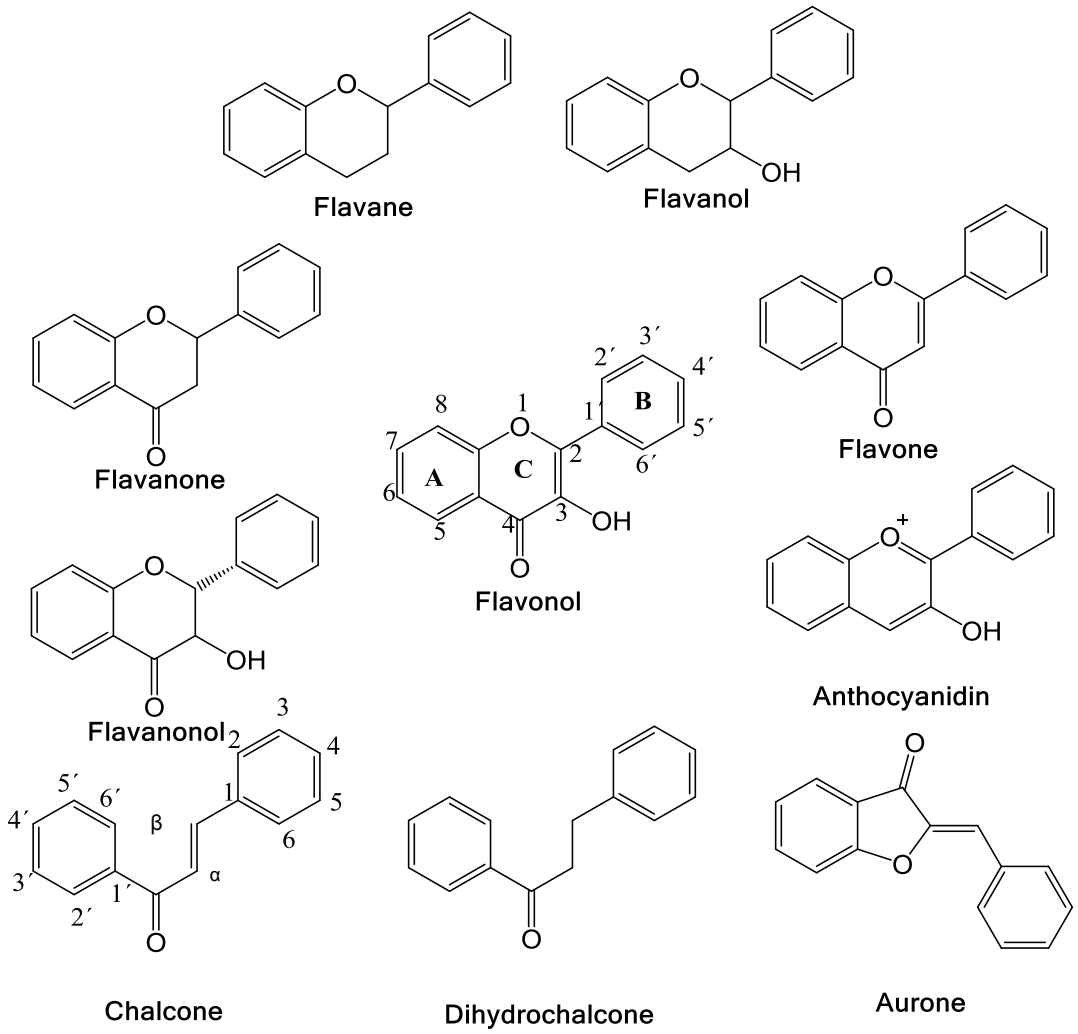

Figure 32: Basic skeletons of several subclasses of flavonoids and numbering of skeletons

All flavonoids are derived from the general phenylpropanoid pathway, one of the best-known pathways in plant secondary metabolism.[46] The first three steps of this pathway (**Figure 33**, **A**) involve the deamination of phenylalamin to cinnamic acid by phenylalanine ammonia lyase (PAL), the oxidation of cinnamic acid to 4-coumaric acid by cinnamate 4-hydroxylase (C4H) and the formation of 4-coumaroyl-CoA by 4-coumaroyl CoA ligase (4CL). Chalcone is obtained by the condensation of three molecules of malonyl-CoA (**Figure 33**, **B**) and one molecule of 4-coumaroyl-CoA by chalcone synthase (CHS) [46]. The subsequent ring closure catalyzed by chalcone isomerase (CHI) produces flavanones which in turn serve as precursor for a large number of different flavonoids (**Figure 33**, **C**). From flavanones the pathway diverges into several side branches, each resulting in a different class of flavonoids. Flavanones can be hydroxylated by flavanone 3β-hydroxylase (FHT) to form a dihydroflavonol, which can subsequently be reduced to leucoanthocyanidin, thereby initiating the synthesis of anthocyanin directed by

dihydroflanonol-4-reductase (DFR) and anthocyanidin synthase (ANS). On the other hand, dihydroflavonol can be directly oxidated by Flavonol synthase (FLS) forming flavonols.[44]

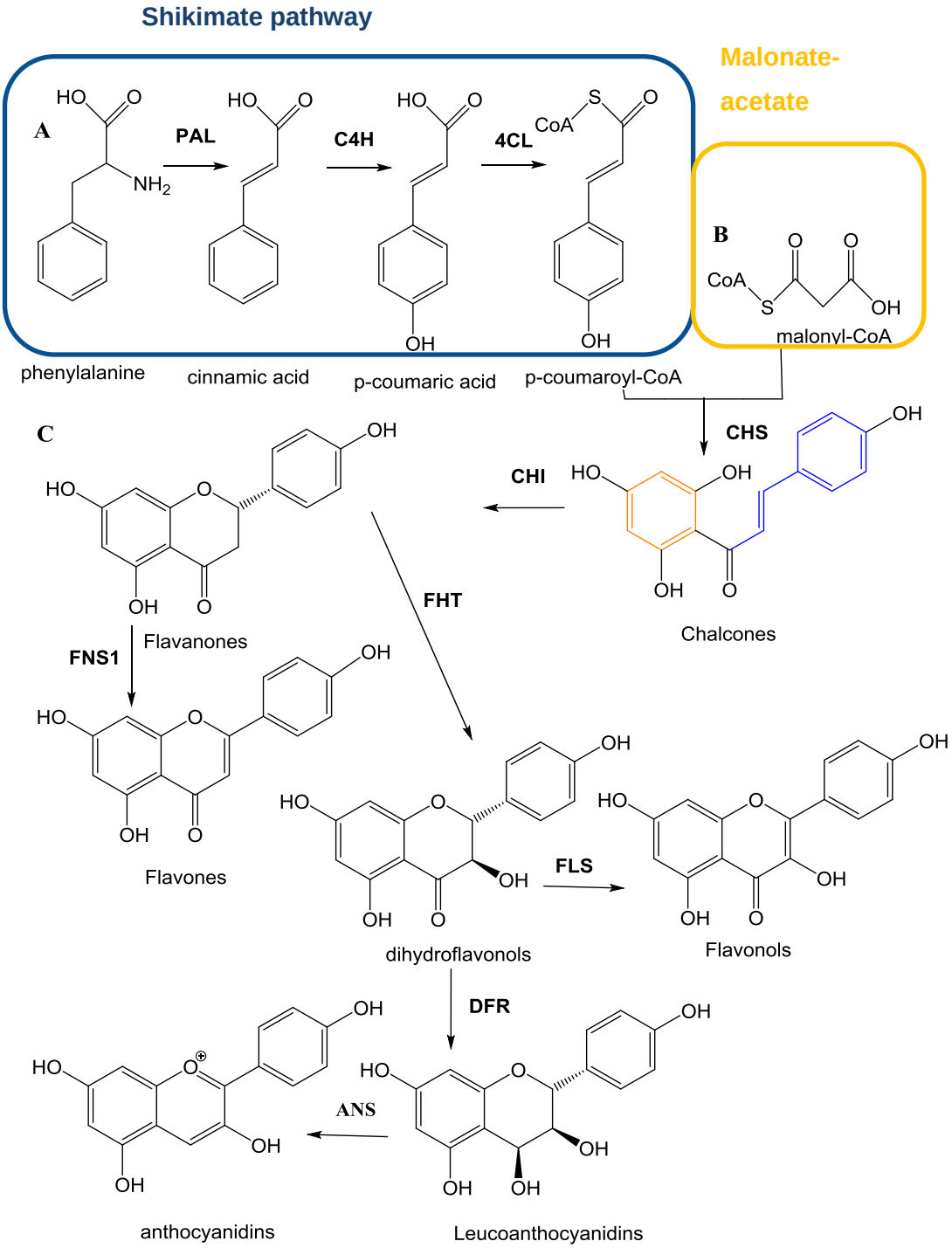

Figure 33: Biosynthesis of flavonoids. PAL: Phenylalanine ammonia-lyase, C4H: Cinnamic acid 4-hydroxylase, 4CL: 4-Coumarate:Coenzyme A ligase, CHS: Chalcone synthase, CHI: Chalcone isomerase, FHT: Flavanone 3β-hydroxylase, FNS I: Flavone synthase I, FLS: Flavonols synthase, DFR: Dihydroflavonols reductase, ANS: Anthocyanidin synthase.
(Adapted). [44]

2.2.1. Biological activities

The diversity of structural patterns has resulted in flavonoids being recognized as a rich source of compounds with diverse biological activities[47], namely antioxidant [42,48], antimutagenic [49], antibacterial [50], antiangiogenic [51,52], anti-inflammatory [53,54], antiallergic [55], and anti-tumor activity [43,56,57]. In addition, these natural products have also been described for their ability to modulate the acivity of several enzymes (lipoxygenase,[58,59] Cytochrome P450 monooxygenases,[60] protein kinase C,[60,61] topoisomesare I,[62] tyrosinase,[63,64] aromatase[65]) as well as to modify the behaviour of many cell systems (functions of inflammatory cells, smooth muscle and cardiac muscle cells, effects on nerve cells).[66]

2.2.1.1. Flavonoids as antitumor agents

Among the activities reported for flavonoids, the antitumor activity is one of the most exhaustively studied. The ability of flavonoids to arrest the cell cycle, induce apoptosis, disrupt mitotic spindle formation, and inhibit angiogenesis makes them promising agents in anticancer research.[51]

Natural flavonoids and their synthetic analogs have been intensely studied in the treatment of ovarian, breast, cervical, pancreatic, and prostate cancers.[51] The interesting anticancer properties of flavonoids in preclinical studies have encouraged their entrance in clinical trials. In fact, the natural flavonoid genistein (**54**, **Figure 34**) and the semi-synthetic flavone flavopiridol (**55**, **Figure 34**) have entered clinical trials for several cancers.[51] Genistein (G-2535), a soy derived isoflavone, was found to be a potent agent in prevention and treatment of cancer.[67] Flavopiridol (NCS 649890) is derived from the indigenous Indian plant *Dysoxylum binectariferum*, and it was the first CDK inhibitor to be tested in clinical trials.[68,69]

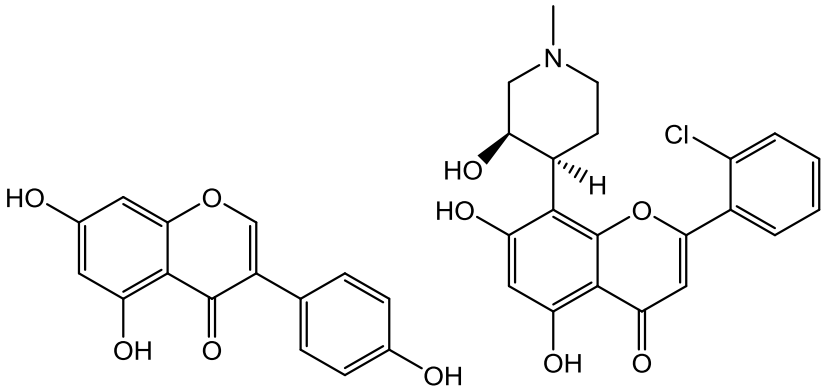

Figure 34: Examples of natural flavonoids that have entered in the late phase of clinical trials for various cancers.

Given the importance of the antitumor activity of flavonoids, several studies have been conducted in order to get some insights into the cellular and molecular mechanisms of action of these compounds. Flavonoids display a vast array of cellular effects, affecting the overall process of carcinogenesis in different stages (initiation, promotion and progression) by several mechanisms (**Figure 35**)[47], including inhibition of DNA topoisomeraseI/II activity[70,71], regulation of reactive oxygen species[72], cell cycle arrest[57], modulation of proliferation pathways[73], and interference with the apoptotic cascade.[74,75]

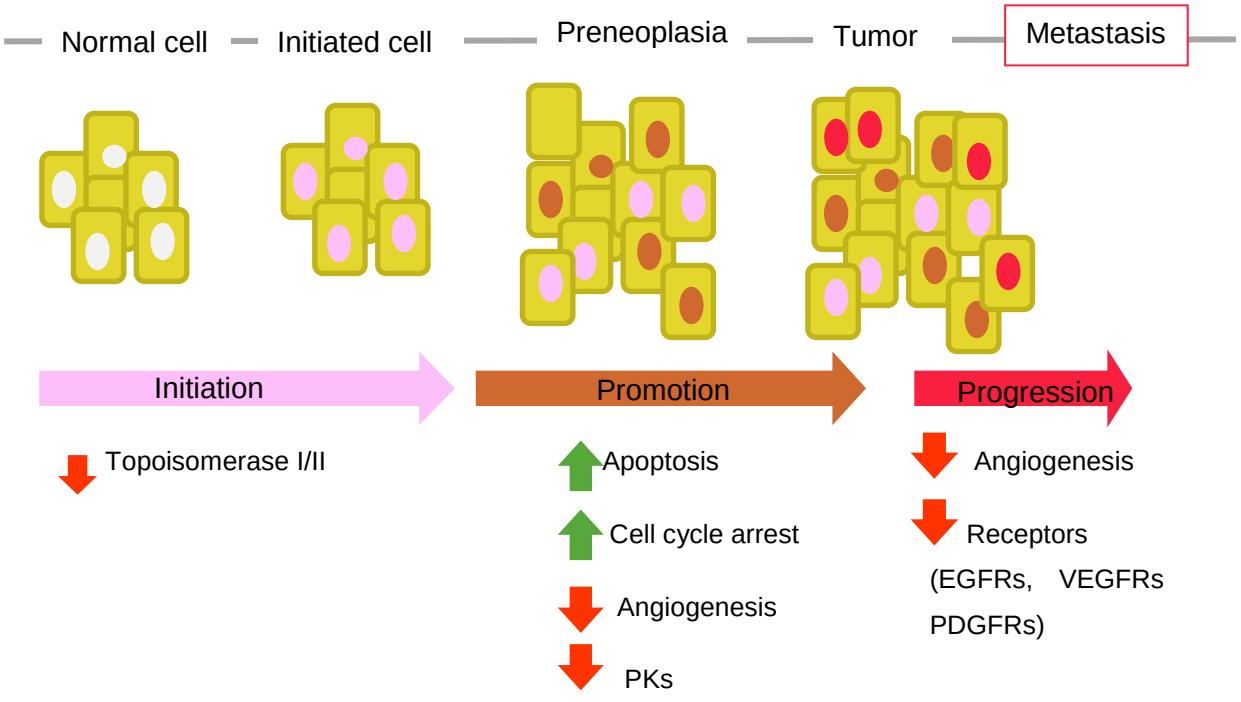

Figure 35: Multistage model of carcinogenesis and potential effects of flavonoids on cancer progression. Red arrows indicate the inhibited systems and the green arrows indicate the activated systems by flavonoids.

Additionally, flavonoids have been reported to modulate several protein kinases. Protein-kinases (PKs) are enzymes that catalyse the phosphorylation of different cellular substrates. Deregulation of PKs can lead to alterations in phosphorylation that result in several abnormalities, namely in uncontrolled cell division and inhibition of apoptosis, being these effects closely linked to various cancers.[76] So, inhibition of PKs is an important aspect in cancer chemoprevention by the flavonoids. Some examples of the protein kinases that are inhibited by flavonoids include serine/threonine kinases, phosphatidylinositol kinase and cyclin-dependent kinases.[51]

Flavonoids are also capable of interact with several receptors which play important roles in cancer pathology [77], namely the epidermal growth factor receptors (EGFRs)[78-80], platelet derived growth factor receptors (PDGFRs), vascular endothelial growth factor receptors (VEGFRs)[81,82] and cyclin-dependent kinases (CDKs).[83]

2.2.1.2. Flavonoids as pro-apoptotic agents in cancer

Activation of apoptosis is a key molecular mechanism responsible for the anticancer activities of several currently studied potential anticancer agents, including flavonoids.[84] Several reports indicate that these compounds may induce apoptosis by affecting the expression or activity of a wide range of molecules involved in apoptosis pathways (**Figure 36**). In fact, the induction of apoptosis by flavonoids can be related to the activation of caspases, decrease of variation of the membrane potential ($\Delta\Psi_m$), release of cytochrome *c* from mitochondria, regulation of Bcl-2 family proteins members, and regulation of IAP by release of Smac/DIABLO from mitochondria, cleavage of poly (ADP-ribose) polymerase (PARP), increase levels of reactive oxygen species (ROS) and activation of death receptors (**Figure 36**).

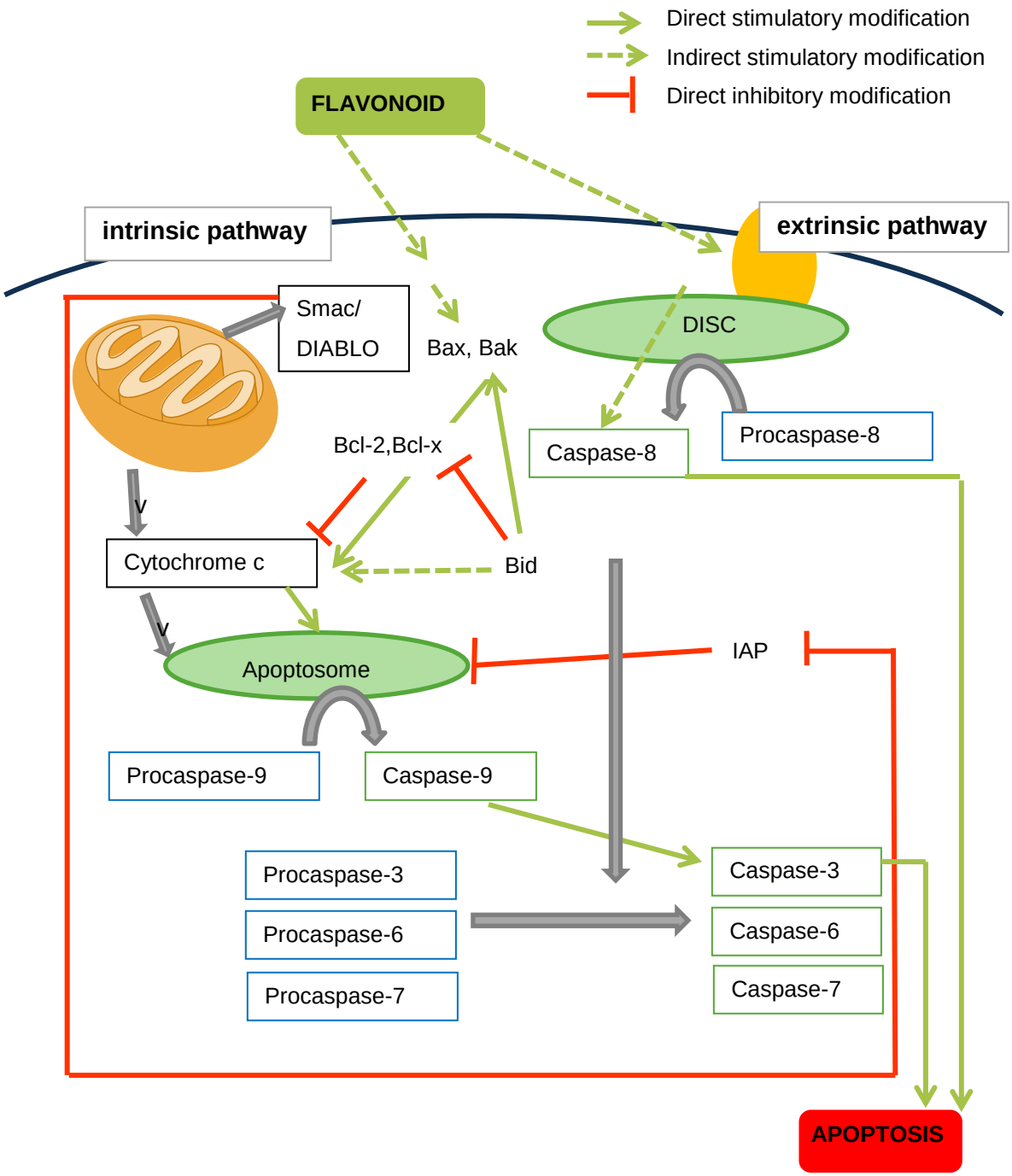

Figure 36: Flavonoids may induce apoptosis by affecting the expression or activity of a wide range of molecules involved in apoptosis pathways.

Some examples of flavonoids that induce apoptosis by modulating different key targets involved in apoptotic pathways, including caspase family proteins are listed in **Table 3.** Despite few structure-activity relatioship studies (SAR) have been conducted regarding antitumor activity of flavonoids, some researchers suggest that flavones and flavonols are the most potent flavonoids.[85] So, the flavonoids listed in **Table 3** are restricted to these two classes of flavonoids.

Table 3: Some flavones and flavonols reported since 2000 as inducers of apoptosis by modulating different key targets involved in apoptotic pathways, including caspase family proteins reported.

Compound	Target or affected process	References
Natural flavones and flavonols		
Methoxyflavones and flavonols		
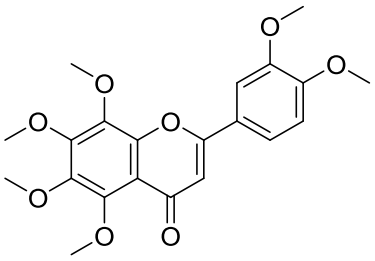 **56**: nobiletin	-Decrease Bcl-2 expression -Increase Bax expression -Increase caspase-3 expression, in HCC cell line SMMC-7721 and HCC cell line H22 -Induction of cell cycle arrest in G0/G1 phase -Inhibition ERK -Activation of p38 -Activation of caspase-8,-9 and -3, in HL-60 AML cells -Cleavage of PARP -Increase caspase-3 activity, in HUVEC -Cleavage of PARP -Decrease Bcl-2 expression -Increase p21 expression -Increase caspase-3,-7 and -9 activities	86-89
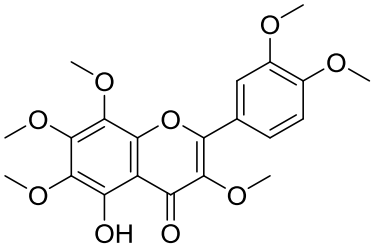 **57**:5-Hydroxy-3,6,7,8,3',4'-hexamethoxyflavone (5-OH-HxMF)	-Decrease $\Delta\Psi m$ -Increase levels of ROS -Increase caspase-2, -3, -6 and -7 activities -Cleavage of PARP -Increase Bad expression, in HL-60 cells	90

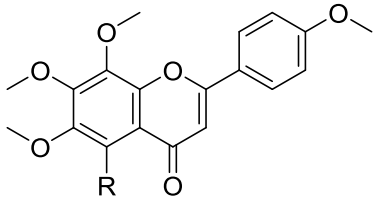 **58:** R=OCH_3, tangeretin **59**: R=OH, 5-DT	-Decrease ΔΨm -Increase caspases-3, -8 and -9 activities -Increase Bax expression -Increase Bid expression -Increase tBid expression -Increase Fas expression -Increase FasL expression -Increase p53 expression, in AGS cells -Arrest cell cycle in G2/M phase -Increase caspases-3, -7 and -9 activities -Decrease Mcl-1 expression -Decrease Bcl-Xl expression, in K562 cells -Increase p53 expression -Increase Bax expression -Decrease cdc-2 (cdk1) and cyclin B1 expression -Increase p21 expression -Cleavage of PARP, in human nonsmall cell lung cancer (H460,H1299 and A549) cells	91-93
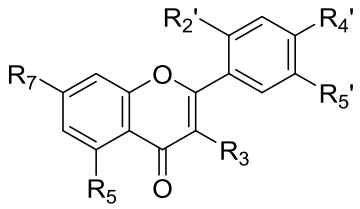 **60**: R_3,R_4´,R_5´=H; R_5,R_7=OCH_3,DMF **61**: R_3,R_5´=H; R_5,R_7,R_4´=OCH_3, TMF **62**: R_3,R_5,R_7,R_5´,R_4´=OCH_3, PMF **63:** R_3,R_7,R_2´R_4´,R_5´=H; R_5=OCH_3, 5-MF **64**: R_3,R_5,R_7,R_4´,R_5´=H R_2´=OCH_3, 2´-MF	-Increase DRs expression -Decrease cFLIP expression -Decrease Mcl-1 expression -Increase Bax expression -Decrease Bid expression -Activation of caspase-3 and -8 -Increase oxidative stress, in human leukemic MOLT-4 cells 5-MF: -Increase caspases-3 and -7 activation -Cleavage of PARP ,in HCT116 colo cancer cells	94,95
Hydroxyflavones and flavonols		

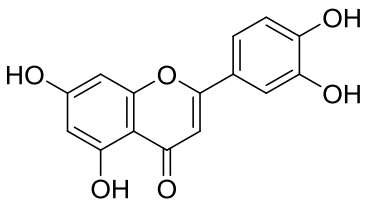 **65**: luteolin	-Decrease ΔΨm -Increase *cit c* release -Cleavage of PARP -Increase Bad expression -Increase Bax expression -Decrease Bcl-2 expression -Decrease Bcl-Xl expression -Induce and increase caspase-3 and -9 activities, in HL-60 cells -Inhibit Bcl-2 expression -Increase Bax expression -Increase caspase-3 activity, in MG-63 cells -increased Fas expression -Activation of caspases-8 and -3, in MDA-MB-231	96-98
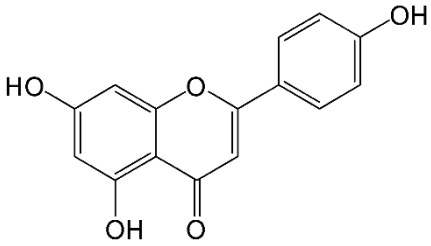 **66:** apigenin	-Increase levels of ROS -Induction of cell cycle arrest in G2/M phase, in SCC25 and A431 cells -Increase TNF-R expression -Increase TRAIL-R expression -Decrease Bcl-2 expression -Activation of caspase-3, in SCC25 cells -Increase levels of ROS -Decrease ΔΨm -Increase *cit c* release -Increase Bax expression -Decrease Bcl-2 expression -Activation caspases-3 and -9, in A375 and A549 cells -Increase *cit c* release -Increase caspase-3 activity, in breast cancer cells (with HER2/*neu*-over-expressing) -Increase caspase-3 and -9 activities -Increase levels of ROS -Activation of ERK and p38, in THP-1 cells -Increase caspase-3 activity -Cleavage of PARP -Increase Bax expression, in NUB-7 cells	99-103

	-Increase levels of ROS -Decrease ΔΨm -Increase *cit c* release -Increase Bax expression -Decrease Bcl-2 expression -Decrease Bcl-xl expression -Cleavage of PARP -Increase caspse-3 and -9 activities, in 22Rv1 cells	
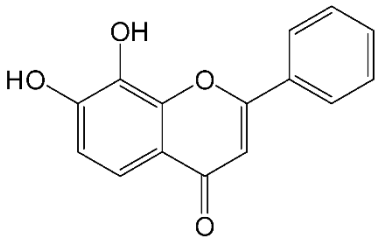 **67:** 7,8-DHF	-Increase Fas expression -Increase FasL expression -Increase DR4 expression -Increase TRAIL expression -Activate caspase-3,-8 and -9 -Cleavage of PARP -Increase Bax expression -Increase *cit c* release -Activation ERK and JNK, in U937 cells	104
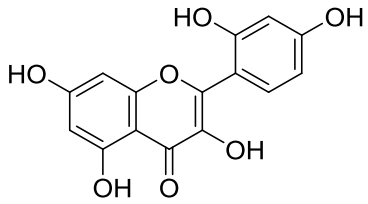 **68**: morin	-Decrease ΔΨm -Increase *cit c* release -Decrease Bcl-2 expression -Increase Bax expression -Cleavage of PARP -Increase caspase-3, -8 and -9 activities, in U937 cells	105
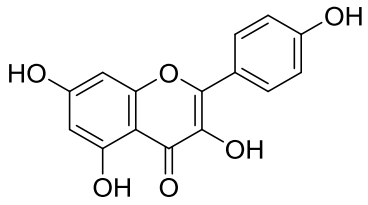 **69**: kaempferol	-Decrease Bcl-xL expression -Increase p53 expresson -Increase Bad expression -Increase Bax expression -increase caspase-3 and -7 activities, in Ovarian cancer cell lines (OVCAR-3, A2780/CP70, and A2780/wt), - Decrease Bcl-xL expression -Increase Bad expression -Cleavage of PARP -Increase caspase-3, -7, -8 and -9 activity in HT-29 Human Colon Cancer Cells -decrease Bcl-2 expression -Increase Bax expression	106-108

	-Cleavage of PARP -increase caspase-3 and -9 activities, in gastric cancer	
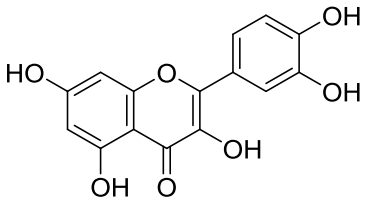 **70**: quercetin	-Decrease ΔΨm -Increase Bax expression -Decrease Bad expression -increase caspase-3,-8 and -9 activities, in MDA-MB-231 cells -Decrease Bcl-xL expression -Increase Bax expression -Increase caspase-3 and -9 activities, in HepG2 cells	109,110
Methoxy- and-Hydroxyflavones and Flavonols		
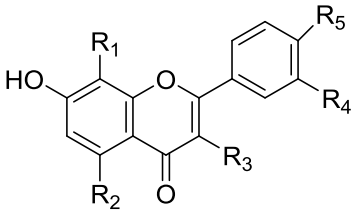 **71**: R_1 =OCH_3; R_2,R_3,R_4,R_5= H, wogonin **72**: R_1, R_2= H; R_3,R_4,R_5=OH, fisetin **73**: R_1=OH; R_2,R_3,R_4,R_5=H, nor-wogonin	wogonin : -Increase levels of ROS -Decrease ΔΨm -Increase caspases-3,-9 and -8 activities -Increase Bax expression -Increase Bad expression -Increase *cit c* release -Increase Fas/CD95 ,In U-2 OS -increase TRAIL-R2 expression, in ATL cells -Increase levels of ROS -Cleavage of PARP -Increase caspase-3 activity, in HL-60 cells -Cleavage of PARP -Increase caspase-3 activity, in SK-HEP-1 cells nor- wogonin: -Increase levels of ROS -Cleavage of PARP -Increase caspase-3 activity, in HL-60 cells Fisetin: Cleavage of PARP -Increase caspase-3 activity, in SK-HEP-1 cells	111-114

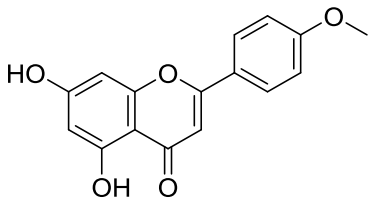 **74**: acacetin	-Induce caspases-3,-8 and -9 activities -Increase FADD expression -Increase FAF1 expression -Increase Apaf-1 expression -Increase cit c expression -Increase Bax expression -Decrease Bcl-2 expression, in human T cell leukemia Jurkat cells -Decrease Bcl-2 expression -Decrease ΔΨm -Increase levels of ROS -Activation of the SAPK/JNK1/2 and c-JUN -Activation of caspase-7 and -8, in MCF-7 cells -Cleavage of PARP -Decrease ΔΨm -Increase levels of ROS -Increase *cit c* release -Increase Bax expression -Increase p53 expression -Increase Fas expression -Increase Bad expression -Decrease Bcl-2 expression -Increase caspase-3 activity, in AGS cells	115 116,117
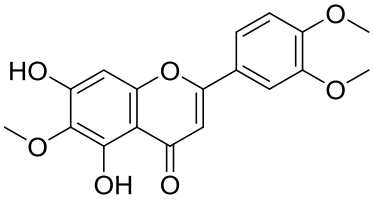 **75**: eupatilin	-Decrese Bcl-2 expression -Increase Bax expression -Cleavage of PARP -Cleavage of caspase-3 -Decrease ΔΨm , in AGS cells	118
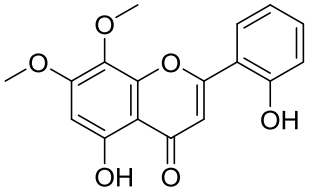 **76**: Skullcapflavone I	-Cleavage of PARP -Increase caspases-3 and -9 activities, in T-HSC/Cl-6 cells	119

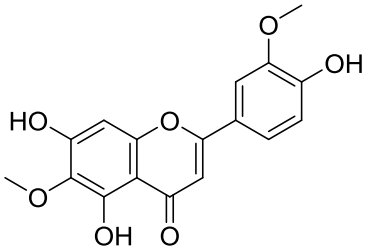 **77:** jaceosidin	-Increase levels of ROS -Cleavage of PARP -Decrease Bcl-2 expression -Increase Bax expression -Increase p53 expression -Inhibition of the ERK pathway, in MCF10A-ras cells	120
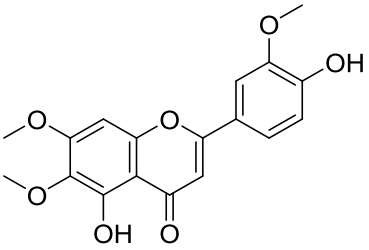 **78:** cirsilineol	-Decrease $\Delta\Psi m$ -Increase *cit c* release -Cleavage of PARP -Increase caspase-3 and -9 activities, in CAov-3 cells	121
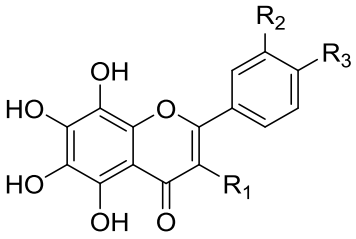 **79:** R_1=H,R_2=OMe,R_3=OMe, 5HPMF **80:** R_1,R_2,R_3=OMe, 5HHMF **81:** R_1=H,R_2=H,R_3=OMe, 5HTMF	-5HPMF induces cell cycle arrest in G2/M in HCT116 and HT29 cells -Cell cycle arrest in G0/G1 phase -Decrease Mcl-1 expression -Cleavage of PARP -Decrease iNOS expression -Decrease COX-2 expression, in H1299 cells -5HTMF induces cell cycle arrest in G0/G1 phase -Decrease Mcl-1 level, in HCT116, HT29 and H1299 cells -Decrease Mcl-1 expression -Cleavage of PARP -Decrease iNOS expression -Decrease COX-2 expression, in H1299 cells - 5HTMF induces cell cycle arrest in G2/M phase -Increase p53 expression -Increase Bax ecpression -Decrease cdc-2 (cdk1) and cyclin B1 expression -Increase p21 expression -Cleavage of PARP, in human nonsmall cell lung cancer (H460,H1299 and A549) cells -Increase Bax expression, in H460 and A549 cells	122-124

	-Increase caspases-3 activity -Cleavage of PARP, in H460, H1299 and A549 cells -5HHMF increase Fas expression -Increase FasL expression -Increase FADD expression -Increase TRADD expression -Increase DR4 expression -Increase caspases-3,-9 and -8 activities -Cleavage of PARP ,in AGS cells	
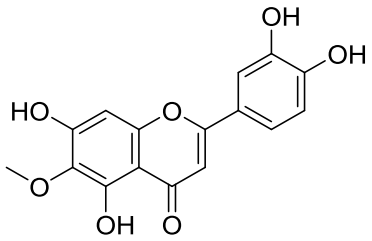 **82:** eupafolin	-Decrease ΔΨm -Increase *cit c* release -Activation caspases-3,-6,-7,-8 and -9 -Decrease Bcl-2 expression -Increase tBid expression, in HeLa cells	125
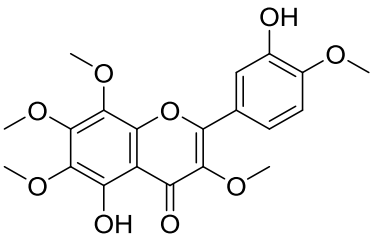 **83**:5,3'-dihydroxy-3,6,7,8,4'-pentamethoxyflavone (DH-PMF)	-Decrease XIAP expression -Decrease cFLIP expression -Decrease Mcl-1 expression -Decrease Bcl-2 expression -Decrease Bcl-Xl expression -Increase Bax expression -Processing procaspase -3, -8 and -9 -Cleavage of PARP -Arrest cell cycle in G2/M phase -Increase p21 expression -Inhibit AKT activity, in human myeloid KBM-5 cells	126
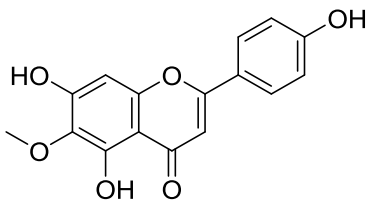 **84:** hispidulin	-Activation of MAPK -Decrease Mcl-1 expression -Cleavage of PARP, in SKOV3 cells -Decrease ΔΨm -Increase ROS level -Increase *cit c* release -Inhibit Akt activation -Cleavage of PARP -Decrease bcl-2 expression	127,128

	-Increase bax expression -Increase caspase-3 activity, in HepG2 cells	
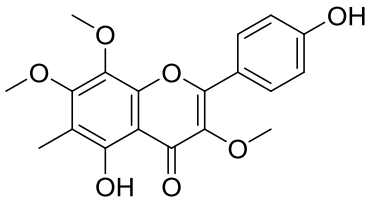 **85**: 5,4'-dihydroxy-3,7,8-trimethoxy-6-c-methylflavone (PD1)	-Decrease $\Delta\Psi m$ -Increase *cit c* release -Activation of caspase-3, in HL-60 human leukaemia cell line	129
Other		
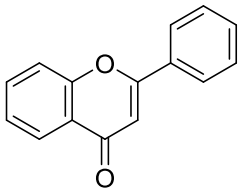 **86**: flavone	-Decrease NF-kB expression -Decrease COX-2 expression -Increase p21 expression -Increase Bak expression -Decrease bcl-X_L expression -Increase caspase-3 activity, in HT-29 cells -Increase levels of ROS -Increase p21 expression -Cleavage of PARP -Increase caspase-3 activity, in HT-29, COLO-205 and COLO-320-HSR cells -Arrest cell cycle in G2/M phase -Decrease bcl-2 expression -Increase caspase-2,-3,-8,-9 and -10 activities, in HCT-116 cells	130-132
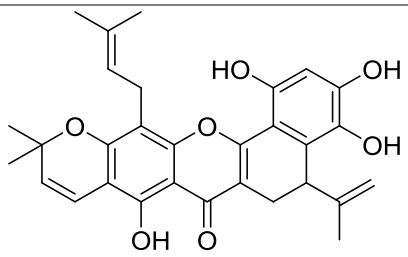 **87**: artonin B	-Decrease $\Delta\Psi m$ -Increase *cit c* release -Decrease Bcl-2 expression -Increase Bax expressiom -Increase Bak expression -Increase caspase-3 activity, in CCRF-CEM cells	133

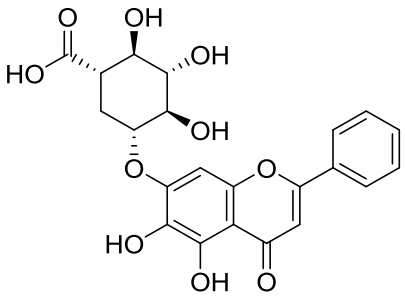 **88:** baicalin	-Increase levels of ROS -Increase activities of caspases-3,-8 and-9, in SW620 cells -Cleavage of PARP -Activation of caspases-3 and-9, in CA46 Burkitt lymphoma cells	134,135
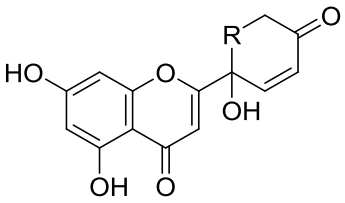 **89**: R= CH, protoapigenone **90**: R= COH, DEDC	-Decrease ΔΨm -Decrease Bcl-2 expression -Decrease Bcl-xL expression -Increase levels of ROS -Activation of caspases-3 and -9 -Cleavage of PARP ,in MDA-MB-231 cells -Decrease Bcl-2 expression -Decrease Bcl-xL expression -Cleavage of PARP -Increase caspase-3 activity, in SKOV3 cells -Arrest cell cycle in S and G2/M phases, in SKOV3 and MDAH-2774 cells -Cleavage of PARP -Increase caspase-3 activity -Activation of ERK and JNK ½ -Arrest cell cycle in S and G2/M phases, in LNCap cells -Decrease ΔΨm -Reduce Bcl-2 expression -Increase *cit c* release -Activation of caspases-3,-8 and -9 -Stimulated phosphorylation of JNK and p38, in HepG2 cells	136-139
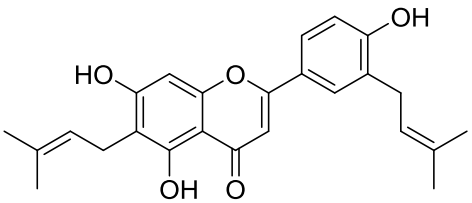 **91**: gancaonin	-Activation of caspase-3 and -7, in CCRF-CEM cells	140

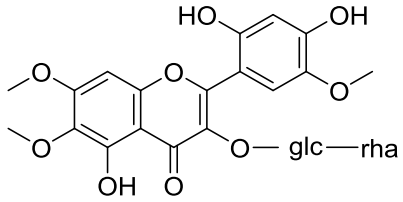 **92**: 5,2´,4´-trihydroxy-6,7,5´ trimethoxyflavone (TTF1)	-Decrease Bcl-2 expression -Increase Bax expression -Increase *cit c* release -Increase caspases-3 and -9 expression ,in HepG-2 cells	141
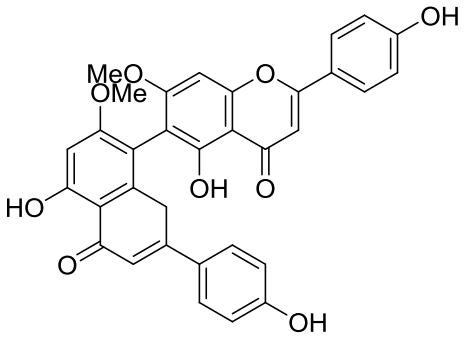 **93**: 7,7''-dimethoxyagastisflavone	-Increase activity of caspase-3 -Decrease ΔΨm, in HT-29 cells	142
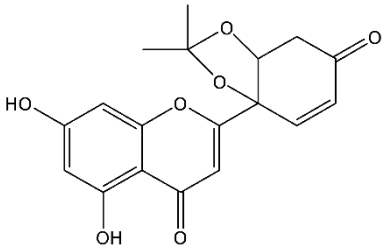 **94:** DICO	-Decrease ΔΨm -Cleavage of PARP -Activation of caspases-3 and -9 -Increase Bax expression -Decrease Blc-2 expression -Increase *cit c* release -Arrest cell cycle in G2/M phase, in HepG2 cells	143
Synthetic Flavones and Flavonols		
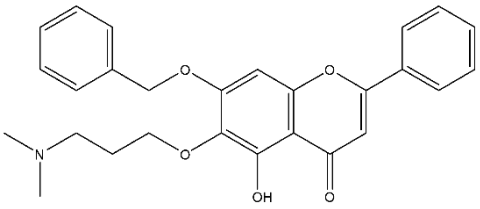 **95**: HQS-3	-Increase Bax expression -Decrease Blc-2 expression -Cleavage of PARP -Increase levels of ROS, in HepG2 cells	144
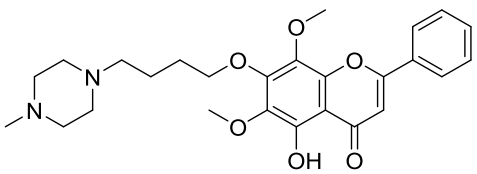 **96:** LYG-202	-Cleavage of PARP -Activation of caspase-3,-8,-9 -Decrease Bcl-2 expression -Increase Bax expression, in S180 and HCT-116 cells -Increase TNF-α activity -Increase caspases-3,-9 and -8 activities -Cleavage of PARP -Cleavage Bid, in HepG2 cells	145-147

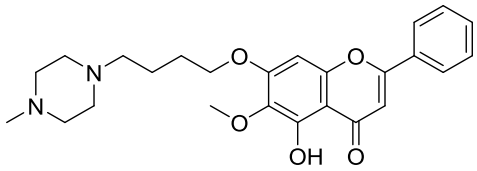 **97:** DHF-18	-Decrease ΔΨm -Increase ROS levels -Increase TNF-R1 -Increase Bid, HepG2 cells	148
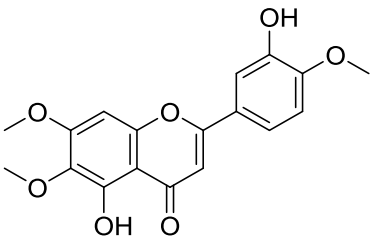 **98**: eupatorin	-Processing and increase caspase-3,-6,-7 -9 and -8 activities -Cleavage of PARP -Increase *cit c* release -Increase AIF release -Increase Smac/ DIABLO release -Decrease Bcl-2 expression or cleavage Bcl-2 -Arrest cell cycle in G2/M phase, in HL-60, U937 and Molt-3 cells -Activation of ERK and JNK, in HL-60 cells -Increase ROS level, in HL-60 and Molt-3 cells	149
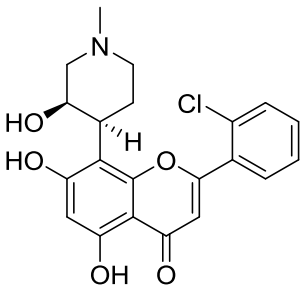 **99**: flavopiridol	-Increase caspase-3 and -8 expression -Increase p53 expression -Arrest cell cycle in G0/G1 and G2/M phase, in CD133^{+high}/ CD44^{+high} prostate CSCs -Inhibits iNOS expression -Cleavage of PARP -Increase caspase-3 activity, in CLL	150,151
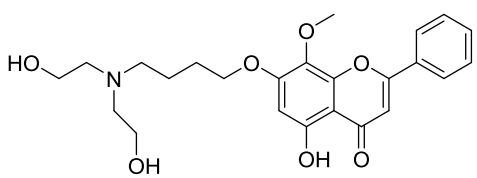 **100**:V8	-Increase levels of ROS -Decrease ΔΨm -Increase *cit c* release -Decrease Bcl-2 expression -Increase BH-3 expression -Increase Bax expression -Processing procaspase-3 and -9, in HepG2 cells	152

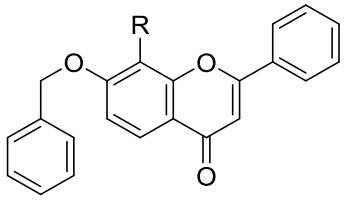 **101:** R=$(CH_2)_5N(CH_2CH_3)_2$ LW-214	-Cleavage of PARP -Increase ROS level -Activation of ASK, in MCF-7 cells	153
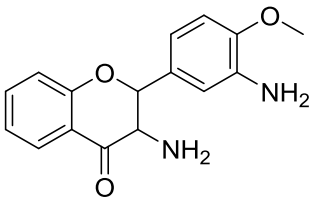 **102**:3,3´-diamino-4´-methoxyflavone(DD1)	-Recruitment of mitochondria -Increase Bax expression -Decrease Bad expression -Activation of caspases-8,-9 and -3 -Cleavage of PARP, in Acute myeloid leukemia (monoblast U937)	154
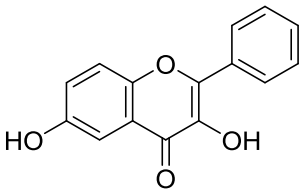 **103**: 3,6-dihydroxyflavone	-Increase ROS level -Cleavage of PARP -Decrease ΔΨm, in leukemia HL-60 cells	155
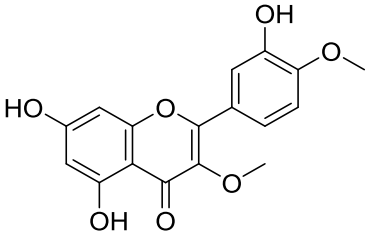 **104**: 5,7,3'-trihydroxy-3,4' dimethoxyflavone (THDF)	-Arrest cell cycle in G2/M phase -Increase *cit c* release -Cleavage of PARP -Processing of caspase-3,-6,-7 and -9 -Inhibition ERK and JNK, in HL-60 and U937 cells	156
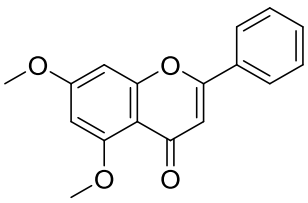 **105**: 5,7-dimethoxyflavone	-Decrease Bcl-xL expression -Increase Bax expression -Increase caspase-3 expression, in HCC cells	157

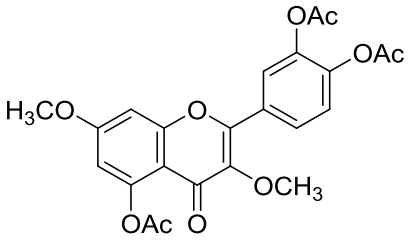 **106**: ayanin diacetate	-Decrease ΔΨm -Increase *cit c* release -Cleavage of PARP -Increase caspase-8 and -9 activities -Decrease Bcl-X_L expression -Cleavage of Bid, in leukemia cells	158
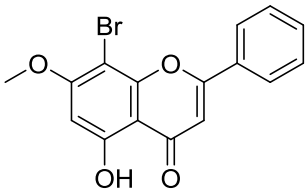 **107**: 8-bromo-7-methoxychrysin	-Arrest cell cycle in G1 phase, in HepG2 and Bel-7402 cells -Increase caspase-3 activity -Increase ROS level, in HepG2 cells	159
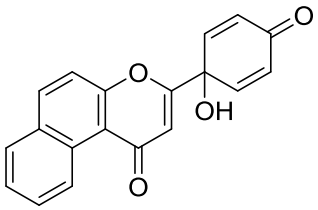 **108**:WYCO2-9	-Increase levels of ROS -Decrease ΔΨm -Activation of caspases-3 and -9 -Cleavage of PARP ,in DU145 prostate cancer cells	160
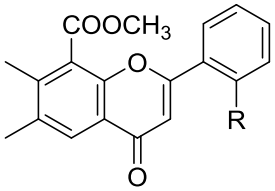 **109:** R=Cl, methyl 2-(2-chlorophenyl)-6,7-dimethyl-4-oxo-4H-chromene-8-carboxylate **110:** R=CH_3, 1 methyl 6,7-dimethyl-4-oxo-2-(o-tolyl)-4H-chromene-8-carboxylate	-Cleavage of PARP -Increase *cit c* realese -Activation of the ERK pathway, in HL-60 cells	161
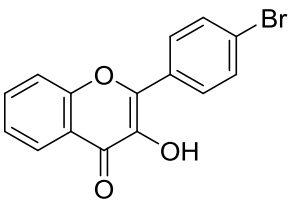 **111**: 4'-bromoflavonol	-Increase caspase-3,-6,-7 -9 and -8 activities -Increase TRAIL expression -Increase DR4 expression -Increase DR5 expression -Decrease Bid expression -Arrest cell cycle in S phase, in HL-60 cells -Decrease Bid expression, in	162

	Molt-3 cells -Increase caspase-3,-6-7,-8 and -9 activities -Increase TRAIL expression -Increase DR4 expression -Increase DR5 expression -Processing of Bid -Arrest cell cycle in S phase, in U937 cells	
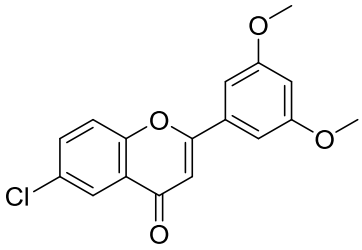 **112**:6-chloro-2-(3,5-dimethoxyphenyl)-4H-chromen-4-one	-Increase caspases-8 and -9 activities -Increase Bax expression -Decrease bcl-2 expression, in HepG-2 cells	163
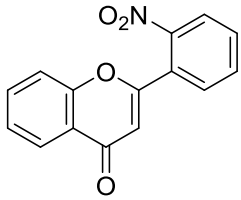 **113:** 2´-Nitroflavone	-Increase TRAIL expression -Increase DR5 expression -Increase Bax expression -Increase *cit c* release -Induction cell cycle arrest in G2/M phase -Activation of p38 and JNK, -Decrease ERK, in HL-60 cells -Increase Bax expression -Increase Fas expression -Increase caspase-3, -8 and-9 activities -Increase *cit c* release -Increase Bax expression -Decrease Bcl-2 expression -Decrease Bcl-Xl expression, in LM3 murine mammary adenocarcinoma cells -Decrease Bcl-xl expression -Increase Bax expression -Increase Fas expression -Increase Fas-L expression -Increase *cit c* release -Increase caspase-3,-8 and -9 activities, in HeLa human cervical carcinoma cells	164-166

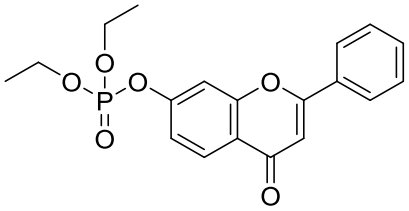 **114**:diethyl flavon-7-yl phosphate (FP)	-Cleavage of PARP -Increase caspase-3 activity, in HeLa cells	167

(PARP= poly (ADP-ribose) polymerase; ASK-1=apoptosis signal regulating kinase 1; ROS= reactive oxygen species; *cit c*=cytochrome c; ΔΨm= variation of the membrane potential; MARK=mitogen-activated protein kinases; ERK=extracellular-regulated kinase; JNK=c-Jun N-terminal kinase; NF-R= tumor necrosis factor receptor; TRAIL-R=TNF-related apoptosis-inducing ligand receptor; Mcl-1=anti-apoptotic BCL-2 protein)

As described in **Table 3**, most flavonoids that significantly induce apoptosis in tumor cells are not direct activators of caspase family proteins, but interfere with other targets related to the intrinsic or extrinsic apoptosis pathways and consequently, increase the caspases expression or levels in tumor cell lines. In fact, the reports about the direct activation of caspases by flavonoids are rare. Recently, in 2014 two activators of caspase-7 (**1** and **2**, **Figure 1**, pag 4) were discovered by Pereira *et al.* (2014). Compounds **1** and **2** are two prenylated derivatives of baicalein (**B**, **Figure 37**) and 3,7-dihydroxyflavone (**H**, **Figure 37**), two natural flavonoids that have shown to be potent inhibitors of tumor cell lines, being this effect attributed at least in part to an apoptotic response.[168-170] Moreover, it was demonstrated that the introduction of prenyl side chains on baicalein (**B**) and 3,7-dihydroxyflavone (**H**) was associated with an increase of their human tumor cell lines growth inhibitory activity.[171]

In this work, innovative assays using *Saccharomyces cerevisiae* individually expressing human caspases-3, -7 or procaspases -3, -7 were developed for screening assays. The validation of this model was accomplished by testing the effect of the known activator of caspase-3 and -7, PAC-1 (**35**, pag 29).[172]

For development of yeast growth-inhibition assays, initially it has been found that the expression of human procaspases-3 and -7 have no effect on cell growth. While the expression of the cleavaged caspases-3 and -7 have a marked effect on cell growth. The relation between this effect and the expression of these human proteins was confirmed by Western Blot analysis.[173,174] It was also found that PAC-1 induced growth inhibition in

yeast cells expressing procaspases-3 and -7 and caspases-3 and -7. These results indicated that PAC-1 was able to activate these caspases, as well as their inactive zymogens, in this model.

Using the same model, flavonoids **1** and **2** also induced procaspase-7-mediated growth inhibition and increase the caspase-7-induced growth inhibition. Nevertheless, no effect on yeast expressing procaspase-3 and caspase-3 were observed with these compounds. These results suggested that, in opposition to PAC-1, flavonoids **1** and **2** were selective activators of caspase-7. *In vitro* processing assays confirmed that both flavonoids **1** and **2** directly processed procaspase-7 to the active caspase-7.[175]

The effect of these flavonoids was also evaluated in HL-60 and MCF-7 human tumor cell lines. HL-60 is an acute promyelocytic leukemia cell line expressing both caspases-3 and -7, while MCF-7 is a breast adenocarcinoma cell line that only expresses caspase-7. The results reveled that both flavonoids inhibit the growth of the two cell lines with a similar GI_{50}, confirming an effect independent of caspase-3.

Considering the structure of flavonoids **1** and **2**, and their building blocks, as no activity was observed for compound **2**, it was suggested that the presence of the 7-prenyl group of flavonoid **1** seems to be associated with selectivity of this flavonoid to caspase-7, and the presence of the 7-geranyl of flavonoid **2** seems to be associated with the caspase-7 activation.

Chapter 3:

Results and Discussion

3.1. Chemistry

Analogues of the prenylflavonoids **FP2** (**1**) and **FP11** (**2**) were synthesized by molecular modification of three natural flavonoids: baicalein (**B**), 3,7-dihydroxyflavone (**H**) and chrysin (**C**) (**Figure 37**).

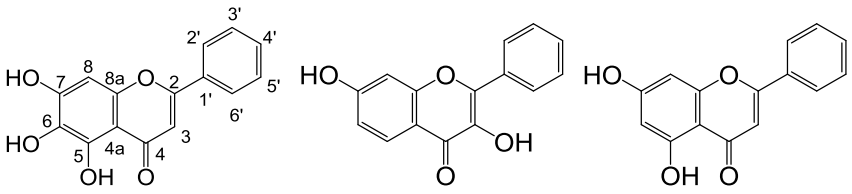

(B) **(H)** **(C)**

Figure 37: Natural flavonoids used as building blocks for molecular modification.

Since baicalein (**B**) and 3,7-dihydroxyflavone (**H**) were the precursors of **FP2** and **FP11**, both natural flavones were chosen as building blocks. Additionally, these natural compounds have already demonstrated to have antitumor activity in human tumor cell lines, which seems to be related to the interference with caspases-dependent pathways.[168,176,177] Similarly, the antitumor activity of chrysin (**C**) has also been described[178], as well as its capacity to induce apoptosis through caspases-dependent pathways[84,179] and the interference with other molecules involved in the apoptotic cascade.[180] Moreover, considering the similarity of the substitution pattern on A ring between, baicalein (**B**), 3,7-dihydroxyflavone (**H**), and chrysin (**C**), the molecular modification of these three building blocks and the study of their caspase modulatory activity will allow to study the influence of the ring-A substitution pattern, namely the hydroxylation pattern, on the caspase modulatory activity.

The molecular modification follow the alkylation of the natural flavonoids using alkylating agents possessing 1-5 carbon atoms, including linear (methyl, ethyl, propyl, allyl, butyl) and branched chains (isopentyl and prenyl) with or without unsaturation, aiming to allow SAR Studies.

The synthesis of the alkylated derivatives followed nucleophilic substitution reactions of the building blocks with alkyl halide in alkaline medium.

3.1.1. Synthesis

3.1.1.1. Optimization of baicalein alkylation

Previous studies revealed that the direct alkylation with prenyl and geranyl bromide of baicalein (**B**) gave a mixture of the mono- and dialkylated derivatives, as well as the building block.[171] In addition, it has been demonstrated that the 7-monoprenylated derivatives were potent inhibitors of human tumor cell lines, in opposite to the 6,7-diprenylated derivatives, being this effect related, at least in part, to the activation of caspase-7.[175] Although no antiproliferative activity have been found for these 6,7-diprenylated derivatives, other 6,7- modified baicalein derivatives have reveal interesting antitumor activity.[181,182] Moreover, several structure related flavones possessing a similar substitution pattern in A ring (hydroxyl group in C-5 and alkyloxy groups in C-6 and C-7) revealed to be potent inhibitors of human tumor cell lines. For example, among the flavones listed in **Table 3** (pag 46, 50 and 51), compounds **78**, **92**, **95**, **97** and **98** showed pro-apoptotic effect by modulating different key targets involved in apoptotic pathways, including caspase family proteins. Therefore, the direct alkylation of this building block was investigated by HPLC-DAD to determine the more suitable amount of alkyl halide necessary to obtain mainly the monoalkylated derivative but also some amount of the dialkylated derivative, to be used in the biological assays. Since it would be difficult to perform this study for all alkylating agents, it was decided to optimize the conditions for the longest and branched chain without unsaturation (isopentyl iodide).

3.1.1.1.1. Optimization of chromatographic conditions

Baicalein mono- (**Biso1**) and diisopentyl- (**Biso2**) derivatives were synthesized as described in **Figure 38** and after their purification and characterization by IR and NMR, were used as standards for the HPLC-DAD study.

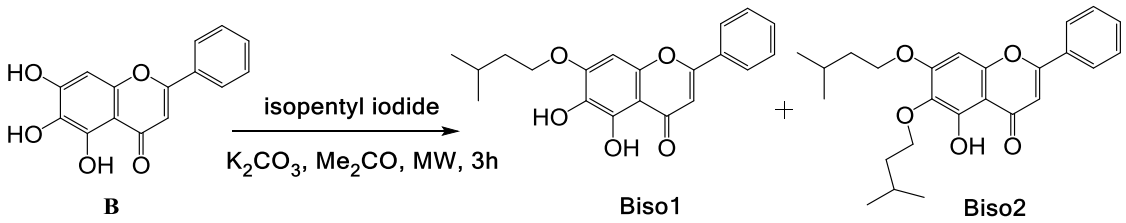

Figure 38: Synthesis of alkylated derivatives of Baicalein (**B**).

Firstly, the chromatographic conditions to quantify **Biso1** and **Biso2** as well as baicalein in the reaction mixture were established. To fullfil this, a mixture of these compounds was analized by HPLC-DAD on C18 HPLC column using several mixtures of MeOH:H_2O:$MeCO_2H$ as mobile phase. As shown in **Figure 39** the mixture MeOH:H_2O:$MeCO_2H$ (95:5:1 v/v/v) allowed to obtain the suitable chromatographic conditions to quantify the major constituents of the reaction with a good resolution (**Figure 39**).

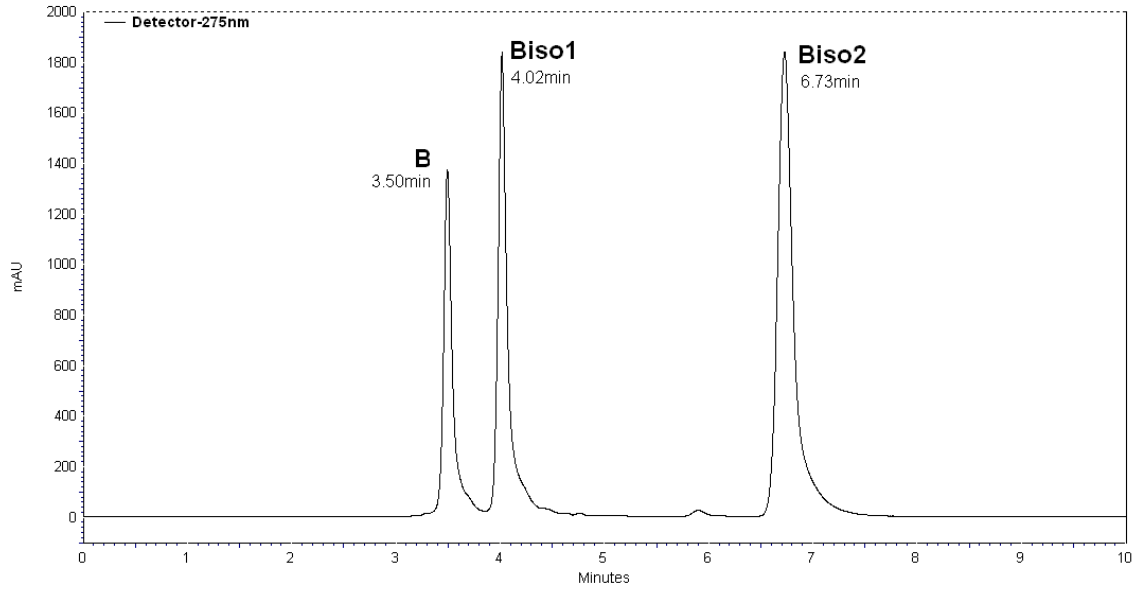

Figure 39: HPLC-DAD chromatogram of a mixture of baicalein (**B**) 5,6-dihydroxy-7-(isopentyloxy)-2-phenyl-4H-chromen-4-one (**Biso1**) and 5-hydroxy-6,7-bis(isopentyloxy)-2-phenyl-4H-chromen-4-one (**Biso2**) at 275 nm with MeOH:H_2O:$MeCO_2H$ (95:5:1 v/v/v) as mobile phase.

However, after the injection of the crude product it was found that the reaction mixture was extremely complex and the peaks of baicalein (**B**) and **Biso1** were overleaped with the peaks of other products, being not possible to quantify baicalein (**B**) and **Biso1** using this chromatographic conditions (**Figure 40 A**).

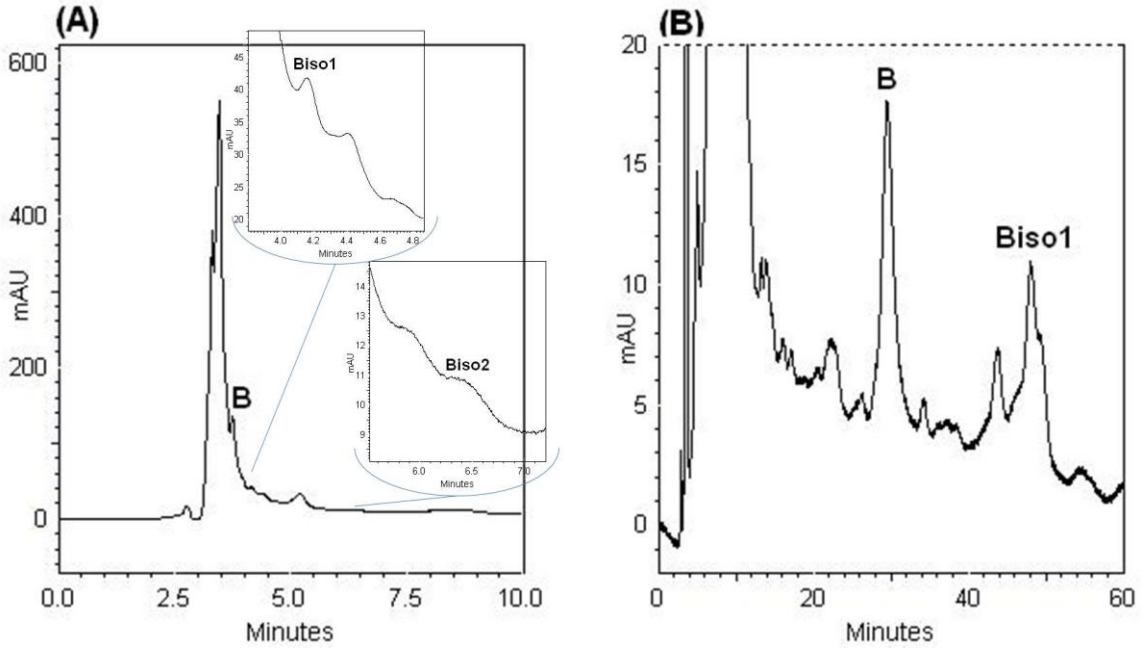

Figure 40: HPLC-DAD chromatograms at 275 nm of the reaction mixture with isopentyl iodide, with **(A)** MeOH:H2O:MeCO2H (95:5:1 v/v/v) and **(B)** MeOH:H2O:MeCO2H (50:50:1 v/v/v) as mobile phase.

Consequently, a new optimization was required for the chromatographic conditions to quantify baicalein (**B**) and **Biso1**. After some attempts, the mixture MeOH:H_2O:$MeCO_2H$ (50:50:1 v/v/v) was considered the best mobile phase for these quantifications (**Figure 40 B**). Therefore, the quantification of **B** and **Biso 1** in the reaction mixture was performed by isocratic elution using a mixture of MeOH:H_2O:$MeCO_2H$ (50:50:1 v/v/v) and the quantification of **Biso2** was achieved by isocratic elution using a mixture of MeOH:H_2O:$MeCO_2H$ (95:5:1 v/v/v).

3.1.1.1.2. Optimization of reaction time

After the optimization of chromatographic conditions, six alkylation reactions of baicalein with isopentyl iodide were performed by MAOS with different irradiation times, as described in section 5.1.1.2.2., and their reaction mixtures were analyzed by HPLC-DAD in order to optimize the reaction time (**Table 4**).

Table 4: Alkylation of baicalein (**B**) with isopentyl iodide with different reaction times.

Reaction time	baicalein (%)	Biso1 (%)	Biso2 (%)
10 min	51.98	26.75	0
20 min	22.83	21.13	0.97
30 min	8.97	18.72	0.97
40 min	8.88	15.83	1.41
50 min	8.79	9.32	4.98
60 min	8.72	5.92	0.53

Comparing the results presented in **Table 4** it was found that the best reaction time for obtaining **Biso1** was 10 min. However, **Biso2** were not detected by HPLC and only half of the starting material was consumed. For reaction times longer than 20 minutes, although more starting material was consumed, a decreased of the amount of **Biso1** and an increase of **Biso2** was detected. This results suggested that **Biso1** was converted into **Biso2**. When using a reaction time of 60 minutes the **Biso1** and **Biso2** yields decreases drastically, even though the amount of baicalein remains the same, being observed the formation of several undesirable by-products. Thus, it was concluded that the reaction time of 20 minutes was the more suitable for obtaining mainly the monoalkylated derivative and also some amount of the dialkylated derivative, to be used in the biological assays.

3.1.1.1.3 Optimization of the amount of alkylating agent

After optimizing the reaction time, the effect of increasing amounts of isopentyl iodide in the presence of the same amount of K_2CO_3 for the alkylation of baicalein after 20 min of MW irradiation was studied (**Table 5**).

Table 5: Alkylation of baicalein with different quantities of isopentyl iodide.

Conditions	0.8 equiv.[a]	1.2 equiv. [a]	1.6 equiv. [a]	2 equiv. [a]
Baicalein[b]	6.24	5.98	n.d.	n.d.
Biso1[b]	22.33	24.61	21.13	7.84
Biso2[b]	0	0	0.97	1.27

n.d.: trace quantities were detected but not determined

[a] 1 equiv. is defined as the stoichiometric amount of isopentyl iodide in the presence of 5 equiv of K_2CO_3.

[b] Yield determined assuming a similar molar extinction coefficient for all the compounds.

According to **Table 5** the reaction with 0.8 and 1.2 equiv. of isopentyl iodide provided the formation of the monoalkylated derivative (**Biso1**), without the formation of the dialkylated flavone (**Biso2**). The use of 1.2 equiv. leaded to a higher yield of **Biso1** and a higher consumption of baicalein (**B**) than when 0.8 equiv. were used.

The use of 1.6 equiv. of isopentyl iodide provides a mixture of mono- and di-alkylated products (**Biso1** and **Biso2**), with a yield of 21.13 % and 0.37 %, respectively. The quantification of the starting material was not possible since only trace amounts were detected and by-products have been formed with similar polarity.

The relative yield of mono- and dialkylated products were different when 2 equiv. of isopentyl iodide were used. It was found a decrease in the yield of monoalkylated derivative and an increase of the yield of the dialkylated product (7.84% and 1.27%, respectively). In addition, once again only trace amounts of baicalein were detected. These results suggested that the dialkylated derivative was obtained by the alkylation of the monoalkylated derivative.

Therefore, it was concluded that the optimal experimental conditions for achieving the objective proposed above would be 1.6 equivalents of isopentyl iodide for a 20 minutes reaction. These conditions have become the reference for all the synthesis described in this work, with the different alkylating agents, both for baicalein (**B**), 3,7-dihydroxyflavone (**H**) and chrysin (**C**), taking into account the scale-up conditions.

3.1.1.2. Derivatives of baicalein

The synthetic approach used for the synthesis of alkylated derivatives of baicalein was based on the reaction of baicalein with 1.6 equivalent of the alkylating agent, namely, isopentyl, butyl, propyl, allyl, ethyl, or methyl iodide, in presence of anhydrous potassium carbonate using MAOS methodology. **Table 6** summarizes the reaction conditions and the results obtained in the synthesis of baicalein alkyl-derivatives.

Table 6: General conditions for the synthesis of alkylated derivatives of baicalein (**B**).

Building block	Reaction conditions	Product	Yield
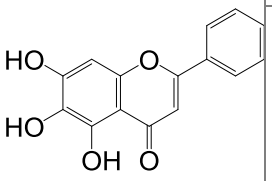 **B**	isopentyl iodide, K_2CO_3, Me_2CO, 3 h	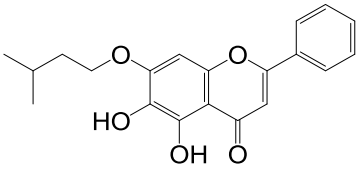 **Biso1**	5.6%
		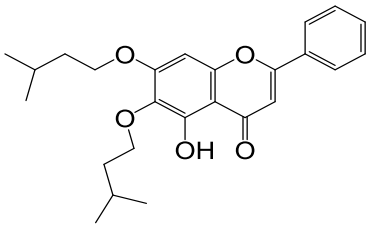 **Biso2**	0.6%
	Butyl iodide, K_2CO_3, Me_2CO, 2 h	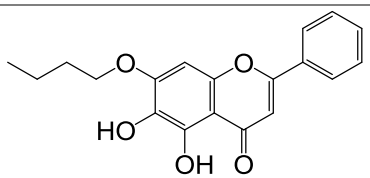 **Butil1**	5.7%
		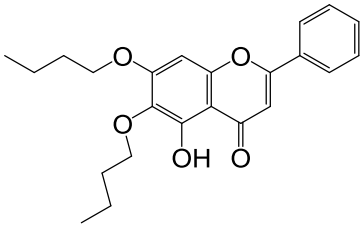 **Butil2**	0.5%
	propyl iodide, K_2CO_3, Me_2CO, 2 h	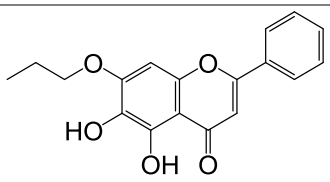 **Brop1**	6.0%

		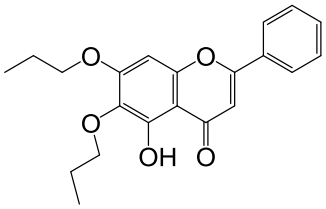 **Brop2**	3.5%
	allyl iodide, K_2CO_3, Me_2CO, 2 h	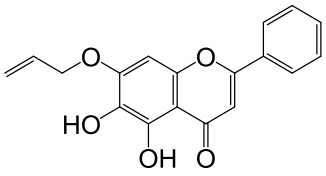 **Bali1**	4.2%
		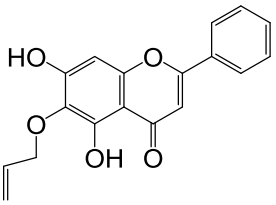 **Bali1'**	1.1%
	ethyl iodide, K_2CO_3, Me_2CO, 2 h	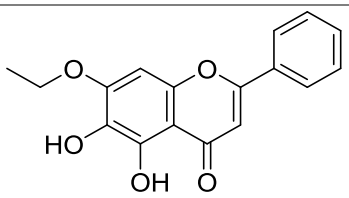 **Betil1**	4.5%
	methyl iodide, K_2CO_3, Me_2CO, 2 h	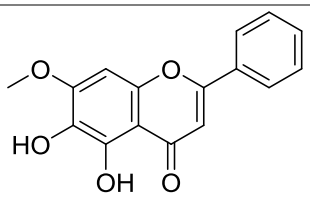 **Bemet 1**	15%
		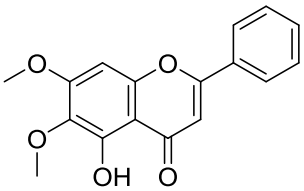 **Bemet 2**	1.5%

For almost all these reactions two alkylated derivatives were obtained. The major products were those with one alkyl side chain on the oxygen at position 7 (**Biso1**, **Butil1**, **Brop1**, **Bali1**, **Betil1** and **Bemet1**), being the products with two alkyloxy side chains on C-6 and C-7 (**Biso2**, **Butil2**, **Brop2** and **Bemet2**) obtained as by-products. The higher yields obtained for monoalkylated derivatives in comparison with the yields obtained for dialkylated derivatives are in accordance with the results obtained in the HPLC studies in

section 3.1.1.1. and suggest that the first hydroxyl group to be alkylated is that on the *para* position to the carbonyl group (C7).

However, the reaction of the baicalein with allyl iodide is one exception. The products of this reaction are two monoalkylated derivatives with one alkylated side chain on the oxygen at position 7 (**Bali1**) and one at position 6 (**Bali1'**). Once more by comparing the yields, it is suggested that the hydroxyl group at position 7 was the first to be alkylated.

For all reactions the obtained yields were low (0.5-15%), being this explained by the fact of the reactions were incompleted and the formation in considerable amounts of more than one product, as illustrated in **Figure 40** in section 3.1.1.1.

3.1.1.3. Derivatives of 3,7-dihydroxyflavone

The alkylated derivatives were obtained by the MW irradiation of 3,7-dihydroxyflavone with 1.6 eq. of the alkylating agent (isopentyl, butyl, propyl, allyl, ethyl, and methyl iodide) or 2 eq. prenyl bromide in presence of anhydrous potassium carbonate. **Table 7** summarizes the reaction conditions and the results obtained in the synthesis of 3,7-dihydroxyflavone alkyl-derivatives.

Table 7: General conditions for the synthesis of alkylated derivatives of 3,7-dihydroxyflavone (**H**).

Building block	Reaction conditions	Product	Yield
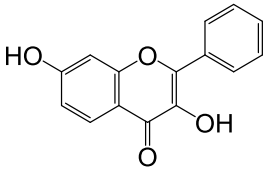 **H**	isopentyl iodide, K_2CO_3, Me_2CO, 2 h	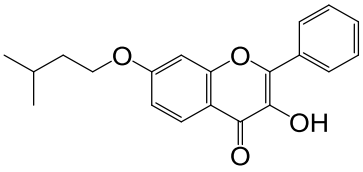 **Hiso**	12.9%
	butyl iodide, K_2CO_3, Me_2CO, 2 h	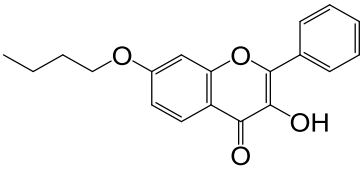 **Hutil 1**	9.7%
		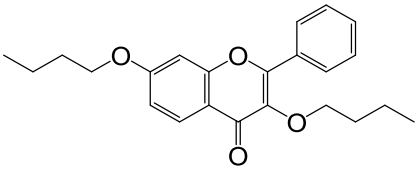 **Hutil 2**	7.1%
	propyl iodide, K_2CO_3, Me_2CO, 2 h	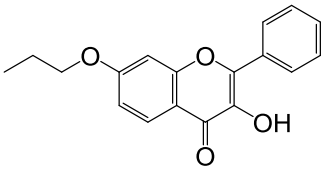 **Hrop**	3.7%
	allyl iodide, K_2CO_3, Me_2CO, 2 h	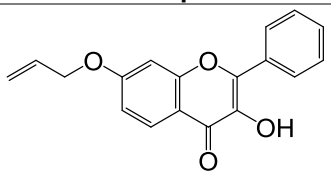 **Hali**	9.3%
	ethyl iodide, K_2CO_3, Me_2CO, 2 h	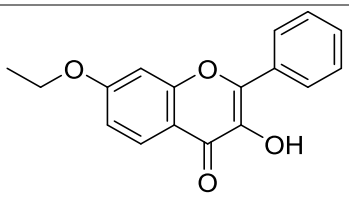 **Hetil**	1.7%
	methyl iodide, K_2CO_3, Me_2CO, 2 h	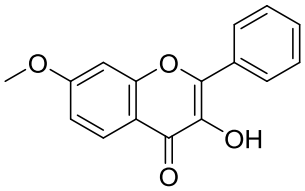 **Hemet**	9.2%
	prenyl bromide, KI, K_2CO_3, Me_2CO, 2 h	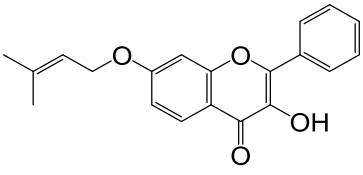 **Hrep**	7.4%

With this building block only the monoalkylated derivatives (**Hiso**, **Hutil1**, **Hrop**, **Hali**, **Hetil**, **Hemet** and **Hrep**) have been isolated, except for the reaction with butyl iodide, for which the dialkylated derivative (**Hutil2**) was also obtained. In fact, for all reactions although two derivatives were detected by TLC in the crude product, successive attempts of purification of the dialkylated derivatives by several methods (flash column chromatography, thin layer chromatography and crystallization) have failed to isolate the dialkylated derivatives.

As already referred for the reactions with baicalein, the yield obtained for the monoalkylated derivative **Hutil1** was slightly higher than the yield obtained for the dialkylated derivative **Hutil2**, suggesting that the hydroxyl group on the *para* position to the carbonyl group (C7) is the first to be alkylated.

Incomplete reactions associated with the time consuming work-up procedure which involved column and preparative thin layer chromatography followed by crystallization justify the low yields of these reactions (1.7-12.9%).

3.2.1.4. Derivatives of chrysin

The synthetic approach used for the synthesis of alkylated derivatives was based on the reaction of chrysin (**C**) with 1.6 eq. of the isopentyl, butyl, propyl, allyl, ethyl, and methyl iodide or 2 eq. of the prenyl bromide in presence of anhydrous potassium carbonate using MAOS methodology. **Table 8** summarizes the reaction conditions and the results obtained in the synthesis of chrysin alkyl-derivatives.

Table 8: General conditions for the synthesis of alkylated derivatives of Chrysin (**C**).

Building block	Reaction conditions	Product	Yield
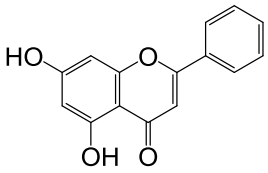 **C**	isopentyl iodide, K_2CO_3, Me_2CO, 1.5 h	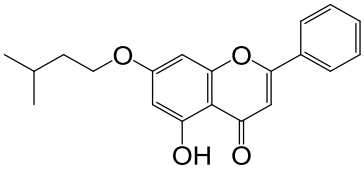 **Ciso**	30%
	butyl iodide, K_2CO_3, Me_2CO, 1.5 h	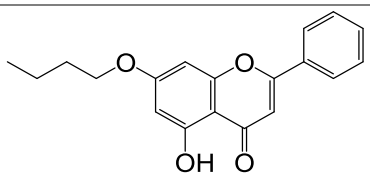 **Cutil**	29%
	propyl iodide, K_2CO_3, Me_2CO, 1.5 h	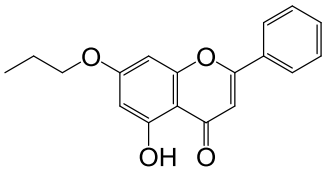 **Crop**	22%
	allyl iodide, K_2CO_3, Me_2CO, 1.5 h	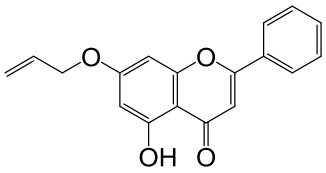 **Cali**	31%
	ethyl iodide, K_2CO_3, Me_2CO, 1.5 h	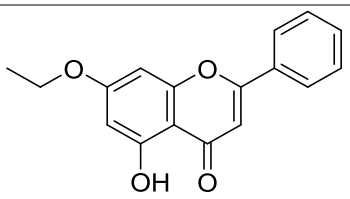 **Cetil**	32%
	methyl iodide, K_2CO_3, Me_2CO, 1.5 h	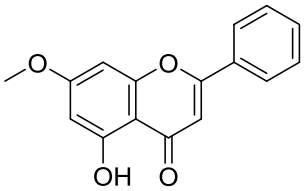 **Cemet**	44%
	prenyl bromide, KI, K_2CO_3, Me_2CO, 1.5 h	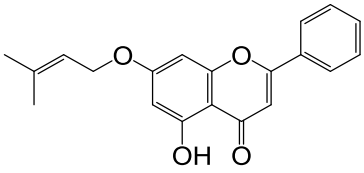 **Crep**	67 %

Unlike reactions with other building blocks, as expected, only the monoalkylated derivatives possessing the alkyloxy group linked to C-7 (**Ciso**, **Cutil**, **Crop**, **Cali**, **Cetil**, **Cemet** and **Crep**) were obtained for reactions with chrysin, being this reflected in the higher yield of these reactions (22-67%).

3.1.2. Structure elucidation

The structure elucidation of all alkylated flavonoids was established on the basis of IR, and NMR techniques. ^{13}C NMR assignments were determined by 2D heteronuclear single quantum correlation (HSQC) and heteronuclear multiple bond correlation (HMBC) experiments.

The numbering concerning the NMR assignments of alkyl groups is presented in **Table 23** and the numbering relative to the NMR assignments of flavonoid scaffolds is presented in **Figure 37**.

3.1.2.1. Derivatives of baicalein

The IR data of all baicalein derivatives were in accordance with the performed molecular modification (**Table 9**). Accordingly, this spectra revealed the presence of at least one free hydroxyl group, attending that a large band of stretching vibration between 3600–3300 cm^{-1} (hydroxyl groups) was visualized for all synthesized compounds, suggesting that the hydroxyl groups were not fully replaced. In addition, the observation of bands at 2961-2851 cm^{-1} (aliphatic C-H) on the IR spectra of baicalein derivatives, in contrast to their starting material, suggested the presence of alkyl groups.

Table 9: IR data of baicalein (**B**) and its alkylated derivatives (**Biso1**, **Biso2**, **Butil1**, **Butil2**, **Brop1**, **Brop2**, **Bali1**, **Bali1'**, **Betil1**, **Bemet1** and **Bemet2)**.

Groups	υ (cm^{-1})					
	B	**Biso1**	**Biso2**	**Butil1**	**Butil2**	**Brop1**
OH	3500-3300	3600-3300	3600-3300	3600-3300	3600-3300	3600-3300
Aliphatic C-H	-	2955 2921 2854	2957 2922 2851	2956 2923 2873	2961 2925 2851	2927 2922 2851
C=O	1651	1657	1653	1655	1657	1617
Aromatic C=C	1609 1573 1498 1462	1489 1477 1450	1559 1497 1457 1419	1502 1584 1464 1451	1497 1457 1419	1559 1489 1473 1459
C-O	1287	1115	1120	1191	1121	1125

Table 9 (contd.): IR data of baicalein (**B**) and its alkylated derivatives (**Biso1**, **Biso2**, **Butil1**, **Butil2**, **Brop1**, **Brop2**, **Bali1**, **Bali1'**, **Betil1**, **Betil2**, **Bemet1** and **Bemet2**).

Groups	υ (cm^{-1})					
	Brop2	**Bali1**	**Bali1'**	**Betil1**	**Bemet1**	**Bemet2**
OH	3600-3300	3600-3300	3600-3300	3600-3300	3600-3300	3600-3300
Aliphatic C-H	2965 2921 2851	2925 2923 2854	2925 2923 2854	2952 2922	2922	2922
C=O	1657	1663	1664	1653	1631	1634
Aromatic C=C	1499 1470 1458	1576 1489 1449	1585 1489 1451	1559 1507 1457	1467	1457
C-O	1122	1252	1115	1189	1131	1129

The ^{1}H and ^{13}C NMR data of baicalein (**B**) and alkyl-derivatives (**Biso1**, **Biso2**, **Butil1**, **Butil2**, **Brop1**, **Brop2**, **Bali1**, **Bali1'**, **Betil1**, **Bemet1** and **Bemet2**) are reported in **Table 10** and **Table 11**, respectively.

The ^{1}H NMR spectra of baicalein (**B**) derivatives showed that all of them have a non-substituted B-ring (H-2', 6': δ_H 7.91-7.87 m; H-3', 4', 5': δ_H 7.58-7.49 m) as the precursor **B**. Like the flavone **B**, ^{1}H NMR spectra of all derivatives showed a signal at δ_H 6.69-6.67 s corresponding to H-3, and a signal at δ_H 6.63-6.55 s corresponding to H-8. For most derivatives, namely **Biso2**, **Brop1**, **Brop2**, **Bali1**, **Bali1'**, **Betil1**, and **Bemet1** a hydrogen-bonded hydroxyl group at C-5 (δ_H 13.04-12.50 s) was also observed, like for the starting material **B**. Besides these, for derivatives **Biso1**, **Brop1**, **Betil1** and **Bemet1** the signal of the hydroxyl group at C6 (δ_H 5.37-5.35 s) was also observed. These data confirms that neither of these positions is substituted.

Considering **Biso1** and **Biso2** the ^{1}H NMR and ^{13}C NMR spectra showed characteristic signals of one or two isopentyl groups (δ_H: 4.18-4.06 t, 1.93-1.65 m, 1.96-1.23 m, 1.01-0.97 d; δ_C: 71.8-67.5, 38.9-37.5, 29.8-29.3, 22.7-22.6, 22.6-22.5) respectively (**Table 10** and **Table 11**). Although, the signal of the hydroxyl group at C-6 was observed for the flavone **Biso1**, the correspondent signal was not observed for the derivative **Biso2,** suggesting that the second isopentyl group should be linked to the hydroxyl group at position 6. For **Biso1** the position of the isopentyl side chain on flavone

skeleton was confirmed by the correlations observed on the HMBC spectra between the proton signals of the oxymethylene group (δ_H 4.18 t) and the carbon signal of C-7 (δ_C 152.3). For **Biso2** a similar correlation was observed for the proton signals of the oxymethylene groups (δ_H: 4.12 t and 4.06 t) and the carbon signals of C-7 (δ_C 158.9) and C-6 (δ_C 131.9), respectively (**Figure 41**).

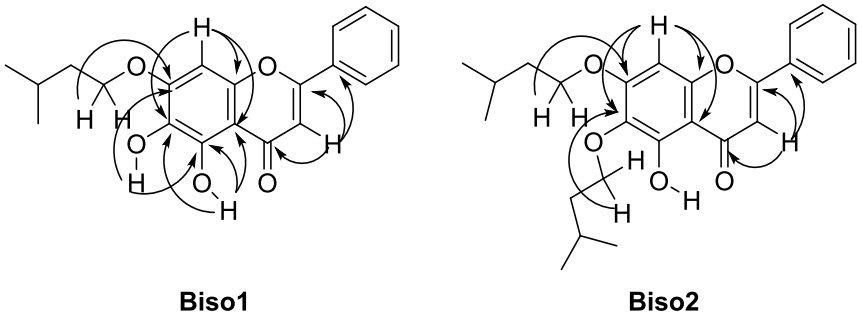

Figure 41: Main connectivities found in the HMBC of derivatives **Biso1** and **Biso2**.

For derivatives **Butil1** and **Butil2**, the ^{1}H and ^{13}C NMR spectra put in evidence the presence of one or two butyl side chains at positions 6 or 7 (**Table 10** and **Table 11**). This group was evidenced by the signals of one oxymethylene group (δ_H 4.16-4.05 t, δ_C 73.1-69.3), two methylenic groups (δ_H 1.94-1.73 m and δ_H 1.62-1.48 m, δ_C 32.2-31.0 and δ_C 19.2) and one methylic group (δ_H 1.02-0.97 t, δ_C 13.9-13.8). As **Butil1** was the major product of the nucleophilic substitution reaction it was proposed that this compound should result from the substitution at position 7. On the contrary **Butil2** should result from the substitution at position 6. This hypothesis was confirmed by the correlation observed in the HMBC spectrum of **Butil1** and **Butil2** (**Figure 42**).

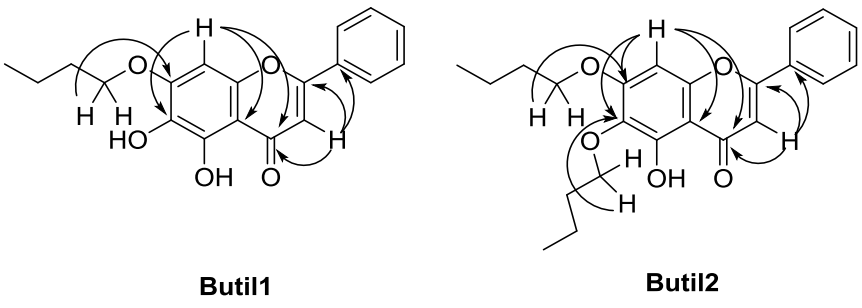

Figure 42: Main connectivities found in the HMBC of derivatives **Butil1** and **Butil2**.

Regarding **Brop1** the ^{1}H NMR spectra displayed two triplets at δ_H 4.12 (2H) and δ_H 1.10 (3H), and one multiplet at δ_H 2.05-1.98 m (2H), suggesting the presence of a propyloxy side chain at C-7. Instead, for **Brop2** the ^{1}H NMR spectra showed four triplets at δ_H 4.05 (2H), δ_H 4.01 (2H), δ_H 1.10 (3H), and δ_H 1.06 (3H) and two multiplets at δ_H 1.96-1.89 (2H) and δ_H 1.85-1.78 (2H), revealing the presence of two propyloxy groups linked to flavone scaffold. Additionally, the signal of the hydroxyl group at C-6 was observed for the flavone **Brop1**. However, the correspondent signal was not observed for the derivative **Brop2**, suggesting that the second propyloxy group should be at position 6. For both propyl derivatives, the linkage of propyloxy groups to C-7 was confirmed by the correlations observed on the HMBC spectra between the proton signals of the oxymethylene group at δ_H 4.12 and δ_H 4.05 and the carbon signals of C-7 δ_C 152.3 and δ_C 158.8, respectively) (**Figure 43**) The linkage of propyloxy group to C-6 for compound **Brop2** was also confirmed by the correlation between the proton signals at δ_H 4.01 t and the carbon signal of C-6 (δ_C 132.0) (**Figure 43**).

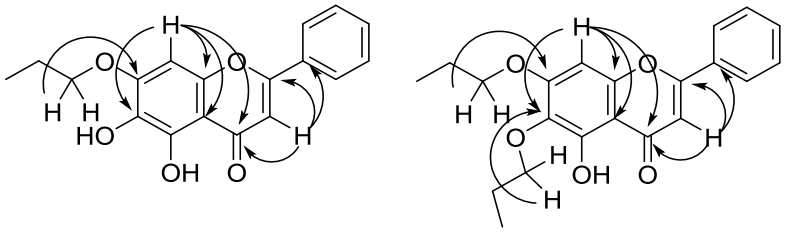

Brop1 **Brop2**

Figure 43: Main connectivities found in the HMBC of derivatives **Brop1** and **Brop2**.

For derivatives **Bali1** and **Bali1'**, the ^{1}H and ^{13}C NMR spectra showed signals that put in evidence the presence of one allyloxy group at positions 6 or 7 (**Table 10** and **Table 11**). This group was evidenced by the signals of one oxymethylene group (δ_H 4.77-4.74 d, δ_C 73.7-70.2), one olephynic proton at δ_H 6.18 -6.01 m linked to a carbon at δ_C 133.0-131.8, other olephinic carbon at δ_C 120.0-119.1 which is linked to two olephynic protons (δ_H 5.51-5.28 m). As **Bali1** was the major product of the nucleophilic substitution reaction it was proposed that this compound should result from the substitution at position 7. On the contrary **Bali1'** should result from the substitution at position 6. This hypothesis was confirmed by the correlation observed in the HMBC spectrum of **Bali1** and **Bali1'** (**Figure 44**).

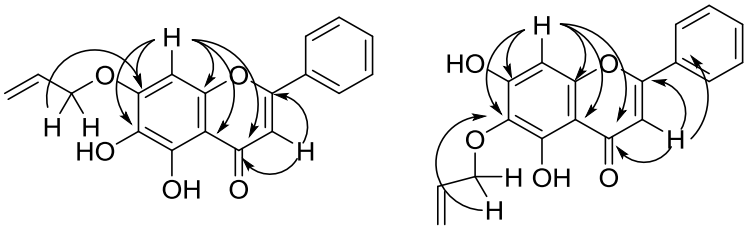

Bali1 **Bali1'**

Figure 44: Main connectivities found in the HMBC of derivatives **Bali1** and **Bali1'**.

Considering **Betil1** the ^{1}H NMR and ^{13}C NMR spectra showed characteristic signals of one ethyl group (δ_H 4.24 q, 1.55 t; δ_C 65.2, 14.6) (**Table 10** and **Table 11**). The correlations observed on the HMBC spectra between the proton signals of the oxymethylene group (δ_H 4.24 q) and the carbon signal of C-7 (δ_C 152.2) confirmed the position of this side chain on the flavone skeleton (**Figure 45**).

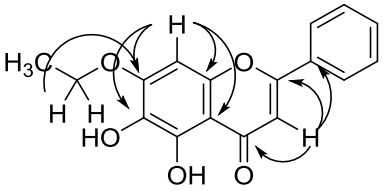

Figure 45: Main connectivities found in the HMBC spectrum of derivative **Betil1**.

Regarding **Bemet1** the ^{1}H and ^{13}C NMR spectra displayed the presence of signals characteristic of one methoxyl group (δ_H 3.94 s, δ_C 60.9) confirming the methylation of one hydroxyl group of the flavone scaffold. Instead, for **Bemet2** the ^{1}H and ^{13}C NMR spectra showed signals of two methoxyl groups (δ_H 3.93-3.98 s, δ_C 56.4-66.9) revealing the methylation of both hydroxyl groups at C-6 and C-7. For both methyl derivatives, the linkage of methoxyl groups to C-7 was confirmed by the correlations observed on the HMBC spectra between the proton signals of the methoxyl group δ_H 3.94 and δ_H 3.98 and the carbon signals of C-7 (δ_C 153.1 and δ_C 159.0) (**Figure 46**). The linkage of methoxyl group to C-6 for compound **Bemet2** was also confirmed by the correlation between the proton signals at δ_H 3.93 s and the carbon signal of C-6 (δ_C 132.7) (**Figure 46**).

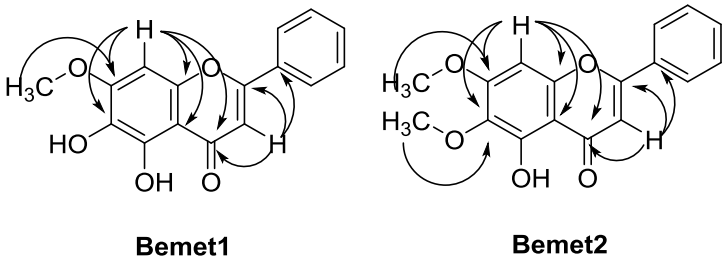

Figure 46: Main connectivities found in the HMBC of derivatives **Bemet1** and **Bemet2**.

For derivatives **Brop2**, **Butil2**, **Bali1**, **Bemet1** and **Bemet2** the ^{1}H and ^{13}C NMR data are in accordance to the published data. [183-185]

Table 10: ^{1}H NMR data of baicalein (**B**) and its alkylated derivatives (**Biso1**, **Biso2**, **Butil1**, **Butil2**, **Brop1**, **Brop2**, **Bali1**, **Bali1'**, **Betil1**, **Bemet1** and **Bemet2**).

	B	**Biso1**	**Biso2**	**Butil1**	**Butil2**	**Brop1**
H-2',6'	7.92-7.88 (*m*)	7.91-7.88 (m)	7.91-7.88 (m)	7.91-7.87 (m)	7.91-7.88 (m)	7.91-7.88 (m)
H-3',4',5'	7.60-7.52 (*m*)	7.54-7-52 (m)	7.54-7.52 (m)	7.54-7.52 (m)	7.54-7.52 (m)	7.55-7.52 (m)
H-3	6.64 (*s*)	6.69 (s)	6.67 (s)	6.68 (s)	6.67 (s)	6.69 (s)
H-5	12.72 (OH, *s*)	n.o	12.61 (OH,s)	n.o	n.o.	12.50 (OH,s)
H-6	n.o.	5.35 (OH,s)	-	n.o	-	5.37 (OH,s)
H-7	n.o.	-	-	-	-	-
H-8	6.60 (*s*)	6.62 (s)	6.56 (s)	6.61 (s)	6.55 (s)	6.61 (s)
H-1''	—	4.18 (t, J=6.6)	4.12 (t, J=6.5)	4.16 (t, J=6.6)	4.09 (t, J=6.5)	4.12 (t, J=6.9)
H-2''	—	1.93-1.77 (m)	1.82-1.75 (m)	1.94-1.85 (m)	1.93-1.83 (m)	2.05-1.98 (m)
H-3''	—	1.29-1.23 (m)	1.96-1.84 (m)	1.61-1.48 (m)	1.62-1.48 (m)	1.10 (t, J=7.4)
H-4''	—	1.01 (d, J=6.3)	1.00 (d, J= 6.5)	1.02 (t, J=7.4)	1.02 (t, J=7.4)	-
H-5''	—			-	-	-
H-1'''	—		4.06 (t, J=6.9)	-	4.05 (t, J=6.6)	-
H-2'''	—		1.72-1.65 (m)	-	1.82-1.73 (m)	-
H-3'''	—		1.96-1.84 (m)	-	1.62-1.48 (m)	-
H-4'''	—		0.97 (d, J=6.6)	-	0,97 (t, J=7.4)	-
H-5'''	—			-	-	-

n.o. not observed; Values in parts *per* million (δ_H). Measured in $CDCl_3$ at 300.13 MHz. J values (Hz) are presented in parentheses.

Table 10 (Contd.): ^{1}H NMR data of baicalein (**B**) and its alkylated derivatives (**Biso1**, **Biso2**, **Butil1**, **Butil2**, **Brop1**, **Brop2**, **Bali1**, **Bali1'**, **Betil1**, **Bemet1** and **Bemet2**).

	Brop2	**Bali1**	**Bali1'**	**Betil1**	**Bemet1**	**Bemet2**
H-2',6'	7.90-7.88 (m)	7.90-7.87 (m)	7.90-7.87 (m)	7.91-7.88 (m)	7.92-7.89 (m)	7.92-7.95 (m)
H-3',4',5'	7.54-7.52 (m)	7.58-7.49 (m)	7.56-7.52 (m)	7.55-7.52 (m)	7.55-7.53 (m)	7.57-7.52 (m)
H-3	6.67 (s)	6.68 (s)	6.67 (s)	6.69 (s)	6.69 (s)	6.68 (s)
H-5	12.50 (OH,s)	13.04 (OH,s)	13.04 (OH,s)	12.55 (OH, s)	12.69 (OH, s)	12.69 (OH, s)
H-6	-	n.o.	-	5.37 (OH,brs)	5.35 (OH,brs)	-
H-7	-	-	n.o.	-	-	-
H-8	6.55 (s)	6.63 (s)	6.62 (s)	6.61 (s)	6.58 (s)	6.58 (s)
H-1''	4.05 (t, J=6.5)	4.74 (brd, J=5.4)	4.77 (dt, J=5.3, 1.2)	4.24 (q, J=7.0)	3.94 (s)	3.98 (s)
H-2''	1.96-1.89 (m)	6.18-6.05 (m)	6.14-6.01 (m)	1.55 (t, J=7.0)	-	-
H-3''	1.10 (t, J=7.4)	5.51-5.45 (m) 5.41-5.37 (m)	5.44-5.37 (m) 5.32-5.28 (m)	-	-	-
H-4''	-	-	-	-	-	-
H-5''	-	-	-	-	-	-
H-1'''	4.01 (t, J=6.7)	-	-	-	-	3.93 (s)
H-2'''	1.85-1.78 (m)	-	-	-	-	-
H-3'''	1.06 (t, J=7.4)	-	-	-	-	-

n.o. not observed; Values in parts *per* million (δ_H). Measured in $CDCl_3$ at 300.13 MHz. J values (Hz) are presented in parentheses.

Table 11: ^{13}C NMR data of baicalein (**B**) and its alkylated derivatives (**Biso1**, **Biso2**, **Butil1**, **Butil2**, **Brop1**, **Brop2**, **Bali1**, **Bali1'**, **Betil1**, **Bemet1** and **Bemet2**).

	B	Biso1	Biso2	Butil1	Butil2	Brop1
C1'	130.9	131.5	131.7	131.5	131.6	131.6
C2'	125.6	126.2	126.2	126.3	126.3	126.2
C3'	128.5	129.1	129.1	129.1	129.1	129.1
C4'	131.1	131.8	131.7	131.8	131.8	131.7
C5'	128.5	129.1	129.1	129.1	129.1	129.1
C6'	125.6	126.2	126.2	126.3	126.3	126.2
C2	163.0	164.0	163.9	164.0	163.8	164.0
C3	104.2	105.4	105.6	105.4	105.6	105.4
C4	182.0	182.7	182.7	182.7	182.7	182.7
C4a	104.4	106.0	106.3	106.0	106.1	106.0
C5	146.5	145.6	145.7	145.7	147.4	145.6
C6	128.7	129.7	131.9	129.7	132.1	129.7
C7	152.8	152.3	158.9	152.3	158.9	152.3
C8	93.7	91.0	91.2	91.1	91.3	91.1
C8a	150.0	150.7	153.3	150.7	153.2	150.7
C1''	-	68.0	67.5	69.3	68.9	71.0
C2''	-	37.5	37.6	31.0	31.0	22.3
C3''	-	29.7	29.3	19.2	19.2	10.4
C4''	-	22.7	22.6	13.8	13.8	-
C5''	-	22.6	22.5	-	-	-
C1'''	-	-	71.8	-	73.1	-
C2'''	-	-	38.9	-	32.2	-
C3'''	-	-	29.8	-	19.2	-
C4'''	-	-	22.7	-	13.9	-
C5'''	-	-	22.6	-	-	-

Values in parts per million (δ_C). Measured in $CDCl_3$ at 75.47 MHz.

Table 11 (Contd.): ^{13}C NMR data of baicalein (**B**) and its alkylated derivatives (**Biso1**, **Biso2**, **Butil1**, **Butil2**, **Brop1**, **Brop2**, **Bali1**, **Bali1'**, **Betil1**, **Bemet1** and **Bemet2**).

	Brop2	Bali1	Bali1'	Betil1	Bemet1	Bemet2
C1'	131.4	131.4	131.3	131.5	131.3	131.3
C2'	126.2	126.2	126.3	126.3	126.3	126.3
C3'	129.1	129.1	129.1	129.1	129.1	129.1
C4'	131.7	131.8	131.9	131.8	131.9	131.9
C5'	129.1	129.1	129.1	129.1	129.1	129.1
C6'	126.2	126.2	126.3	126.3	126.3	126.3
C2	163.8	164.1	164.1	164.1	164.0	164.0
C3	105.6	105.4	105.3	105.5	105.7	105.7
C4	182.7	182.6	183.0	182.7	182.8	182.8
C4a	106.1	106.1	106.1	106.0	106.1	106.3
C5	140.0	145.8	152.1	145.7	145.5	153.1
C6	132.0	129.8	128.7	129.7	129.7	132.7
C7	158.8	151.7	155.5	152.2	153.1	159.0
C8	91.2	91.6	93.4	91.1	90.7	90.7
C8a	153.2	150.5	153.3	150.7	151.1	153.4
C1''	70.6	70.2	73.7	65.2	60.9	56.4
C2''	22.3	131.8	133.0	14.6	-	.
C3''	10.4	119.1	120.0	-	-	.
C4''	-	-	-	-	-	.
C5''	-	-	-	-	-	.
C1'''	75.0	-	-	-	-	66.9
C2'''	22.7	-	-	-	-	.
C3'''	10.5	-	-	-	-	.
C4'''	-	-	-	-	-	.
C5'''	-	-	-	-	-	.
Values in parts per million (δ_C). Measured in $CDCl_3$ at 75.47 MHz or 125.77 MHz						

3.1.2.2. Derivatives of 3,7-dihydroxyflavone

The IR data of 3,7-dihydroxyflavone (**H**) and its alkylated derivatives are presented in **Table 12.** The presence of alkyl groups was suggested by the observation of bands at 2999-2854 cm^{-1}. Additionally, the presence of one free hydroxyl group was revealed by the presence of a large band of stretching vibration between 3600-3100 cm^{-1}, for all synthesized compounds except for **Hutil2**, suggesting that alkylation of both hydroxyl groups have occurred only for **Hutil2**.

Table 12: IR data of 3,7-dihydroxyflavone (**H**) and its alkylated derivatives (**Hiso**, **Hutil1**, **Hutil2**, **Hrop**, **Hali**, **Hetil**, **Hemet** and **Hrep**).

Groups	υ (cm^{-1})								
	H	**Hiso**	**Hutil1**	**Hutil2**	**Hrop**	**Hali**	**Hetil**	**Hemet**	**Hrep**
OH	3400-3100	3600-3300	3600-3300	-	3600-3300	3600-3300	3600-3300	3600-3300	3600-3300
Aliphatic C-H	-	2958 2921 2854	2958 2922 2854	2958 2936 2873	2970 2920	2999 2964 2921	2026	2922	2974 2920 2854
C=O	1623	1605	1604	1623	1603	1615	1614	1622	1613
Aromatic C=C	1571 1451 1414	1504 1467 1452 1410	1566 1462 1452 1419	1499 1466 1447	1567 1504 1432 1412	1564 1503 1473 1453	1504 1457 1408	1508 1456 1401	1566 1463 1451 1408
C-O	1280	1260	1250	1260	1259	1260	1262	1262	1258

The ^{1}H and ^{13}C NMR data of 3,7-dihydroxyflavone (**H**) and alkyl-derivatives (**Hiso**, **Hutil1**, **Hutil2**, **Hrop**, **Hali**, **Hetil**, **Hemet** and **Hrep**) are reported in **Table 13** and **Table 14**.

The ^{1}H NMR spectra of 3,7-dihydroxyflavone (**H**) derivatives demonstrated that all of them have a non-substituted B-ring (H-2',6': δ_H 8.25-8.07 *m*; H-3', 4', 5': δ_H 7.61-7.42 *m*) as the precursor **H**. Moreover, three signals of A ring aromatic protons had been found namely signals for H-5 (δ_H 8.15-8.12 d), H-6 (δ_H 7.03-6.96 dd), and H-8 (δ_H 6.97-6.90 d), like the starting material (H) (δ_H 8.04 d, δ_H 6.96 m and δ_H 6.93 m, respectively).

Like for baicalein (**B**) derivatives, in addition to the signals described before, the ^{1}H and ^{13}C NMR spectra of all 3,7-dihydroxyflavone (**H**) derivatives showed signals that put in

evidence the presence of one alkyl side chain, except for derivative **Hutil2,** for which characteristic signals of two butyl side chains are observed, as illustrated in **Figure 47**.

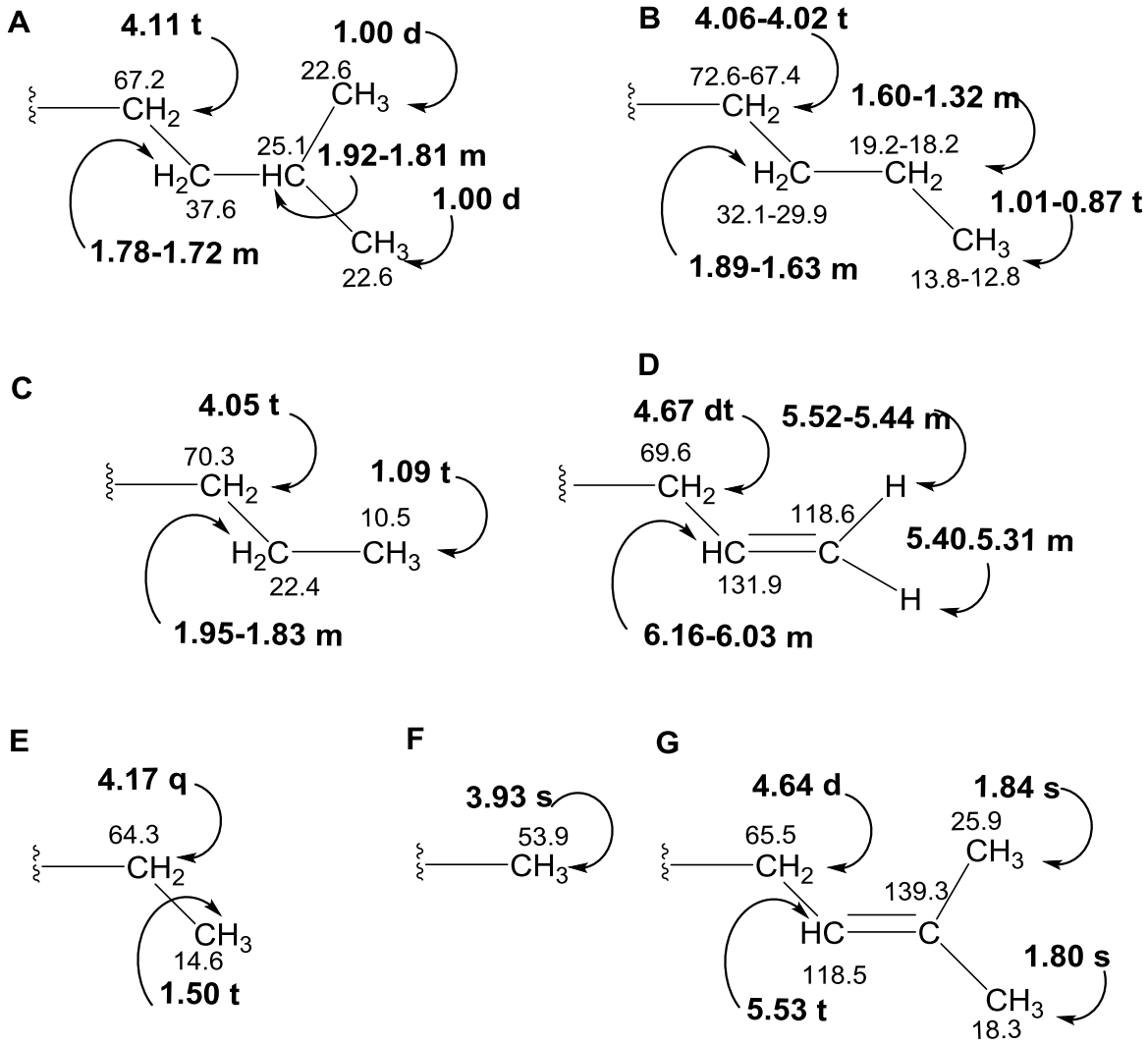

Figure 47: ^{1}H and ^{13}C NMR data for the alkyl groups of derivatives **Hiso** (A), **Hutil1/2** (B), **Hrop** (C), **Hali** (D), **Hetil** (E), **Hemet** (F) and prenyl group of derivative **Hrep** (G).

The structure of **Hrep** was confirmed by comparison with the ^{1}H and ^{13}C NMR data previously reported.[171]

For all derivatives, the position of alkyl side chains was evidenced by the correlations found in the HMBC spectra between the proton signals of the methylene

groups (H-1", H-1"') and the carbon signals of C7 (δ_C 163.9-162.9) and C3 (δ_C 140.5-137.1), respectively (**Figure 48**).

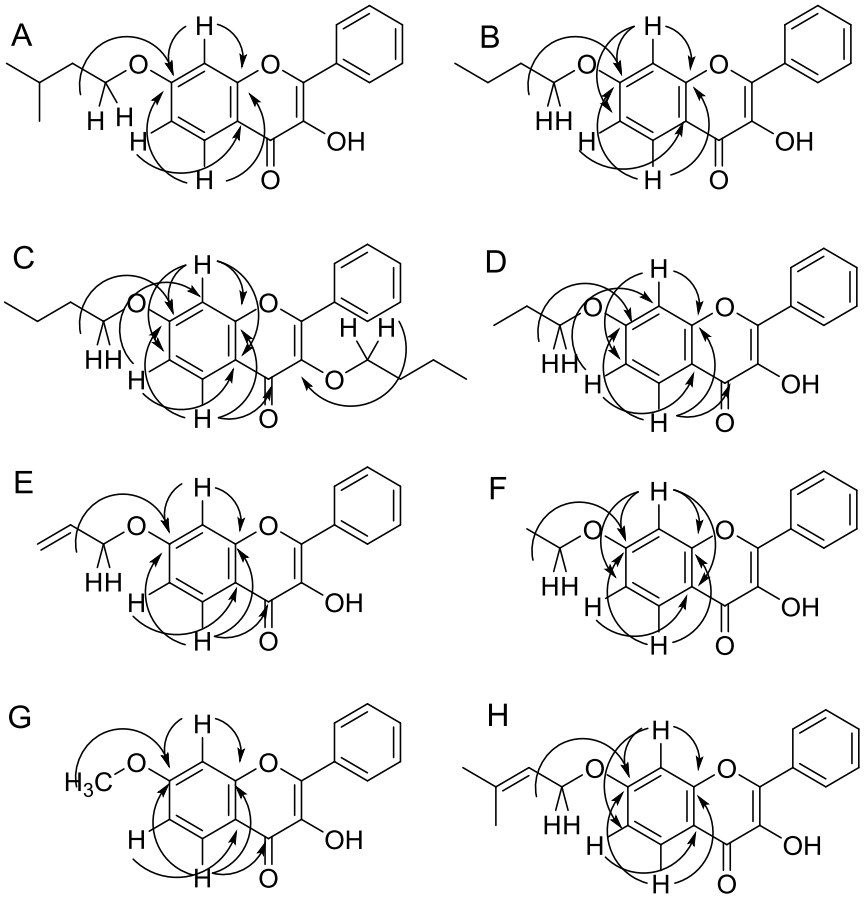

Figure 48: Main connectivities found in the HMBC of alkylated derivatives of 3,7-dihydroxyflavone (**Hiso** (A), **Hutil1** (B),**Hutil2** (C), **Hrop** (D), **Hali** (E), **Hetil** (F), **Hemet** (G) and **Hrep** (H)).

Table 13: ^{1}H NMR data of 3,7-dihydroxyflavone (**H**) and its alkylated derivatives (**Hiso**, **Hutil1, Hutil2**, **Hrop**, **Hali**, **Hetil**, **Hemet** and **Hrep**).

	H	Hiso	Hutil1	Hutil2	Hrop	Hali	Hetil	Hemet	Hrep
H-2',6'	8.24-8.21 (*m*)	8.25- 8.23 (m)	8.25-8.22 (m)	8.10-8.07 (m)	8.25-8.22 (m)	8.25-8.22 (m)	8.25-8.22 (m)	8.24-8.21 (m)	8.25-8.22 (m)
H-3',4',5'	7.53-7.43 (*m*)	7.56-7.42 (m)	7.56-7.43 (m)	7.52-7.49 (m)	7.61-7.43 (m)	7.61-7.43 (m)	7.56-7.43 (m)	7.55-7.42 (m)	7.56-7.43 (m)
H-3	n.o.	n.o.	n.o.	-	n.o.	n.o.	n.o.	n.o.	n.o.
H-5	8.04 (*d*, *J*=8.0)	8.12 (d, J=8.9)	8.13 (d, J=8.6)	8.14 (d, J=8.9)	8.13 (d, J=8.9)	8.15 (d, J= 8.9)	8.13 (d, J= 8,9)	8.13 (d, J=8.9)	8.13 (*d*, *J*=8.8)
H-6	6.96 (*m*)	6.98 (dd, J=8.9, 2.3)	7.00 (dd, J=8.8, 2.3)	6.96 (dd, J=8.9, 2.3)	7.00 (dd, J=10.4, 2.3)	7.03 (dd, J= 8.6, 2.3)	6.99 (dd, J=8.9, 2.1)	6.99 (dd, J=8.9, 2.3)	7.00 (dd, J=8.8, 2.2)
H-7		-	-	-	-	-	-	-	-
H-8	6.93 (m)	6.94 (d, J=2.2)	6.95 (d, J=2.3)	6.90 (d, J=2.3)	6.97 (d, J=2.3)	6.97 (d, J=2.3)	6.95 (d, J=2.1)	6.94 (d, J=2.3)	6.97 (d, J=2.2)
H-1''	-	4.11 (t, J=6.6)	4.09 (t, J=6.5)	4,06 (t, J=6.5)	4.05 (t, J=6.6)	4.67 (dt, J=5.3, 1.5)	4.17 (q, 6.9)	3.93 (s)	4.64 (d, J=6.8)
H-2''	—	1.78-1.72 (m)	1.89-1.80 (m)	1.87-1.78 (m)	1.95-1.83 (m)	6.16-6.03 (m)	1.50 (t, J=6.9)	-	5.53 (t, J=6.8, 2.0)
H-3''	—	1.92-1.81 (m)	1.60-1.47 (m)	1.59-1.49 (m)	1.09 (t, J=7.4)	5.52-5.44 (m) 5.40-5.31 (m)	-	-	-
H-4''	—	1.00 (d, J= 6.5)	1.01 (t, J=7.4)	1.00 (t, J=7.4)	-	-	-	-	1.84 (s)
H-5''	—		-	-	-	-	-	-	1.80 (s)
H-1'''	—	-	-	4.02 (t, J=6.5)	-	-	-	-	-
H-2'''	—	-	-	1.73-1.63 (m)	-	-	-	-	-
H-3'''	—	-	-	1.42-1.32 (m)	-	-	-	-	-
H-4'''	—	-	-	0.87 (t, J=7.4)	-	-	-	-	-
H-5'''	_	-	-	-	-	-	-	-	-

n.o. not observed; Values in parts per million (δ_H). Measured in $CDCl_3$ at 300.13 MHz. J values (Hz) are presented in parentheses.

Table 14: ^{13}C NMR data of 3,7-dihydroxyflavone (**H**) and its alkylated derivatives (**Hiso**, **Hutil1**, **Hutil2**, **Hrop**, **Hali**, **Hetil**, **Hemet** and **Hrep**).

	H	Hiso	Hutil1	Hutil2	Hrop	Hali	Hetil	Hemet	Hrep
C1'	131.0	131.3	131.3	131.3	131.3	131.2	131.3	131.2	131.3
C2'	127.0	127.5	127.5	128.5	127.5	127.5	127.5	127.5	127.5
C3'	127.9	128.6	128.9	128.3	128.6	128.6	128.8	128.6	128.6
C4'	129.1	129.9	130.2	130.4	129.9	129.9	129.9	129.9	129.9
C5'	127.9	128.6	128.9	128.3	128.6	128.6	128.8	128.6	128.6
C6'	127.0	127.5	127.5	128.5	127.5	127.5	127.5	127.5	127.5
C2	143.5	144.1	143.1	155.3	144.1	144.1	144.1	144.2	144.2
C3	137.7	138.1	137.1	140.5	138.1	138.1	138.1	138.1	139.5
C4	172.4	172.9	206.0	174.8	172.9	172.8	172.9	172.8	207.0
C4a	113.5	115.1	113.4	118.0	114.4	114.7	114.4	114,6	114.7
C5	126.2	126.7	126.5	127.1	126.7	126.8	126.7	126.8	126.7
C6	114.7	115.3	114.2	114.8	115.3	115.2	115.2	114.9	115.4
C7	162.4	163.9	162.9	163.6	163.9	163.2	163.7	164.3	163.6
C8	101.9	100.3	99.3	100.3	100.3	100.8	100.3	99.8	100.6
C8a	156.7	157.4	156.4	157.1	157.4	157.3	157.4	157.4	157.4
C1''	-	67.2	67.4	68.4	70.3	69.6	64.3	53.9	65.5
C2''	-	37.6	29.9	31.0	22.4	131.9	14.6	-	118.5
C3''	-	25.1	18.2	19.1	10.5	118.6	-	-	31.0
C4''	-	22.6	12.8	13.8	-	-	-	-	25.9
C5''	-		-	-	-	-	-	-	18.3
C1'''	-		-	72.6	-	-	-	-	-
C2'''	-		-	32.1	-	-	-	-	-
C3'''	-		-	19.2	-	-	-	-	-
C4'''	-		-	13.8	-	-	-	-	-
C5'''	-		-	-	-	-	-	-	-
Values in parts per million (δ_C). Measured in $CDCl_3$ at 75.47 MHz.									

3.1.2.3. Derivatives of chrysin

The IR data of chrysin (**C**) as well as chrysin derivates (**Ciso**, **Cutil**, **Crop**, **Cali**, **Cetil**, **Cemet** and **Crep**) are presented in **Table 15**. The observation of bands at 2985-2851 cm $^{-1}$ (aliphatic C-H), suggested the presence of alkyl groups. The presence of a large band of stretching vibration at 3451-3441 cm $^{-1}$ corresponding to hydroxyl groups is an indicator that the alkylation did not occur at both hydroxyl groups of the precursor (**C**).

Table 15: IR data of chrysin (**C**) and its alkylated derivatives (**Ciso**, **Cutil**, **Crop**, **Cali**, **Cetil**, **Cemet** and **Crep**).

Groups	υ (cm^{-1})							
	C	**Ciso**	**Cutil**	**Crop**	**Cali**	**Cetil**	**Cemet**	**Crep**
OH	3600-3400	3600-3400	3600-3400	3600-3400	3600-3400	3600-3400	3600-3400	3600-3400
Aliphatic C-H	-	2956 2921 2851	2952 2933 2868	2964 2920 2874	2961 2920 2851	2985 2924 2852	2923 2854	2967 2917 2853
C=O	1652	1662	1664	1661	1665	1663	1668	1659
Aromatic C=C	1577 1555 1499	1588 1452	1589 1569 1450 1442	1585 1569 1507 1451	1586 1506 1451	1586 1509 1454	1588 1495 1452 1436	1588 1504 1449
C-O	1168	1169	1170	1173	1170	1173	1160	1178

The ^{1}H and ^{13}C NMR data of chrysin (**C**) and its alkyl-derivatives (**Ciso**, **Cutil**, **Crop**, **Cali**, **Cetil**, **Cemet** and **Crep**) are reported in **Table 16** and**Table 17.**

The ^{1}H NMR spectra of chrysin (**C**) derivatives indicated that all of them have a non-substituted B-ring (H-2',6' δ_H 7.91-7.82 m; H-3',4',5' δ_H 7.58-7.48 m) as the precursor **C**. Like for chrysin (**C**), the ^{1}H NMR spectra showed signals for two A-ring aromatic protons (H-6: δ_H 6.40-6.33 d, H-8: δ_H 6.53-6.46 d) and a signal at δ_H 6.68-6.61 s corresponding to H-3. In addition, the signal of the hydroxyl group at C-5 (δ_H 12.73-12.69 s) was also observed for all derivatives, except for **Cutil** and **Cetil**.

Besides these signals, the ^{1}H and ^{13}C NMR spectra of chrysin (**C**) derivatives showed characteristic signals of one prenyl (**Crep**), isopentyl (**Ciso**), butyl (**Cutil**), propyl (**Crop**), allyl (**Cali**), ethyl (**Cetil**), or methyl (**Cemet**) side chain, as illustrated in **Figure 49**.

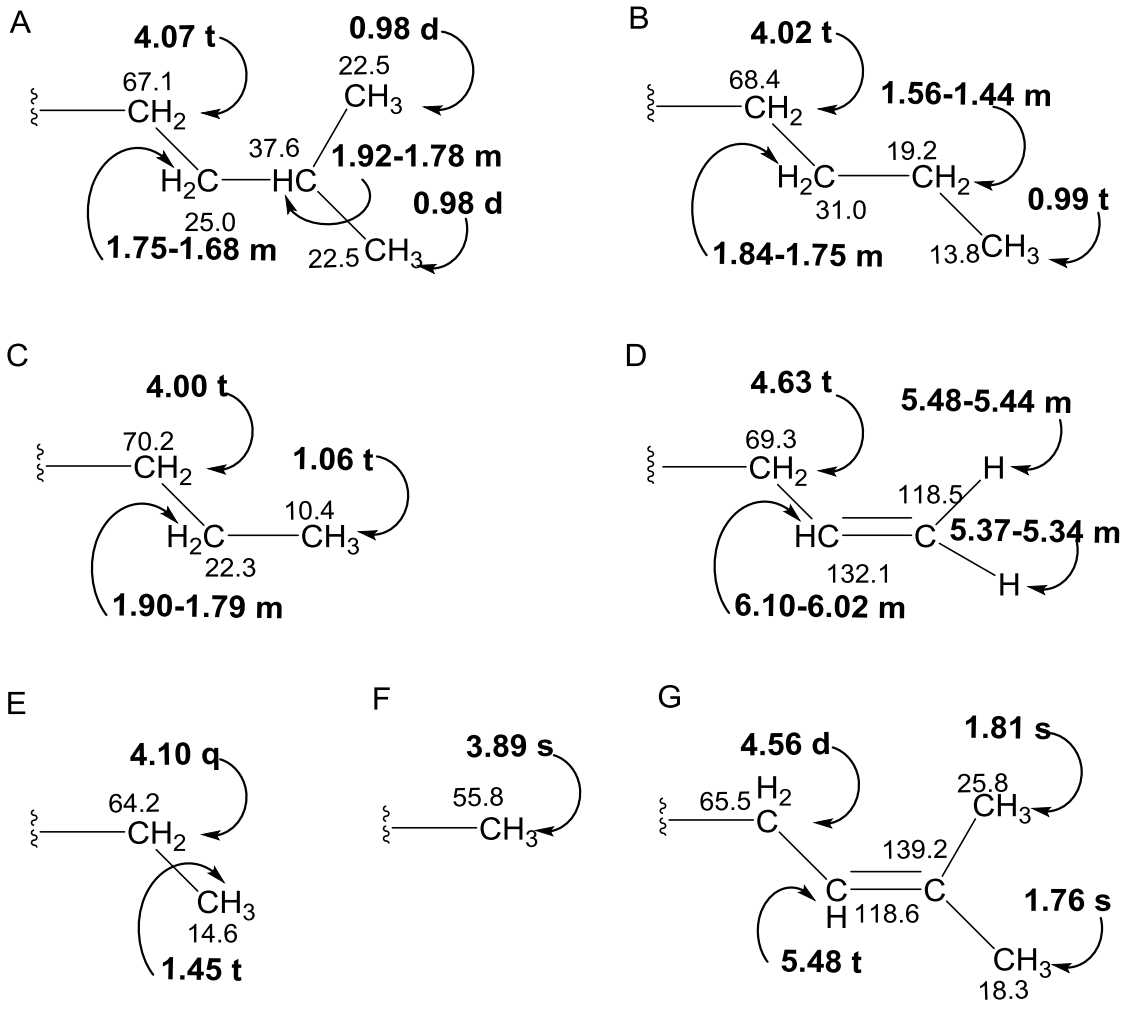

Figure 49:[1]H and [13]C NMR data for the alkyl groups of derivatives **Ciso** (A), **Cutil** (B), C**rop** (C), C**ali** (D), **Cetil** (E), C**emet** (F) and prenyl group of derivative **Crep** (G).

The position of these side chains was evidenced by the correlations found in the HMBC as indicated in **Figure 50**.

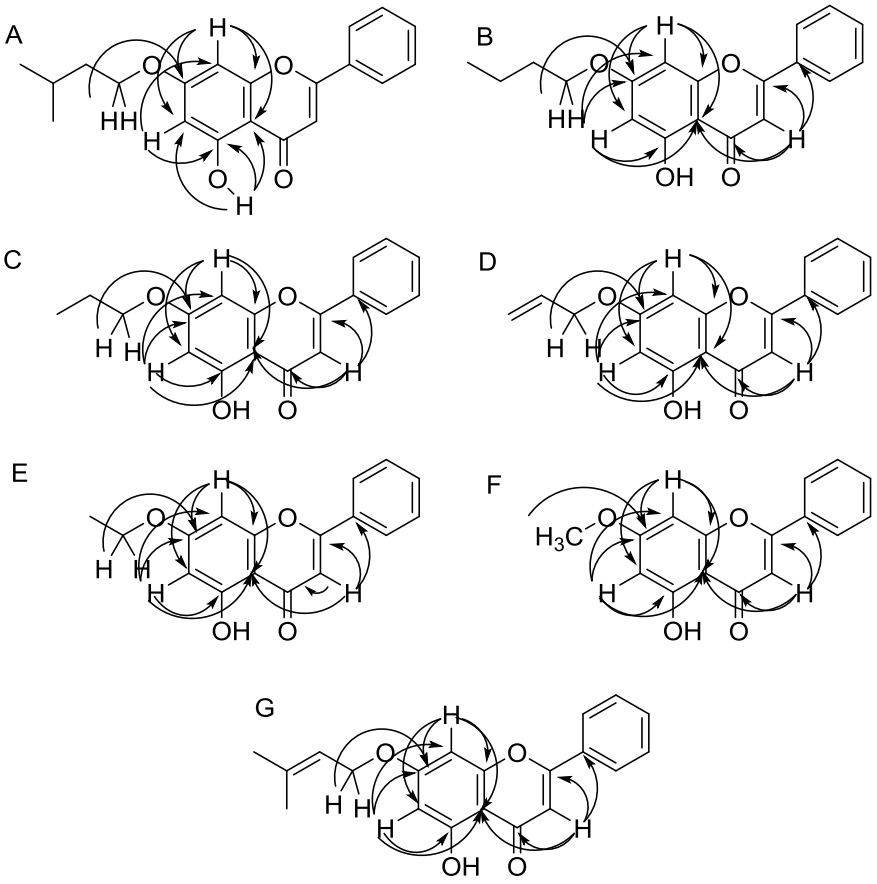

Figure 50: Main connectivities found in the HMBC of alkylated derivatives of chrysin (**Ciso** (A), **Cutil** (B), **Crop** (C), **Cali** (D), **Cetil** (E), **Cemet** (F) and **Crep** (G)).

For derivatives **Cali, Cetil** and **Cemet,** the ^{1}H and ^{13}C NMR data obtained are in accordance to the published data. [186-188]

Table 16: ^{1}H NMR data of chrysin (**C**) and its alkylated derivatives (**Ciso**, **Cutil**, **Crop**, **Cali**, **Cetil**, **Cemet** and **Crep**).

	C	Ciso	Cutil	Crop	Cali	Cetil	Cemet	Crep
H-2',6'	7.90-7.87 (m)	7.90-7.88 m	7.87-7.84 (m)	7.90-7.87 (m)	7.90-7.88 (m)	7.89-7.86 (m)	7.91-7.88 (m)	7.86-7.82 (m)
H-3',4',5'	7.55-7.52 (m)	7.55-7.52 (m)	7.52-7.50 (m)	7.56-7.49 (m)	7.58-7.51 (m)	7.53-7.51 (m)	7.55-7.52 (m)	7.51-7.48 (m)
H-3	6.67 (s)	6.67 (s)	6.63 (s)	6.66 (s)	6.68 (s)	6.65 (s)	6.67 (s)	6.61 (s)
H-5	12.70 (OH, s)	12.71 (OH,s)	n.o.	12.70 (OH,s)	12.72 (OH,s)	n.o.	12.73 (OH,s)	12.69 (OH,s)
H-6	6.30 (d, J=2.2)	6.37 (d, J=2.2)	6.34 (d, J=2.2)	6.37 (d, J=2.2)	6.40 (d, J=2.2)	6.35 (d, J=2.2)	6.38 (d, J=2.3)	6.33 (d, J=2.2)
H-7	6.14 (OH,s)	-	-	-	-	-	-	-
H-8	6.48 (d, J=2.2)	6.50 (d, J=2.2)	6.47 (d, J=2.2)	6.50 (d, J=2.2)	6.53 (d, J=2.2)	6.48 (d, J=2.2)	6.51 (d, J=2.3)	6.46 (d, J=2.2)
H-1''		4.07 (t, J=6.6)	4.02 (t, J=6.5)	4.00(t, J=6.6)	4.63 (dt, J=5.2, 1.4)	4.10 (q, J=7.0)	3.89 (s)	4.56 (d, J=6.9)
H-2''		1.75-1.68 (m)	1.84-1.75 (m)	1.90-1.79 (m)	6.10-6.02 (m)	1.45 (t, J=7.0)	-	5.48 (t, J=6.7)
H-3''		1.92-1.78 (m)	1.56-1.44 (m)	1.06 (t, J= 7.4)	5.48-5.44 (m) 5.37-5.34 (m)	-	-	-
H-4''		0.98 (d, J=6.5)	0.99 (t, J=7.4)		-	-	-	1.81 (s)
H-5''			-	-	-	-	-	1.76 (s)

n.o. not observed; Values in parts per million (δ_H). Measured in $CDCl_3$ at 300.13 MHz or 500 MHz. J values (Hz) are presented in parentheses.

Table 17: ^{13}C NMR data of Chrysin (**C**) and its alkylated derivatives (**Ciso**, **Cutil**, **Crop**, **Cali**, **Cetil**, **Cemet** and **Crep**).

	C	Ciso	Cutil	Crop	Cali	Cetil	Cemet	Crep
C1'	131.9	131.8	131.3	131.4	131.4	131.3	131.3	131.2
C2'	126.3	126.3	126.2	126.3	126.3	126.3	126.3	126.2
C3'	129.1	129.1	129.1	129.1	129.1	129.1	129.1	129.0
C4'	131.9	131.8	131.8	131.8	131.9	131.8	131.9	131.8
C5'	129.1	129.1	129.1	129.1	129.1	129.1	129.1	129.0
C6'	126.3	126.3	126.2	126.3	126.3	126.3	126.3	126.2
C2	163.9	163.9	163.8	163.9	164.0	163.9	164.0	163.8
C3	105.9	105.9	105.8	105.9	105.9	105.8	105.9	105.7
C4	182.4	182.5	182.4	182.5	182.5	182.5	182.5	182.4
C4a	105.6	105.6	105.5	105.6	105.8	105.6	105.7	105.6
C5	162.0	162.1	162.1	162.1	162.2	162.1	162.2	162.0
C6	99.5	98.6	98.6	98.6	98.8	98.6	98.2	98.8
C7	165.0	168.2	165.2	165.2	164.6	165.0	165.6	164.9
C8	94.2	93.1	93.0	93.1	93.4	93.1	92.7	93.2
C8a	157.8	158.0	157.8	157.8	157.8	157.8	157.8	157.7
C1''	-	67.1	68.4	70.2	69.3	64.2	55.8	65.5
C2''	-	25.0	31.0	22.3	132.1	14.6	-	118.6
C3''	-	37.6	19.2	10.4	118.5	-	-	139.2
C4''	-	22.5	13.8	-	-	-	-	25.8
C5''	-		-	-	-	-	-	18.3

Values in parts per million (δ_C). Measured in $CDCl_3$ at 75.47 MHz or 125.77 MHz

3.2. Peck purity

For baicalein (**B**) derivatives **Biso1, Brop1 and Bali1**, prior to their biological activity evaluation, their purity was evaluated by HPLC-DAD as described in chapter 5. A percentage of purity greater than 95% was found for all derivatives (**Table 18**).

Table 18: Purity values of the alkylated derivatives of baicalein (**Biso1**, **Brop1** and **Bali1**).

Compound	Peak purity
Biso1	99.7%
Brop1	99.7%
Bali1	99.8%

3.3. Biological activity

3.3.1. Modulation of procaspase-3 and -7 activity*

In this section it is discussed the results obtained in the evaluation of the procaspases-3 and -7 modulatory activity of some synthesized flavonoids (the alkylated derivatives **Biso1, Brop1** and **Bali1**).

The effect of the derivatives **Biso1**, **Brop1** and **Bali1** on the activity of human procaspases-3 and -7 was evaluated using yeast cell assays. In this yeast assay, the expression of procaspases-3 and -7 does not affect the yeast growth, but activators of procaspases-3 and -7, such as PAC-1 (positive control[33]) induce yeast growth inhibition. Using this approach, the effect of 0.1-50 μM PAC-1 and 0.1-15 μM flavonoids on the growth of yeast individually expressing procaspases-3 or -7 was evaluated and the percentage of drug-induced growth inhibition was estimated, considering 100% growth the number of colony-forming units (c.f.u.) obtained with DMSO only. The results are summarized in **Figure 51**.

*Work developed by the Master student Sofia Salazar under the supervision of Professor Lucília Saraiva (FFUP) – ongoing studies.

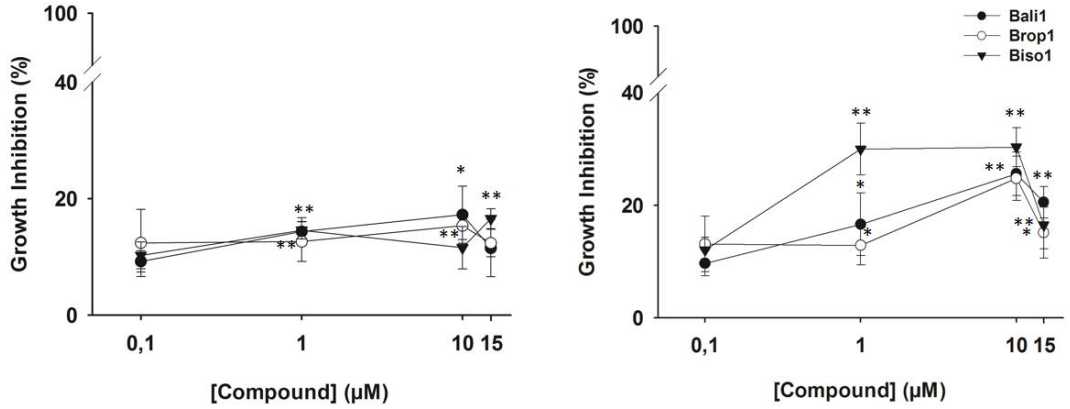

Figure 51: Concentration-response curves for the effects of flavonoids **Biso1**, **Brop1** and **Bali1** on the growth of yeast expressing human procaspase-3 (**A**) or -7 (**B**), for 24 hours treatment. The percentage of drug-induced growth inhibition was estimated considered 100% growth the number of CFU obtained with DMSO only. Data are mean ± SEM of six independent experiments; values significantly different from DMSO are indicated (**p*=0.01, ***p*=0.001; unpaired student *t*' test).

The results indicate that compounds **Biso1**, **Brop1** and **Bali1**, induced growth inhibition in yeast cells expressing procaspase-7 at 0.1 - 15 µM (**Figure 51**, **B**)**,** with the maximal effect achieved at 10 µM for **Brop1** and **Bali1** and 1 µM for **Biso1**, without interfering with the growth of control yeast (data not shown). Interestingly, the effect of these compounds was less pronounced in yeast cells expressing procaspase-3 (**Figure 51**, **A**)**.** The comparison of the concentration-response curves for the effect of flavonoid **Biso1** here reported with those reported for the baicalein derivative **FP2** [175], revealed that at the concentration of 1 µM (minimum concentration for which the maximal effect was achieved for **Biso**) the percentage of inhibition for **Biso1** (about 30 %) was higher than the percentage of inhibition obtained for **FP2** (about 8 %), suggesting that **Biso1** was more potent than **FP2**.

For procaspase-7, the GI_{25} values was obtained from concentration–response curves (**Table 19**).

Table 19: GI_{25} values obtained for PAC-1 and flavonoids **Biso1**, **Brop1** and **Bali1**.

Compounds	GI25	
	procaspase-3	procaspase-7
PAC-1	16.6 ± 2.87	24.5 ± 4.82
Biso1	ND	1.2 ± 2.26**
Brop1	ND	12.5 ± 4.91
Bali1	ND	9.3 ± 2.23*

GI_{25} values correspond to the concentration that caused 25% growth inhibition of yeast cells expressing procaspase-3 or -7 after treatment with 0.1 - 15 μM flavonoids **Biso1**, **Brop1** and **Bali1**, and 0.1 - 50 μM PAC-1 (positive control). Data are mean ± SEM of six independent experiments.; values significantly different from PAC-1 are indicated (*p=0.01, **p=0.001; unpaired). *ND* – Not determined.

The GI_{25} revealed that all tested flavones were more potent than PAC-1, being compound **Biso1**, the most potent derivative. Additionally, contrary to PAC-1 that activates both procaspases-3 and -7, the results seggested that all tested flavonoids appear to be selective for procaspase-7.

3.4. Docking study

An *in silico* docking study was performed using executioner procaspases-3, -6, and -7 as targets, and the derivatives already tested in the biological assays (**Biso1**, **Brop1** and **Bali1**) as potential ligands. In addition to that compounds, docking studies were also performed for the baicalein derivative **FP2**, already reported as a procaspase-7 activator[175]. Docking scores were obtained, which consist of approximations of the free energy ΔG of the ligand-macromolecule complex. In this computational study, a series of compounds already described in the literature as procaspases modulators[189,190,190] (**Figure 52**) were used as positive controls.

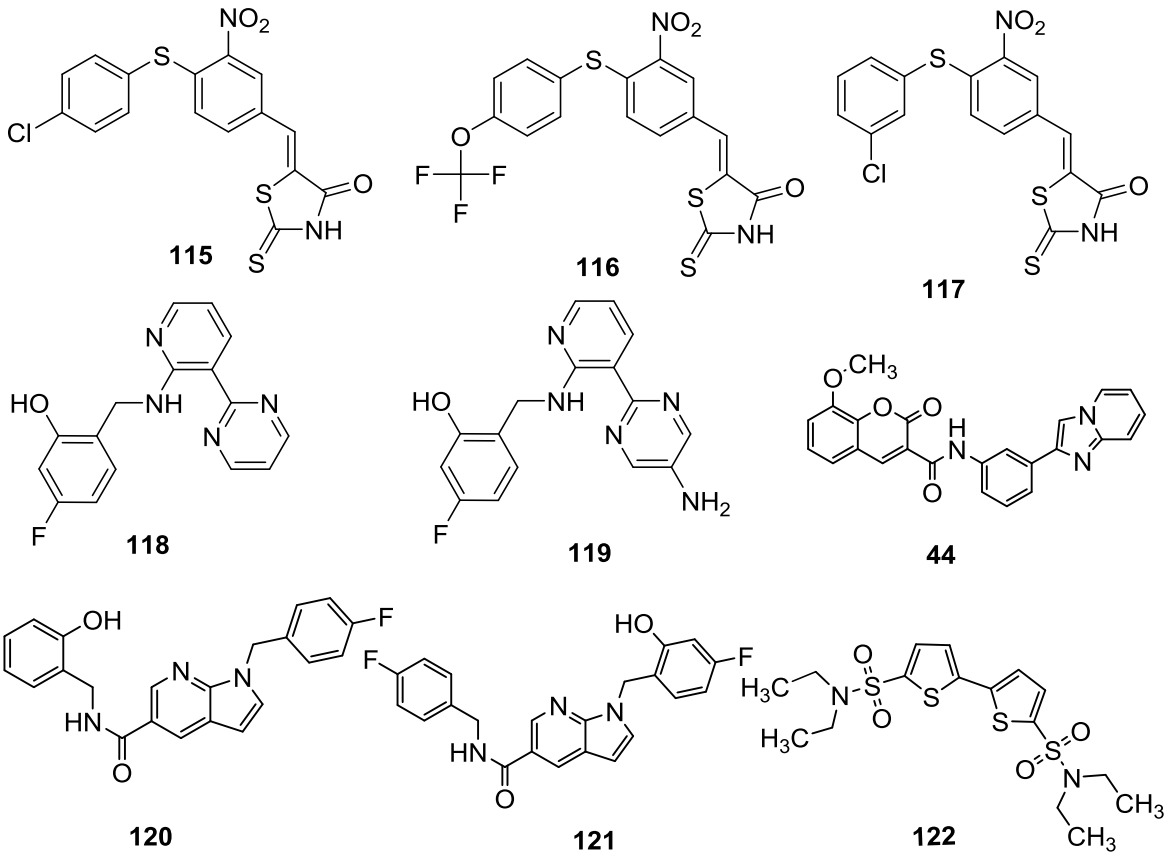

Figure 52: Structures of the positive controls used in the docking study.

The obtained docking scores are represented in **Table 20**.

Table 20: Docking scores (Kcal.mol-1) for procaspase activators described in the literature and derivatives **Biso1**, **Brop1** and **Bali1**.

		Procaspase-3	Procaspase-7	Procaspase-6
Controls	**115***		-6.1	
	116*	-7.6	-6.1	
	117*		-6.4	
	118*			-9
	119*			-9
	44*	-9		-9.9
	120*			-11.4
	121*			-11.4
	122*	-7.1		
Tested compounds	**FP2**	-7.3	-7.7	-9
	Biso1	-7.2	-7.7	-8.7
	Brop1	-6.7	-6.9	-8.7
	Bali1	-6.9	-6.2	-8.7

used as positive controls for one, two, or three of the tested procaspases, according to the activation capacity previously described in the literature for those targets*[189,190,190]*.***

Considering procaspase-3, compounds **116**, **44** and **122** were used as positive controls (**Table 20** and **Figure 53**). By analysis of the obtained docking results, in general it was found that all positive controls, particularly compound 1541 (**44**), had a lower docking score and thus formed a more stable complex with procaspase-3 than the synthesized compounds. However, **Biso1** and **FP2** exhibited a ΔG value (-7.2 and 7.3 Kcal/mol, respectively) similar to the positive control **122**, suggesting also the formation of a stable complex with procaspase-3.

For procaspase-7, **Biso1, Brop1,** and **Bali1** revealed a more negative docking scores (-7.1, -6.9, and -6.2 Kcal/mol, respectively) than the known activators (compounds **115- 117** and **Figure 54**). As with procaspase-3, among the tested compounds **Biso1** and **FP2** are predicted to form more stable complexes with procaspase-7. In addition, both derivatives are predicted to bind with the same affinity, as a similar docking score was observed for both derivatives. Pereira et al. (2014) verified that **FP2** was evolved in the activation of procaspase-7 and inhibited the growth of HL-60 and MCF-7 human tumor cells[175]. Therefore, the results obtained for this docking study are in accordance to the results already reported.[175] Furthermore, a correlation between ΔG and GI_{25} can be observed for derivatives **Biso1, Brop1,** and **Bali1**. Indeed, for procaspase-7, among the tested compounds **Biso1** was the most potent compound with a GI_{25} value of 1.3 ± 2.2 μM.

In vitro studies were not performed for procaspase-6. However, it is important to study *in silico* possible interactions in order to understand if there is the possibility of

activation of procaspases-6 by these compounds. The analysis of the results for procaspase-6 show that that the prenylated (**FP2**) and alkylated derivatives of baicalein (**Biso1**, **Brop1** and **Bali1**) have the same (-9 Kcal/mol) or similar (-8.7 Kcal/mol) docking scores as controls **117** and **118** (**Table 20**, Figure 55). However, both synthesized compounds and **FP2** had higher ΔG values than other known activators described in the literature (**120**, **121** and **44**; **Table 20**, Figure 55).

In addition to the docking scores, it is important to analyze the possible polar interactions established between the tested compounds and procaspases. In **Figure 56, Figure 57** and **Figure 58**, the most stable docking conformations of tested compounds into procaspase-3, -7 and -6, and polar interactions are represented.

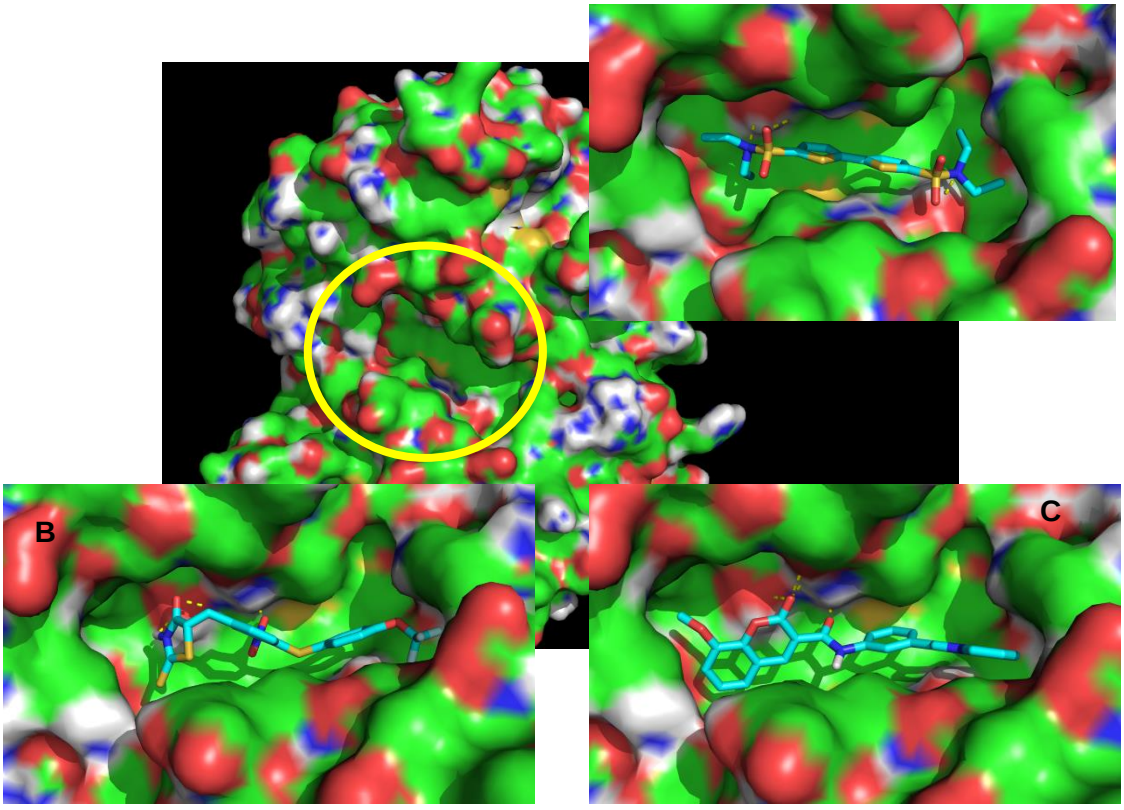

Figure 53: Compound **122** (A), **116** (B) and **44** (**1541**) (C) docked into procaspase-3. Small molecules are represented as blue sticks, and procaspase-3 is represented as surface. Carbon, oxygen, nitrogen and sulphur atoms of the target are represented in green, red, blue, and yellow, respectively. Polar interactions are represented as yellow broken line.

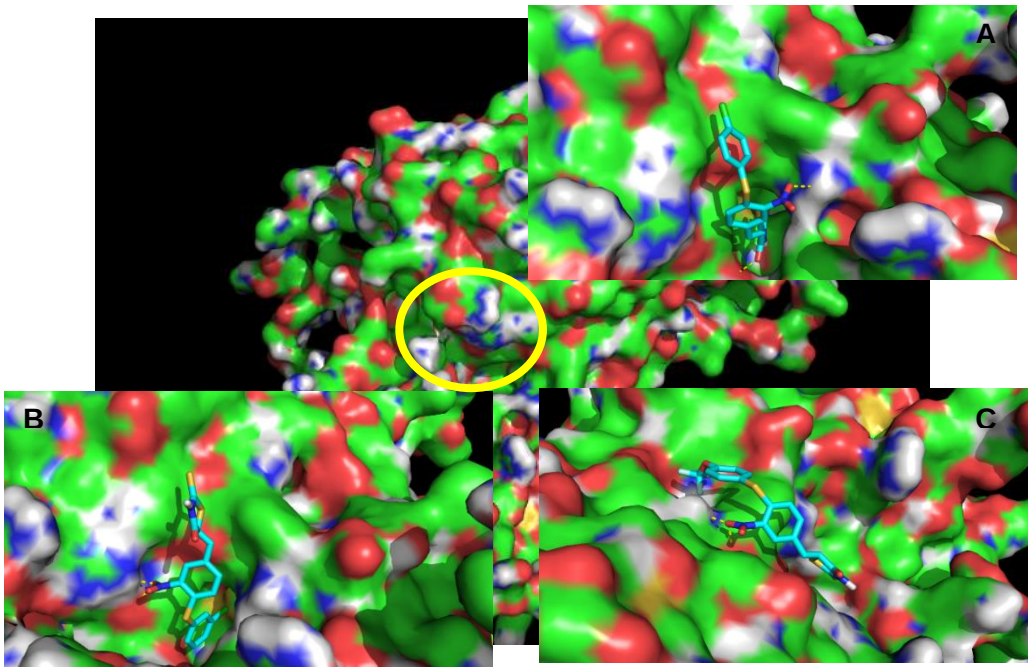

Figure 54: compound **115** (A), **117** (B) and **116** (C) docked into procaspase-7. Small molecules are represented as blue sticks, and procaspase-7 is represented as surface. Carbon, oxygen, nitrogen and sulphur atoms of the target are represented in green, red, blue, and yellow, respectively. Polar interactions are represented as yellow broken line.

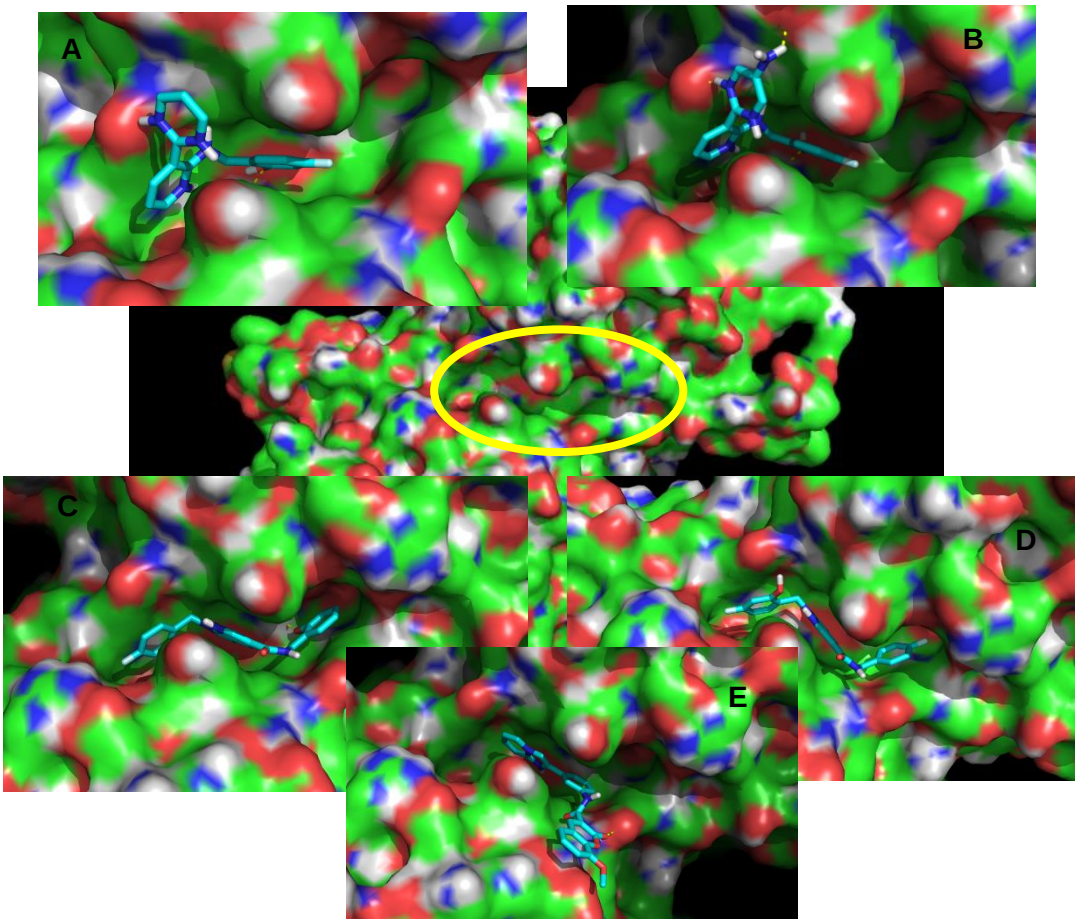

Figure 55: compound **118** (A), **119** (B), **120** (C), **121** (D) and **44** (1541) (E) docked into procaspase-6. Small molecules are represented as blue sticks, and procaspase-6 is represented as surface. Carbon, oxygen, nitrogen and sulphur atoms of the target are represented in green, red, blue, and yellow, respectively. Polar interactions are represented as yellow broken line.

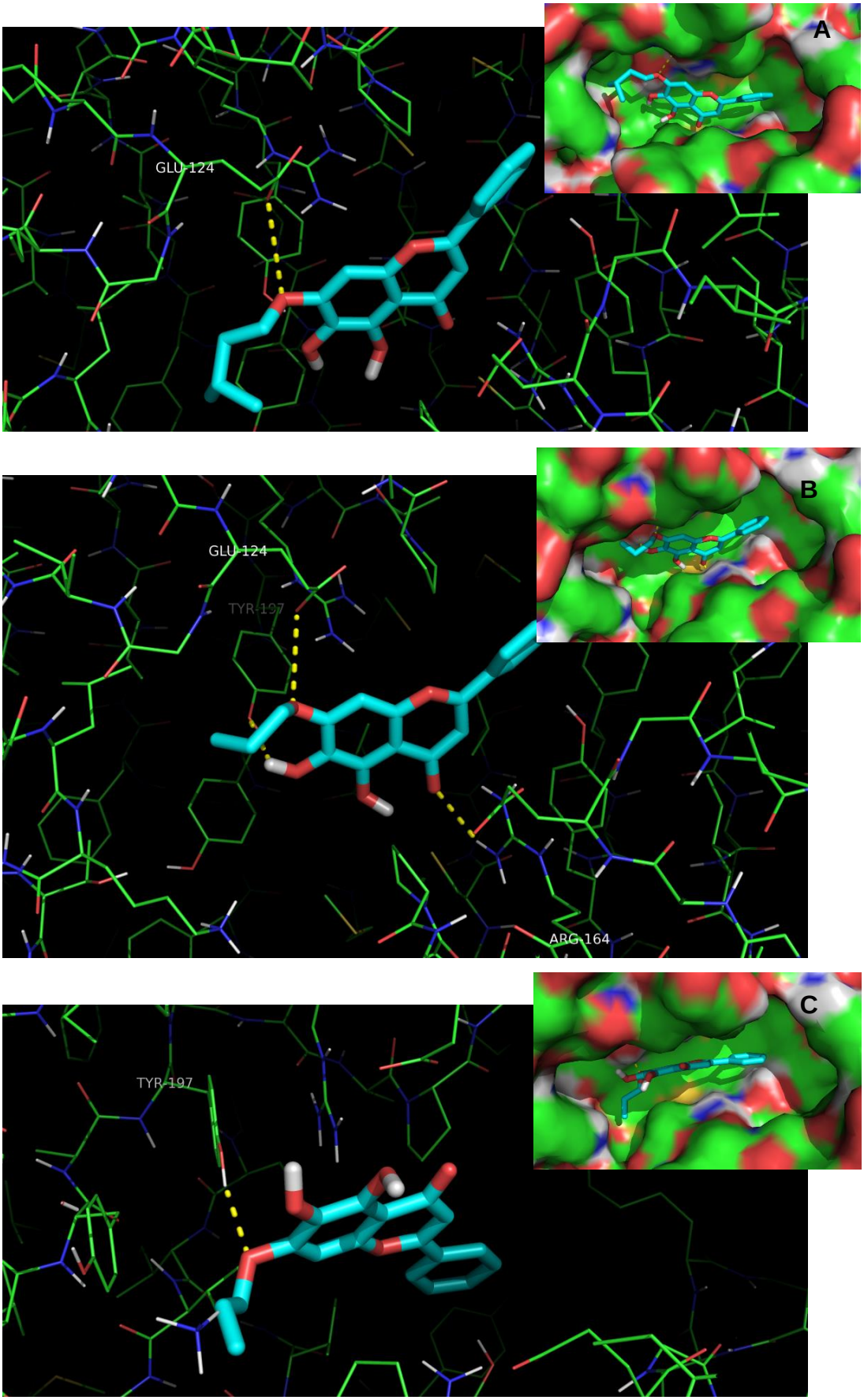

Figure 56: Interactions of **Biso1** (A) **Brop1** (B) and **Bali1** (C) (blue sticks) with residues in the allosteric site of procaspase-3. Polar interactions are represented as yellow broken lines. Carbon, oxygen, nitrogen and sulphur atoms of the target are represented in green, red, blue, and yellow, respectively.

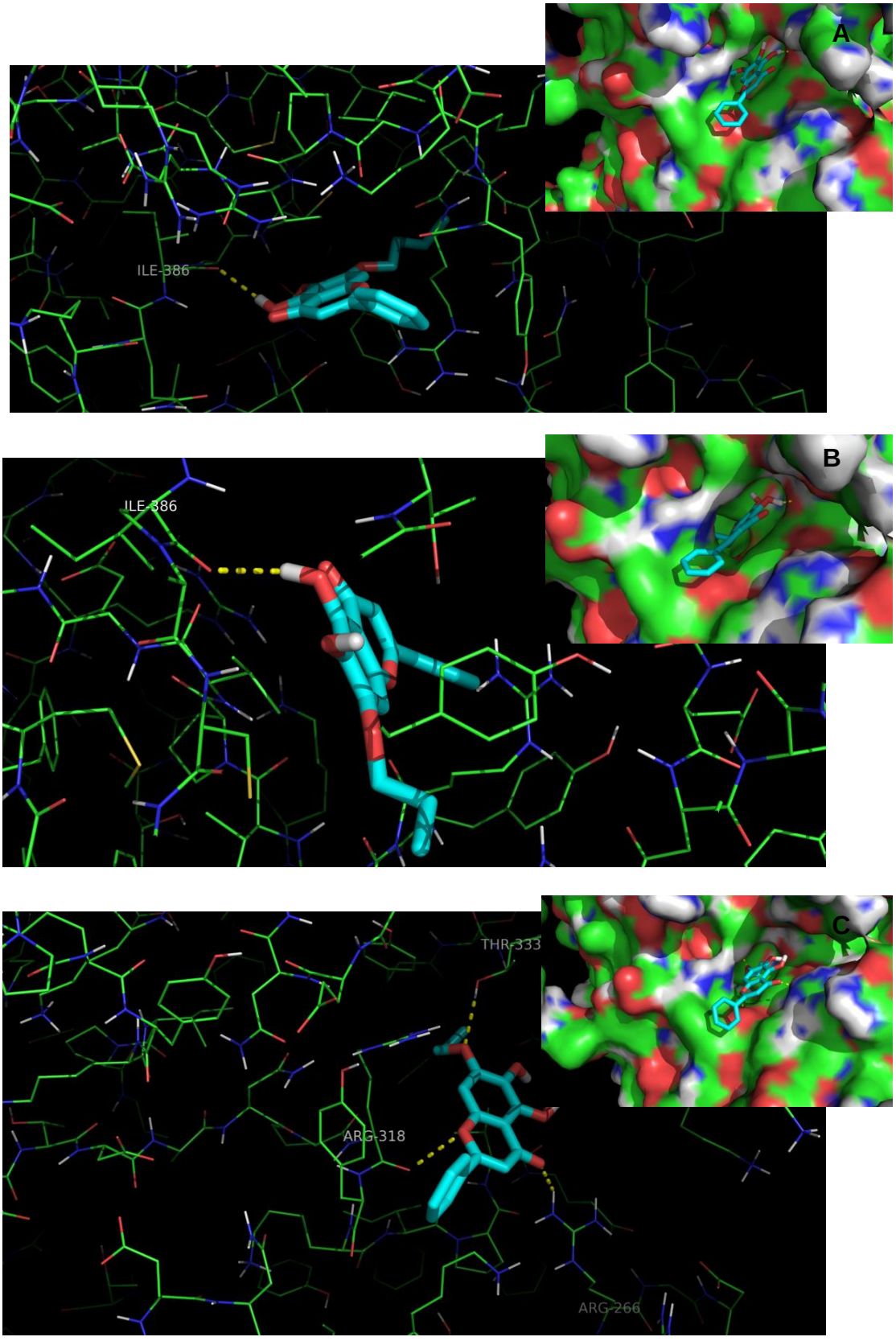

Figure 57: Interactions of **Biso1** (A) **Brop1** (B) and **Bali1** (C) (blue sticks) with residues in the allosteric site of procaspase-7. Polar interactions are represented as yellow broken lines. Carbon, oxygen, nitrogen and sulphur atoms are represented in green, red, blue, and yellow, respectively.

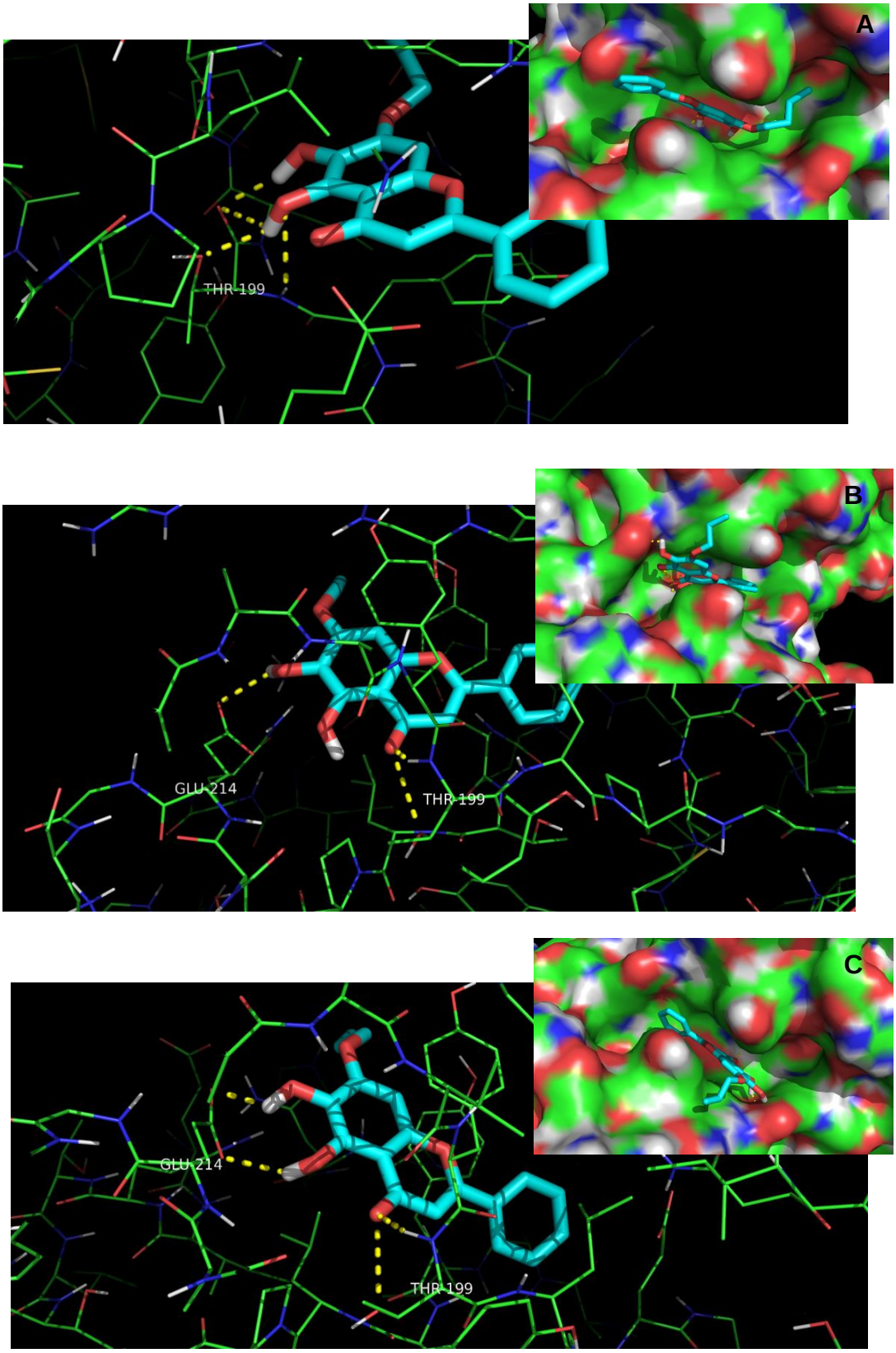

Figure 58: Interactions of **Biso1** (A) **Brop1** (B) and **Bali1** (C) (blue sticks) with residues in the allosteric site of procaspase-6. Polar interactions are represented as yellow broken lines. Carbon, oxygen, nitrogen and sulphur atoms are represented in green, red, blue, and yellow, respectively.

All alkylated derivatives (**Biso1**, **Brop1** and **Bali1**) of baicalein (**B**) establish polar interactions with procaspase-3, -7, and -6 allosteric sites. The different residues involved in polar interaction are listed in **Table 21**.

Table 21: Residues of procaspases-3, -7, and -6 involved in polar interactions with alkylated derivatives (**Biso1**, **Brop1** and **Bali1**).

Tested compounds	Procaspase-3	Procaspase-7	Procaspase-6
Biso1	GLU 124	ILE 886	TYR 199
Brop1	GLU 124 TYP 197 ARG 164	ILE 886	GLU 114 THP 199
Bali1	TYR 197	THP 333 ARG 318 ARG 266	GLU 214 THP 199

Biso1 is the most active procaspase activator both *in vitro* and *in silico*. Despite not containing the largest number of polar interactions *in silico*. Nonetheless, it is necessary not to disregard the non-polar interactions. Besides establishing polar interactions, the isopentoxyl group allows a more favorable orientation and a deeper insertion of the molecule into the allosteric groove of the target, as well as the establishment of additional van der Waals interactions with the hydrophobic cavity.

Once **Biso1** showed to be the most active derivative, we decided to make an *in silico* docking study to predict the procaspases modulatory activity of other synthesized derivatives possessing a 7-isopentyloxy group (derivatives **Hiso** and **Ciso**) (**Table 22**).

Table 22: Docking scores (Kcal.mol^{-1}) for modulators described in the literature and alkylated derivatives of baicalein (**Biso1**), 3,7-dihydroxyflavone (**Hiso**) and chrysin (**Ciso**).

		Procaspase-3	Procaspase-7	Procaspase-6
Controls	**115***		-6.1	
	116*	-7.6	-6.1	
	117*		-6.4	
	118*			-9
	119*			-9
	44*	-9		-9.9
	120*			-11.4
	121*			-11.4
	122*	-7.1		
Tested compounds	**Biso1**	-7.2	-7.7	-8.7
	Hiso	-6.8	-9.6	-7.6
	Ciso	-7.1	-9.3	-6.3

used as positive controls for one, two, or three of the tested procaspases, according to the activation capacity previously described in the literature for those targets*[189,190,190].**

By analysis of the results obtained for procaspase-3, it was found that **Hiso** and **Ciso** had docking scores similar with **Biso1**. However, for procaspase-6 the results of **Hiso** and **Ciso** were worse than **Biso1**. Curiously, in procaspase-7 the compound **Hiso** had the best result and **Ciso** had a similar result. These results suggest that the hydroxyl group in position 6 may be detrimental to the interaction with procaspase-7. Concerning procaspase-3, the results suggest that the hydroxyl group in position 5 is important for interaction with procaspase-3. Furthermore, concerning modulation of procaspase-6, the presence of two hydroxyl groups in C-5 and C-6 in the flavone scaffold seems to be associated to a higher modulatory activity than the presence of just one hydroxyl group in C-5.

Chapter 4:

Conclusions

Cancer is an increasing concern of our aging society, being responsible for a high mortality rate. Thus, cancer has been the focus of a great concern in general society, leading to numerous research studies by the scientific community. Considering that the resistance to apoptosis is one of the hallmarks of cancer, the search for compounds that induce apoptosis may be a key to the discovery of new antitumor agents.

Caspases are involved in a cascade cellular of events that results in activation of initiator caspases and consequently in the activation of effector caspases triggering the apoptosis. Thus, the search for modulators of caspases with the ability to promote their activation might be an effective strategy to the activation of apoptosis in tumor cells.

Flavonoids have a wide range of biological activities including antitumor activity. Many flavonoids and in particular prenyl- and alkyl-flavonoids were described as inducers of apoptosis by affecting the expression or activity of a wide range of molecules involved in apoptosis pathways, namely caspases. However, the reports about the direct activation of caspases by flavonoids are scarce and recent.

The current work allowed the synthesis and identification of twenty-six flavonoids, being sixteen described for the first time, using MAOS methodologies. For three synthesized alkylated flavonoids (**Biso1**, **Brop1** and **Bali1**) their ability to modulate the activity of procaspases-3 and -7 was evaaluated, using yeast-based assays. For bioactive compounds were performed docking studies with procaspases-3,-6 and -7.

Considering the aims proposed for this dissertation, it is possible to conclude that the synthesis of alkylflavonoids by molecular modification of three naturally occurring compounds using non-classic methodologies (MAOS) were successfully accomplished. However other strategies to obtain these derivatives with a higher yield should be investigated in the future. All tested compounds revealed to be procaspase-7 activators, particularly **Biso1,** which showed a lower GI_{25} value (1.2 ± 2.26 μM) than the positive control, PAC-1 (24.5 ± 4.82 μM). Futher studies must be perform in order to evaluate their potency and selectivity for procaspases-3, -6 and -7, particularly in comparison to that obtained with their starting materials.

The results presented in this dissertation also suggest that the suitable alkylation of flavonoid scaffolds may result in interesting derivatives with the ability to modulate the procaspases activity, which deserve further studies in order to confirm the results obtained in the yeast cell model. In the future it would be also important to investigate the

procaspases modulatory activity of other synthesized compounds using yeast cell assays and assays with tumor cell lines to establish structure-activity relationship (SAR).

Chapter 5:

Experimental Procedures

5.1 Chemistry

5.1.1. Synthesis

5.1.1.1. General methods

MW reactions were performed using a glassware setup for atmospheric-pressure reactions and a 100 mL or 30 ml Teflon reactor (internal reaction temperature measurements with a fiber-optic probe sensor) and were carried out using an Ethos MicroSYNTH 1600 Microwave Labstation from Milestone.

All the reactions were monitored by thin-layer chromatography (TLC).

Purifications of compounds were carried out by flash chromatography using Macherey-Nagel silica gel 60 (0.04-0.063 mm), preparative TLC using Macherey-Nagel silica gel 60 (GF254) plates, and crystallization.

Melting points were obtained in a Köfler microscope and are uncorrected.

IR spectra were obtained in KBr microplate in a FTIR spectrometer Nicolet iS10 from Thermo Scientific with Smart OMNI-Transmisson accessory (Software OMNIC 8.3).

^{1}H and ^{13}C NMR spectra were taken in CDCl3 at r.t., on Bruker Avance 300 and 500 instruments (300.13 MHz for ^{1}H and 75.47 MHz for ^{13}C). Chemical shifts are expressed in δ (ppm) values relative to tetramethylsilane (TMS) used as an internal reference; ^{13}C NMR assignments were made by 2D (HSQC and HMBC) NMR experiments (long-range ^{13}C-1H coupling constants were optimized to 7 Hz).

The commercial available reagents were purchased from Sigma Aldrich Co.

Analytical HPLC-DAD analyses were performed on a SpectraSYSTEM (Thermo Fisher Scientific, Inc, USA) equipped with a P4000 pump, an AS3000 autosampler and a diode array detector UV8000. The separation was carried out on a 250 x 4.6 mm i.d. FortisBIO C18 (5 µm) (Fortis™ Technologies Ltd, Cheshire, UK). LC analysis was performed by isocratic elution using a mixture of MeOH:H_2O:$MeCO_2H$ (50:50:1 v/v/v) or (95:5:1) as mobile phase and the flow rate was set at 1 mL/min. The injected volume was

20 µL and the eluent was monitored at 275 nm. ChromQuest 5.0 (version 3.2.1) software (Thermo Fisher Scientific Inc.) managed chromatographic data. Methanol (HPLC grade) was obtained from Carlo Erba Reagents, (Val de Reuil, Italy), acetic acid (HPLC grade) was obtained from Romil Pure Chemistry (Cambridge, UK) and HPLC grade water obtained from a Simplicity® UV Ultrapure Water System, Millipore Corporation, USA. Prior to use, mobile phase solvents were degassed in an ultrasonic bath for 15 min.

All commercially available reagents were purchased from Sigma Aldrich Co. Reagents and solvents were purified and dried according to the usual procedures described elsewhere.[191] The following materials were synthesized and purified by the described procedures.

5.1.1.2. Optimization of baicalein alkylation

5.1.1.2.1. HPLC-DAD analysis and quantification

The HPLC-DAD analyses of **Biso1** and baicalein (**B**) was performed by isocratic elution using a mixture of MeOH:H_2O:$MeCO_2H$ (50:50:1 v/v/v). The analyses of **Biso2** was performed by isocratic elution using a mixture of MeOH:H_2O:$MeCO_2H$ (95:5:1 v/v/v). Calibration curves for **Biso1** (5, 10, 25, 30, 50, 100, 150 and 200 µg/mL), **Biso2** (5, 10, 25, 30 and 50ug/mL) and baicalein (**B**) (25, 30, 50, 100, 150 and 200 µg/ mL) were prepared by injecting, in triplicate, different concentrations of standard samples, recording their peak areas and plotting peak areas *vs* concentration of the standard. Calibration curves exhibited good linear regressions (y = 195215x, r^2 = 0.9899 for **Biso1** (Rt = 48 min), y = 146214x, r^2 = 0.9721 for **Biso2** (Rt = 7 min) and y = 192828x; r^2 = 0.9969 for **B** (Rt = 28 min)).

5.1.1.2.2. Optimization of reactional time

Six independent mixtures of baicalein (**B**) (0.020 g, 0.074 mmol), isopentyl iodide (0.118 mmol) and anhydrous K_2CO_3 (0.052 g, 0.37 mmol) in anhydrous acetone (11 mL) were submitted to microwave irradiation at 200 W of power. The final temperature was 60

°C and the total irradiation time was 10, 20, 30, 40, 50 or 60 min. After cooling, the solid was filtered and the solvent removed under reduced pressure to afford the crude product. The solid obtained was dissolved in methanol and, without purification, was analyzed by HPLC-DAD, according to 5.1.1.2.1.

5.1.1.2.3. Optimization of the amount of the alkylating agent

A mixture of baicalein (**B**) (0.020 g, 0.074 mmol), isopentyl iodide (0.059, 0.089, 0.118 or 0.148 mmol) and anhydrous K_2CO_3 (0.052 g, 0.37 mmol) in anhydrous acetone (11 mL) was submitted to microwave irradiation at 200 W of power. The final temperature was 60 °C and the total irradiation time was 20 min. After cooling, the solid was filtered and the solvent removed under reduced pressure to afford the crude product. The solid obtained was dissolved in methanol and, without purification, was analyzed by HPLC-DAD, according to 5.1.1.2.1.

5.1.1.3. Derivatives of baicalein

5.1.1.3.1. Alkylated derivatives of baicalein

A mixture of baicalein (**B**) (0.20 g, 0.74 mmol), isopentyl / butyl / propyl / allyl / ethyl / methyl iodide (1.18 mmol) and anhydrous K_2CO_3 (0.55 g, 3.7 mmol) in anhydrous acetone (60 mL) was submitted to successive 30 min of microwave irradiation at 200 W of potency. The final temperature was 60 °C and the total irradiation time was 2h, except for the reaction with isopentyl iodide, for which the reaction time was 3 h. After cooling, the solid was filtered and the solvent removed under reduced pressure to afford the crude product. The yellow-orange solid obtained was dissolved in acetone and purified as described below.

5,6-dihydroxy-7-(isopentyloxy)-2-phenyl-4H-chromen-4-one (Biso1). Purified by flash chromatography (SiO_2; n-hexane: EtOAc, 7:3). Yield: 5.6 %; mp 175-178 ºC; IR (kBr) υ_{max}: 3600-3300, 2955, 2921, 2854, 1657, 1489, 1477, 1450, 1115 cm^{-1}; ^1H NMR ($CDCl_3$, 300.13 MHz) δ= 7.91-7.88 (2H, m, H-2', 6'), 7.54-7.52 (3H, m, H-3', 4', 5'), 6.69 (1H, s, H-

3), 6.62 (1H, s, H-8), 5.35 (OH, s, H-6), 4.18 (2H, t, J=6.6, H-1''), 1.93-1.77 (2H, m, H-2''), 1.29-1.23 (1H, m, H-3''), 1.01 (6H, d, J=6.3, H-4'',5''); ^{13}C NMR ($CDCl_3$, 75.47 MHz) *δ*= 182.7 (C4), 164.0 (C2), 152.3 (C7), 150.7 (C8a), 145.6 (C5), 131.8 (C4'), 131.5 (C1'), 129.7 (C6), 129.1 (C3', 5'), 126.2 (C2', 6'), 106.0 (C4a), 105.4 (C3), 91.0 (C8), 68.0 (C1''), 37.5 (C2''), 29.7 (C3''), 22.7 (C4''), 22.6 (C5'').

5-hydroxy-6,7-bis(isopentyloxy)-2-phenyl-4H-chromen-4-one (Biso2). Purified by flash chromatography (SiO_2; n-hexane: EtOAc, 9:1) followed by preparative TLC (SiO_2; n-hexane: EtOAc, 8:2). Yield: 0.6 %; mp 85-87 ºC; IR (kBr) υmax: 3600-3300, 2957, 2922, 2851, 1653, 1559, 1497, 1457, 1419 cm $^{-1}$; ^{1}H NMR ($CDCl_3$, 300.13 MHz) *δ*= 12.61 (OH, s, H-5), 7.91-7.88 (2H, m, H-2', 6'), 7.54-7.52 (3H, m, H-3', 4', 5'), 6.67 (1H, s, H-3), 6.67 (1H, s, H-3), 6.56 (1H, s, H-8), 4.12 (2H, t, J=6.5, H-1''), 4.06 (2H, t, J=6.9, H-1'''), 1.96-1.84 (2H, m, H-3'',3'''), 1.79 (2H, q, J=6.6, H-2''), 1.69 (2H, q, J=6.8, H-2'''), 1.00 (6H, d, J=6.5, H-4'', H-5'') 0.97 (6H, d, J=6.6, H-4''',5'''); ^{13}C NMR ($CDCl_3$, 75.47 MHz) *δ*= 182.7 (C4), 163.9 (C2), 158.9 (C7), 153.3 (C8a), 145.7 (C5), 131.9 (C6), 131.7 (C1'), 129.1 (C3', C5'), 126.2 (C2', 6'), 106.3 (C4a), 105.6 (C3), 91.2 (C8), 71.8 (C1'''), 67.5 (C1''), 38.9 (C2'''), 37.6 (C2''), 29.8 (C3'''), 29.3 (C3''), 22.7 (C4'''), 22.6 (C4'',5'''), 22.5 (C5'').

7-butoxy-5,6-dihydroxy-2-phenyl-4H-chromen-4-one (Butil1). Purified by flash chromatography (SiO_2; petroleum ether: EtOAc, 7:3). Yield: 5.7%; mp 169-172 ºC; IR (kBr) υmax: 3600-3300, 2956, 2923, 2873, 1655, 1502, 1584, 1464, 1451, 1191 cm^{-1}; ^{1}H NMR ($CDCl_3$, 300.13M Hz) *δ*= 7.91-7.87 (2H, m, H-2', 6'), 7.54-7.52 (3H, m, H-3', 4', 5'), 6.68 (1H, s, H-3), 6.61 (1H, s, H-8), 4.16 (2H, t, J=6.6, H-1''), 1.94-1.85 (2H, m, H-2''),1.61-1.48 (2H, m, H-3''), 1.02 (3H, t, J=7.4, H4''); ^{13}C NMR ($CDCl_3$, 75.47 MHz) *δ*= 182.7 (C4), 164.0 (C2), 152.3 (C7), 150.7 (C8a), 145.7 (C5), 131.8 (C4'), 131.5 (C1'), 129.7 (C6), 129.1 (C3', 5'), 126.3 (C2', 6'), 106.0 (C4a), 105.4 (C3), 91.1 (C8), 69.3 (C1''), 31.0 (C2''), 19.2 (C3''), 13.8 (C4'').

6,7-dibutoxy-5-hydroxy-2-phenyl-4H-chromen-4-one (Butil2). Purified by flash chromatography (SiO_2; petroleum ether: EtOAc, 9:1). Yield: 0.5 %; mp 103-106 ºC; IR (kBr) υmax: 3600-3300, 2961, 2925, 2851, 1657, 1497, 1457, 1419, 1121 cm^{-1}; ^{1}H NMR ($CDCl_3$, 300.13 MHz) *δ*= 7.91-7.88 (2H, m, H-2', 6'), 7.54-7.52 (3H, m, H-3', 4', 5'), 6.67 (1H, s, H-3), 6.55 (1H, s, H-8), 4.09 (2H, t, J=6.5, H-1''), 4.05 (2H, t, J=6.6, H-1'''), 1.93-1.83 (2H, m, H-2''), 1.82-1.73 (2H, m, H-2'''), 1.62-1.48 (4H, m, H-3'',3'''), 1.02 (3H, t, J=, H4''); 0.97 (3H, t, J=, H-4'''); ^{13}C NMR ($CDCl_3$,75.47 MHz) *δ*= 182.7 (C4), 163.8 (C2),

158.9 (C7), 153.2 (C8a), 147.4 (C5), 131.8 (C4'), 131.6 (C1'), 132.1 (C6), 129.1 (C3', 5'), 126.3 (C2', 6'), 106.1 (C4a), 105.6 (C3), 91.3 (C8), 73.1 (C1'''), 68.9 (C1''), 32.2 (C2''), 31.0 (C2''), 19.2 (C3'', C3'''), 13.9 (C4'''), 13.8 (C4'').

5,6-dihydroxy-2-phenyl-7-propoxy-4H-chromen-4-one (Brop1). Purified by flash chromatography (SiO_2; petroleum ether: EtOAc, 8:2). Yield: 3.5%; mp 167-170 ºC; IR (kBr) υmax: 3600-3300, 2927, 2922, 2851, 1617, 1559, 1489, 1473, 1459, 1458 cm^{-1}; ^1H NMR (CDCl3, 300.13 MHz) *δ*= 12.50 (OH, s, H-5), 7.91-7.88 (2H, m, H-2', 6'), 7.55-7.52 (3H, m, H-3', 4', 5'), 6.69 (1H, s, H-3), 6.61 (1H, s, H-8), 5.37 (OH, s, H-6), 4.12 (2H, t, J=6.9, H-1''), 2.05-1.98 (2H, m, H-2''), 1.10 (3H, t, J=7.4, H-3''); ^{13}C NMR (CDCl3, 75.47 MHz) *δ*= 182.7 (C4), 164.0 (C2), 152.3 (C7), 150.7 (C8a), 145.6 (C5), 131.7 (C4'),131.6 (C1'), 129.7 (C6), 129.1 (C3', 5'), 126.2 (C2', 6'), 106.0 (C4a), 105.4 (C3), 91.1 (C8), 71.0 (C1''), 22.3 (C2''), 10.4 (C3'').

5-hydroxy-2-phenyl-6,7-dipropoxy-4H-chromen-4-one (Brop2). Purified by flash chromatography (SiO_2; petroleum ether: EtOAc, 9:1). Yield: 6.0%; mp 77-80 ºC; IR (kBr) υmax: 3600-3300, 2965, 2921, 2851, 1657, 1499, 1470, 1458, 1416, 1122 cm^{-1}; ^1H NMR ($CDCl_3$, 300.13MHz) *δ*= 12.50 (OH, s, H-5), 7.90-7.88 (2H, m, H-2', 6'), 7.54-7.52 (3H, m, H-3', 4', 5'), 6.67 (1H, s, H-3), 6.55 (1H, s, H-8), 4.05 (2H, t, J=6.5, H-1''), 4.01 (2H, t, J=6.7, H-1'''), 1.96-1.89 (2H, m, H-2''), 185-1.78 (2H, m, H-2'''), 1.10 (3H, t, J=7.4, H-3''), 1.06 (3H, t, J=7.4, H-3'''); ^{13}C NMR ($CDCl_3$, 75.47 MHz) *δ*= 182.7 (C4), 163.8 (C2), 158.8 (C7), 153.2 (C8a),140.0 (C5), 132.0 (C6), 131.7 (C4'),131.4 (C1'), 129.1 (C3', 5'), 126.2 (C2', 6'), 106.1 (C4a), 105.6 (C3), 91.2 (C8), 75.0 (C1'''), 70.6 (C1''), 22.7 (C2'''), 22.3 (C2''), 10.5 (C3'''), 10.4 (C3'').

7-(allyloxy)-5,6-dihydroxy-2-phenyl-4H-chromen-4-one (Bali1). Purified by flash chromatography (SiO_2; n-hexane: EtOAc, 7:3). Yield: 4.2%; mp 160-162 ºC; IR (kBr) υmax: 3600-3300, 2925, 2923, 2854, 1663, 1576, 1489, 1449, 1252 cm^{-1}; ^1H NMR ($CDCl_3$, 300.13 MHz) *δ*= 13.04 (OH, s, H-5), 7.90-7.87 (2H, m, H-2', 6'), 7.58-7.49 (3H, m, H-3', 4', 5'), 6.68 (1H, s, H-3), 6.63 (1H, s, H-8), 6.18-6.05 (1H, m, H-2''), 5.51-5.45 (1H, m, H-3''a), 5.41-5.37 (1H, m, H-3''b), 4.74 (2H, brd, J=5.4, H-1''); ^{13}C NMR ($CDCl_3$, 75.47 MHz) *δ*= 182.6 (C4), 164.1 (C2), 151.7 (C7), 150.5 (C8a), 145.8 (C5), 131.8 (C4', C2''), 131.4 (C1'), 129.8 (C6), 129.1 (C3', 5'), 126.2 (C2', 6'), 119.1 (C3''), 106.1 (C4a), 105.4 (C3), 91.6 (C8), 70.2 (C1'').

6-(allyloxy)-5,7-dihydroxy-2-phenyl-4H-chromen-4-one (Bali1'). Purified by flash chromatography (SiO_2; n-hexane: EtOAc, 9:1) followed by preparative TLC (SiO2; n-hexane: EtOAc, 8:2). Yield: 1.1%; 166-168 ºC; IR (kBr) υmax: 3600-3300, 2925, 2923, 2854, 1664, 1585, 1489, 1451, 1115 cm^{-1}; ^{1}H NMR ($CDCl_3$, 300.13 MHz) *δ*= 13.04 (OH, s, H-5), 7.90-7.87 (2H, m, H-2', 6'), 7.56-7.52 (3H, m, H-3', 4', 5'), 6.67 (1H, s, H-3), 6.62 (1H, s, H-8), 6.14-6.01 (1H, m, H-2''),5.44-5.37 (1H, m, H-3''a), 5.32-5.28 (1H, m, H-3''b), 4.77 (2H, dt, J=3.3,1.2, H-1''); ^{13}C NMR ($CDCl_3$, 75.47 MHz) *δ*= 183.0 (C4), 164.1 (C2), 155.5 (C7), 153.3 (C8a), 152.1 (C5), 133.0 (C2''), 131.9 (C4'), 131.3 (C1'), 129.1 (C3', 5'), 128.7 (C6), 126.3 (C2', 6'), 120.0 (C3''), 106.1 (C4a), 105.3 (C3), 93.4 (C8), 73.7 (C1'').

7-ethoxy-5,6-dihydroxy-2-phenyl-4H-chromen-4-one (Betil1). Purified by flash chromatography (SiO_2; n-hexane: EtOAc, 9.5:0.5). Yield: 4.5 %; mp 159-161 ºC; IR (kBr) υmax: 3600-3300, 2952, 2922, 1653, 1559, 1507, 1457, 1189 cm^{-1}; ^{1}H NMR ($CDCl_3$, 300.13 MHz) *δ*= 12.55 (OH, s, H-5), 7.91-7.88 (2H, m, H-2',6'), 7.55-7.53 (3H, m, H-3',4',5'), 6.69 (1H, s, H-3), 6.61 (1H, s, H-8), 5.37 (OH, brs, H-6), 4.24 (2H, q, J=14.0, 7.0, H-1''), 1.55 (3H, t, J=7.0, H-2''); ^{13}C NMR ($CDCl_3$, 75.47 MHz) *δ*= 182.7 (C4), 164.1 (C2), 152.2 (C7), 150.7 (C8a), 145.7 (C5), 131.8 (C4'), 131.5 (C1'), 129.7 (C6), 129.1 (C3', 5'), 126.3 (C2', 6'), 106.0 (C4a), 105.5 (C3), 91.1 (C8), 65.2 (C1''), 14.6 (C2'').

5,6-dihydroxy-7-methoxy-2-phenyl-4H-chromen-4-one (Bemet1). Purified by flash chromatography (SiO_2; n-hexane: EtOAc, 9:1) followed by flash chromatography (SiO2; n-hexane). Yield: 15 x%; mp 203-205 ºC; IR(kBr) υmax: 3600-3300, 2922, 1631, 1467 cm^{-1}; 1H NMR (CDCl3, 300.13MHz) *δ*= 12.69 (OH, s, H-5), 7.92-7.89 (2H, m, H-2', 6'), 7.55-7.53 (3H, m, H-3', 4', 5'), 6.69 (1H, s, H-3), 6.58 (1H, s, H-8), 5.35 (OH, brs, H-6), 3.94 (3H, s, H-1''); ^{13}C NMR ($CDCl_3$, 75.47 MHz) *δ*= 182.8 (C4), 164.0 (C2), 153.1 (C7), 151.1 (C8a), 145.5 (C5), 131.9 (C4'), 131.3 (C1'), 129.7 (C6), 129.1 (C3', 5'), 126.3 (C2', 6'), 106.1 (C4a), 105.7 (C3), 90.7 (C8), 60.9 (C1'').

5-hydroxy-6,7-dimethoxy-2-phenyl-4H-chromen-4-one (Bemet2). Purified by flash chromatography (SiO_2; n-hexane: EtOAc, 9.5:0.5) followed by flash chromatography (SiO2; n-hexane). Yield: 1.5x%; mp 150-152 ºC; IR(kBr) υmax: 3600-3300, 2922, 1634, 1505, 1457, 1413 cm^{-1}; 1H NMR (CDCl3, 300.13MHz) *δ*= 12.69 (OH, s, H-5), 7.92-7.85 (2H, m, H-2', 6'), 7.57-7.52 (3H, m, H-3', 4', 5'), 6.68 (1H, s, H-3), 6.58 (1H, s, H-8), 3.98 (3H, s, H-1''), 3.93 (3H, s, H-1'''); ^{13}C NMR ($CDCl_3$, 75.47 MHz) *δ*= 182.8 (C4), 164.0 (C2),

159.0 (C7), 153.4 (C8a), 145.8 (C5), 131.9 (C4'), 131.3 (C1'), 132.7 (C6), 129.1 (C3', 5'), 126.3 (C2', 6'), 106.1 (C4a), 105.7 (C3), 90.7 (C8), 66.9 (C1'''), 56.4 (C1'').

5.1.1.4. Derivatives of 3,7-dihydroxyflavone

5.1.1.4.1. Alkylated derivatives of 3,7-dihydroxyflavone

A mixture of 3,7-dihydroxyflavone (**H**) (0.19g, 0.74mmol), isopentyl / butyl / propyl / allyl / ethyl / methyl iodide (1.18 mmol) and anhydrous K_2CO_3 (0.55 g, 3.7 mmol) in anhydrous acetone (60 mL) was submitted to successive 30 min of microwave irradiation at 200 W of potency. Total irradiation time was 2h and the final temperature was 60C. After cooling, the solid was filtered and the solvent removed under reduced pressure to afford the crude product. The yellow-green solid obtained was dissolved in acetone and purified as described below.

3-hydroxy-7-(isopentyloxy)-2-phenyl-4H-chromen-4-one (Hiso). Purified by flash chromatography (SiO_2; petroleum ether: EtOAc, 9.5:0.5) followed by preparative TLC (SiO2; n-hexane: EtOAc, 8:2) and crystallization (chloroform: n-hexane). Yield: 12.9 x %; mp = 181-184ºC; IR (kBr) υmax: 3600-3300, 2958, 2921, 2854, 1605, 1504, 1467, 1452, 1410, 1260 cm^{-1}; *δ*= 8.25-8.22 (2H, m, H-2', 6'), 8.12 (1H, d, J=8.9, H-5), 7.56-7.42 (3H, m, H-3', 4', 5'), 6.98 (1H, dd, J=8.9, 2.3, H-6), 6.94 (1H, d, J= 2.3, H-8), 4.11 (2H, t, J= 6.6, H-1''), 1.92-1.81 (1H, m, H-3''), 1.78-1.72 (2H, m, H-2''), 1.00 (6H, d, J=6.5, H-4'', 5''). ^{13}C NMR ($CDCl_3$, 75.47 MHz) *δ*= 172.9 (C4), 163.9 (C7), 157.4 (C8a), 144.1 (C2), 138.1 (C3), 131.3 (C1'), 129.6 (C4'), 128.6 (C3', 5'), 127.5 (C2', 6'), 126.7 (C5), 115.3 (C6), 115.1 (C4a), 100.3 (C8), 67.2 (C1''), 37.6 (C2''), 25.1 (C3''), 22.6 (C4'', 5'').

7-butoxy-3-hydroxy-2-phenyl-4H-chromen-4-one (Hutil1). Purified by flash chromatography (SiO_2; n-hexane : EtOAc, 9.5;0.5) followed by preparative TLC (SiO2; n-hexane: EtOAc, 8:2) and crystallization (chloroform: n-hexane) Yield: 9.7 x %; mp= 149-151ºC ; IR (kBr) υmax: 3600-3300, 2958, 2922, 2854, 1604, 1566, 1462, 1452, 1419, 1250 cm^{-1}; ^1H NMR ($CDCl_3$, 300.13 MHz) *δ*= 8.25-8.22 (2H, m, H-2', 6'), 8.13 (1H, d, J=8.6, H-5), 7.56-7.43 (3H, m, H-3', 4', 5'), 7.00 (1H, dd, J=8.8, 2.3, H-6), 6.95 (1H, d, J= 2.3, H-8), 4.09 (2H, t, J= 6.5, H-1''), 1.89-1.80 (2H, m, H-2''), 1.60-1.47 (2H, m, H-3''), 1.01

(3H, t, J=7.4, H-4''). ^{13}C NMR ($CDCl_3$, 75.47 MHz) *δ*= 206.0 (C4), 162.9 (C7), 156.4 (C8a), 143.1 (C2), 137.1 (C3), 131.3 (C1'), 130.2 (C4'), 128.9 (C3', 5'), 127.5 (C2', 6'), 126.5 (C5), 114.2 (C6), 113.4 (C4a), 99.3 (C8), 67.4 (C1''), 29.9 (C2''), 18.2 (C3''), 12.8 (C4'').

3,7-dibutoxy-2-phenyl-4H-chromen-4-one (Hutil2). Purified by flash chromatography (SiO_2; n-hexane : EtOAc, 9.75:0.25). Yield: 7.1 x%; mp= 190-193ºC ; IR(kBr) υmax: 3600-3300, 2936, 1873, 1623, 1499, 1466, 1447, 1260 cm^{-1}; ^{1}H NMR ($CDCl_3$, 300.13 MHz) *δ*= 8.10-8.07 (2H, m, H-2', 6'), 8.14 (1H, d, J=8.9, H-5), 7.52-7.49 (3H, m, H-3', 4', 5'), 6.96 (1H, dd, J=8.9, 2.3, H-6), 6.90 (1H, d, J= 2.3, H-8), 4.06 (2H, t, J=6.5, H-1''), 4.02 (2H, t, J=6.5, H-1'''), 1.87-1.78 (2H, m, H-2''), 1.73-1.63 (2H, m, H-2'''), 1.59-1.49 (2H, m, H-3''), 1.42-1.32 (2H, m, H-3'''), 1.00 (3H, t, J=7.4, H-4''), 0.87 (3H, t, J=7.4, H-4'''). ^{13}C NMR ($CDCl_3$, 75.47 MHz) *δ*= 174.8 (C4), 163.6 (C7), 157.1 (C8a), 155.3 (C2), 140.5 (C3), 131.3 (C1'), 130.4 (C4'), 128.3 (C2', 6'), 128.7 (C3'. C5'), 127.1 (C5), 114.8 (C6), 113.6 (C4a), 100.3 (C8), 72.6 (C1'''), 68.4 (C1''), 32.1 (C2'''), 31.0 (C2''), 19.2 (C3'''), 19.1 (C3''), 13.8 (C4'', 4''').

3-hydroxy-2-phenyl-7-propoxy-4H-chromen-4-one (Hrop). Purified by flash chromatography (SiO_2; petroleum ether: EtOAc, 95:5) followed by preparative TLC (SiO2; n-hexane: EtOAc, 8:2) and crystallization (chloroform: n-hexane). Yield: 3.7 x% as yellow crystals; mp= 173-174ºC; IR (kBr) υmax: 3600-3300, 2970, 1920, 1603, 1576, 1504, 1432, 1412, 1259 cm^{-1}; ^{1}H NMR ($CDCl_3$, 300.13 MHz) *δ*= 8.25-8.22 (2H, m, H-2', 6'), 8.13 (1H, d, J=8.9, H-5), 7.61-7.43 (3H, m, H-3', 4', 5'). 7.00 (1H, dd, J= 10.4, 2.3, H-6), 6.97 (1H, d, J=2.3, H-8), 4.05 (2H, t, J=6.6, H-1''), 1.95-1.83 (2H, m, H-2''), 1.09 (3H, t, J=7.4, H-3''). ^{13}C NMR ($CDCl_3$,75.47 MHz) *δ*= 172.9 (C4), 163.9 (C7), 157.4 (C8a), 144.1 (C2), 138.1 (C3), 131.3 (C1'),129.9 (C4'), 128.6 (C3', 5'), 127.5 (C2', 6'), 126.7 (C5), 115.3 (C6), 113.6 (C4a), 100.3 (C8), 70.3(C1''), 22.4 (C2''), 10.5 (C3'').

7-(allyloxy)-3-hydroxy-2-phenyl-4H-chromen-4-one (Hali). Purified by flash chromatography (SiO_2; n-hexane: EtOAc, 9.75:0.25) followed by preparative TLC (SiO2; n-hexane: EtOAc, 8:2) and crystallization (chloroform: n-hexane). Yield: 9.3 x%; mp= 144-146ºC; IR(kBr) υmax: 3600-3300, 2999, 2964, 2921, 2847, 1615, 1564, 1503, 1473, 1453, 1260 cm^{-1}; ^{1}H NMR ($CDCl_3$, 300.13 MHz) *δ*= 8.25-8.22 (2H, m, H-2', 6'), 8.15 (1H, d, J=8.9, H-5), 7.03 (1H, dd, J= 8.6, 2.3, H-6), 6.97 (1H, d, J=2.3, H-8), 6.16-6.03 (1H, m, H-2''), 5.52-5.44 (2H, m, H-3''a), 5.40-5.31 (2H, m, H-3''b), 4.67 (2H, dt, J=5.3, 1.5, H-1''). ^{13}C NMR ($CDCl_3$, 75.47 MHz) *δ*= 172.8 (C4), 163.2 (C7), 157.3 (C8a), 144.1 (C2), 138.1

(C3),131.9 (C2'') 131.2 (C1'), 129.9 (C4'), 128.6 (C3', 5'), 127.5 (C2', 6'), 126.8 (C5),118.6 (C3''), 115.2 (C6), 100.3 (C8), 69.6 (C1'').

7-ethoxy-3-hydroxy-2-phenyl-4H-chromen-4-one (Hetil). Purified by flash chromatography (SiO_2; n-hexane: EtOAc, 9.75:0.25) followed by preparative TLC (SiO2; n-hexane: EtOAc, 8:2) and crystallization (chloroform: n-hexane). Yield: 1.7 %; mp=195-197ºC; IR(kBr) υmax: 3600-3300, 2926, 1614, 1504, 1457, 1408, 1262 cm^{-1}; ^1H NMR ($CDCl_3$, 300.13 MHz) δ= 8.25-8.22 (2H, m, H-2', 6'), 8.13 (1H, d, J=8.9, H-5),7.56-7.43 (3H, m, H-3', 4', 5'), 6.99 (1H, dd, J= 8.9, 2.1, H-6), 6.95 (1H, d, J=2.4, H-8), 4.17 (2H, q, J= 6.9, H-1''), 1.50 (3H, t, J=6.9, H-2''). ^{13}C NMR ($CDCl_3$, 75.47 MHz) δ= 172.9 (C4), 163.7 (C7), 157.4 (C8a), 144.1 (C2), 138.1 (C3), 131.3 (C1'), 129.9 (C4'), 128.8 (C3', 5'), 127.5 (C2', 6'), 126.7 (C5), 115.2 (C6), 114.4 (C4a), 100.3 (C8), 64.3 (C1''), 14.6 (C2'').

3-hydroxy-7-methoxy-2-phenyl-4H-chromen-4-one (Hemet). Purified by flash chromatography (SiO_2; n-hexane: EtOAc, 9.75:0.25) followed by preparative TLC (SiO2; n-hexane: EtOAc, 8:2) and crystallization (chloroform: n-hexane). Yield: 9.2x%; mp 180-182 ºC; IR(kBr) υmax: 3600-3300, 2922, 1622, 1508, 1456, 1401, 1262 cm^{-1}; ^1H NMR ($CDCl_3$, 300.13 MHz) δ= 8.24-8.21 (2H, m, H-2', 6'), 8.13 (1H, d, J=8.9, H-5), 7.55-7.42 (3H, m, H-3', 4', 5'), 6.99 (1H, dd, J= 8.9, 2.3, H-6), 6.94 (1H, d, J=2.3, H-8), 3.93 (3H, s, H-1''). ^{13}C NMR ($CDCl_3$, 75.47 MHz) δ= 172.8 (C4), 164.3 (C7), 157.4 (C8a), 144.2 (C2), 138.1 (C3), 131.2 (C1'), 129.9 (C4'), 128.6 (C3', 5'), 127.5 (C2', 6'), 126.8 (C5), 115.2 (C6), 114.9 (C4a), 99.8 (C8), 53.9 (C1'').

5.1.1.4.2. Prenylated derivative of 3,7-dihydroxyflavone

A mixture of 3,7-dihydroxyflavone (**H**) (0.188 g, 0.74 mmol), prenyl bromide (171µl, 1.48 mmol), potassium iodide (0.012 g, 0.074 mmol) and anhydrous K_2CO_3 (0.55g, 3.7mmol,) in anhydrous acetone (60ml) was submitted to successive 15 min of microwave irradiation at 200 W of potency. Total irradiation time was 45 min and the final temperature was 60 °C. After cooling, the solid was filtered and the solvent removed under reduced pressure to afford the crude product. The solid obtained was dissolved in acetone and purified by flash chromatography (SiO_2; petroleum ether: EtOAc, 9.75:0.25) and then by preparative TLC (SiO_2; n-hexane: EtOAc, 7:3) and crystallization (chloroform: n-hexane). One compound was obtained (**Hrep**).

3-hydroxy-7-((3-methylbut-2-en-1-yl)oxy)-2-phenyl-4H-chromen-4-one (Hrep). Yield: 7.4 x%; mp= 174-176ºC; IR (kBr) υmax: 3600-3300, 2974, 2920, 2854, 1613, 1566, 1463, 1451, 1408, 1258 cm^{-1}; ^{1}H NMR ($CDCl_3$, 300.13 MHz) *δ*= 8.25-8.22 (2H, m, H-2' H-6'), 8.13 (1H, d, J=8.7, H-5), 761-7.44 (3H, m, H-3' H-4' H-5'), 7.02 (1H, d, J=2.3, H-6) ou 6.98 (1H, dd, J= 6.2, 2.2, H-6), 7.01 (1H, dd, J=8.8, 2.3, H-8) ou 6.97 (1H, d, J=2.2, H-8), 5.56-5.51 (1H, m, H-2'), 4.64 (2H, d, J=6.7, H-1''), 1.84 (3H, s, H-4''), 1.80 (3H, s, H-5''). ^{13}C NMR ($CDCl_3$, 75.47 MHz) *δ*= 207.0 (C4), 163.6 (C7), 157.4 (C8a), 144.2 (C2), 139.5 (C3), 131.3 (C1'), 129.9 (C4'), 128.6 (C3', 5'), 127.5 (C2', 6'), 126.7 (C5), 118.5 (C2''), 115.4 (C6), 114.7 (C4a), 100.6 (C8), 65.5 (C1''), 31.0 (C3''), 25.9 (C4'''), 18.3 (C5'').

5.1.1.5. Derivatives of chrysin

5.1.1.5.1. Alkylated derivatives of chrysin

A mixture of chrysin (**C**) (0.188g, 0.74mmol), isopentyl / butyl / propyl / allyl / ethyl / methyl iodide (1.18 mmol) and anhydrous K_2CO_3 (0.55 g, 3.7 mmol) in anhydrous acetone (60 mL) was submitted to successive 30 min of microwave irradiation at 200 W of potency. Total irradiation time was 90 min and the final temperature was 60 °C. After cooling, the solid was filtered and the solvent removed under reduced pressure to afford the crude product. The solid obtained was dissolved in acetone and purified by flash chromatography (SiO_2; n-hexane: EtOAc; 9:1).

5-hydroxy-7-(isopentyloxy)-2-phenyl-4H-chromen-4-one (Ciso). Yield: 30%; mp 129-132 ºC; IR (kBr) υmax: 3600-3400, 2956, 2921, 1851, 1662, 1588, 1452, 1169 cm^{-1}; ^{1}H NMR ($CDCl_3$, 300.13 MHz) *δ*= 12.71 (OH, s, H-5), 7.90-7.87 (2H, m, H-2', 6'), 7.55-7.52 (3H, m, H-3', 4', 5'), 6.67 (1H, s, H-3), 6.50 (1H, d, J=2.2, H-8), 6.37 (1H, d, J=2.2, H-6), 4.06 (2H, t, J=6.6, H-1''), 1.92-1.78 (1H, m, H-3''), 1.75-1.68 (2H, m, H-2''), 0.98 (6H, d, J=6.5, H-4'', 5''). ^{13}C NMR ($CDCl_3$, 75.47 MHz) *δ*= 182.5 (C4), 168.2 (C7), 163.9 (C2), 162.1 (C5), 131.8 (C1'), 129.1 (C3', 5'), 126.3 (C2', 6'), 105.9 (C3), 98.6 (C6), 93.1 (C8), 67.1 (C1''), 37.6 (C2''), 25.0 (C3''), 22.5 (C4'', 5'').

5-hydroxy-2-phenyl-7-propoxy-4H-chromen-4-one (Cutil). Yield: 29%; mp 145-148 ºC; IR (kBr) υmax: 3600-3400, 2952,2933, 2868, 1664, 1589, 1569, 1450, 1442,

1274, 1170 cm^{-1}; ^{1}H NMR ($CDCl_3$, 300.13 MHz) *δ*= 7.87-7.84 (2H, m, H-2', 6'), 7.52-7.50 (3H, m, H-3', 4', 5'), 6.63 (1H, s, H-3), 6.47 (1H, d, J=2.2, H-8), 6.34 (1H, d, J=2.2, H-6), 4.02 (2H, t, J=6.5, H-1''), 1.84-1.75 (2H, m, H-2''), 1.56-1.44 (2H, m, H-3''), 0.99 (3H, t, J=7.4, H-4''); ^{13}C NMR ($CDCl_3$, 75.47 MHz) *δ*= 182.4 (C4), 165.2 (C7), 163.8 (C2), 162.1 (C5), 157.8 (C8a), 131.8 (C4'), 131.3 (C1'), 129.1 (C3', 5'), 126.2 (C2', 6'), 105.8 (C3), 105.5 (C4a), 98.6 (C6), 93.0 (C8), 68.4 (C1''), 31.0 (C2''), 19.2 (C3''), 13.8 (C4'').

5-hydroxy-2-phenyl-7-propoxy-4H-chromen-4-one (Crop). Yield: 22%; mp 132-135 ºC; IR (kBr) υmax: 3600-3400, 2964, 2920, 2874, 1661, 1585, 1569, 1507, 1451, 1173 cm^{-1}; ^{1}H NMR ($CDCl_3$, 300.13 MHz) *δ*= 12.70 (OH, s, H-5), 7.90-7.87 (2H, m, H-2', 6'), 7.56-7.49 (3H, m, H-3', 4', 5'), 6.66 (1H, s, H-3), 6.50 (1H, d, J=2.2, H-8), 6.37 (1H, d, J=2.2, H-6), 4.00 (2H, t, J=6.6, H-1''), 1.90-1.79 (2H, m, H-2''), 1.06 (3H, t, J=7.4, H-3''). ^{13}C NMR ($CDCl_3$,75.47 MHz) *δ*= 182.5 (C4), 165.2 (C7), 163.9 (C2), 162.1 (C5), 157.8 (C8a), 131.8 (C4'), 131.4 (C1'), 129.1 (C3', 5'), 126.3 (C2', 6'), 105.9 (C3), 105.6 (C4a), 98.6 (C6), 93.1 (C8), 70.2 (C1''), 22.3 (C2''), 10.4 (C3'').

7-(allyloxy)-5-hydroxy-2-phenyl-4H-chromen-4-one (Cali). Yield: 31%; mp 118-120 ºC; IR (kBr) υmax: 3600-3400, 2961, 2920, 2851, 1665, 1586, 1506, 1451, 1203, 1170 cm^{-1}; ^{1}H NMR ($CDCl_3$, 300.13 MHz) *δ*= 12.72 (OH, s, H-5), 7.90-7.88 (2H, m, H-2, 6'), 7.58-7.51 (3H, m, H-3', 4', 5'), 6.68 (1H, s, H-3), 6.53 (1H, d, J=2.3, H-8), 6.40 (1H, d, J=2.3, H-6), 6.10-6.02 (1H, m, H-2'') 5.48-5.44 m (1H, m, H-3''a), 5.37-5.34 (1H, m, H-3''b), 4.63 (2H, dt, J=5.2, 1.4, H-1''); ^{13}C NMR ($CDCl_3$, 75.47 MHz) *δ*= 182.5 (C4), 164.6 (C7), 164.0 (C2), 162.2 (C5), 157.8 (C8a), 132.1 (C2''), 131.9 (C4'), 131.4 (C1'), 129.1 (C3', 5'), 126.3 (C2', 6'), 118.5 (C3'''), 105.9 (C3), 105.8 (C4a), 98.8 (C6), 93.4 (C8), 69.3 (C1'').

7-ethoxy-5-hydroxy-2-phenyl-4H-chromen-4-one (Cetil). Yield: 32%; mp 153-154 ºC; IR (kBr) υmax: 3600-3400, 2985, 2924, 2852, 1663, 1586, 1509, 1454, 1204, 1173 cm^{-1}; ^{1}H NMR ($CDCl_3$, 300.13 MHz) *δ*= 7.89-7.86 (2H, m, H-2',6'), 7.53-7.51 (3H, m, H-3', 4', 5'), 6.65 (1H, s, H-3), 6.48 (1H, d, J=2.2, H-8), 6.35 (1H, d, J=2.2, H-6), 4.10 (2H, q, J=7.0, H-1''), 1.45 (3H, t, J=7.0, H-2''); ^{13}C NMR ($CDCl_3$, 75.47 MHz) *δ*= 182.5 (C4), 165.0 (C7), 163.9 (C2), 162.1 (C5), 157.8 (C8a), 131.8 (C4'), 131.3 (C1'), 129.1 (C3', 5'), 126.3 (C2', 6'), 105.8 (C3), 105.6 (C4a), 98.6 (C6), 93.1 (C8), 64.2 (C1''), 14.6 (C2'').

5-hydroxy-7-methoxy-2-phenyl-4H-chromen-4-one (Cemet). Yield: 44%; mp 165-168 ºC; IR(kBr) υmax: 3600-3400, 2923, 2854, 1668, 1588, 1495, 1452, 1436, 1202, 1160 cm^{-1}; ^{1}H NMR ($CDCl_3$, 300.13 MHz) *δ*= 12.73 (OH, s, H-5), 7.91-7.88 (2H, m, H-2', 6'), 7.55-7.52 (3H, m, H-3', 4', 5'), 6.67 (1H, s, H-3), 6.51 (1H, d, J=2.2, H-8), 6.38 (1H, d, J=2.2, H-6), 3.89 (3H, s, H-1''); ^{13}C NMR ($CDCl_3$, 75.47 MHz) *δ*= 182.5 (C4), 165.6 (C7), 164.0 (C2), 162.2 (C5), 157.8 (C8a), 131.9 (C4'), 131.3 (C1'), 129.1 (C3', 5'), 126.3 (C2', 6'), 105.9 (C3), 105.7 (C4a), 98.2 (C6), 92.7 (C8), 55.8 (C1'').

5.1.1.5.2. Prenylated derivative of chrysin

A mixture of Chrysin (**C**) (0.188 g, 0.74 mmol), prenyl bromide (171 µL, 1.48 mmol), potassium iodide (0.012 g, 0.074 mmol) and anhydrous K_2CO_3 (0.55 g, 3.7 mmol) in anhydrous acetone (60 mL) was submitted to successive 30 min of microwave irradiation at 200 W of potency. Total irradiation time was 90 min and the final temperature was 60 °C. After cooling, the solid was filtered and the solvent removed under reduced pressure to afford the crude product. The yellow-orange solid obtained was dissolved in acetone and purified by flash chromatography (SiO_2; n-hexane: EtOAc; 9:1). One compound was isolated (**Crep**).

5-hydroxy-7-((3-methylbut-2-en-1-yl)oxy)-2-phenyl-4H-chromen-4-one (Crep): Yield: 67%; mp 104-107 ºC; IR (kBr) υmax: 3600-3400, 2967, 2917, 2853, 1659, 1588, 1504, 1449, 1178 cm^{-1}; ^{1}H NMR ($CDCl_3$, 300.13 MHz) *δ*= 12.69 (OH, s, H-5), 7.86-7.82 (2H, m, H-2', 6'), 7.51-7.48 (3H, m, H-3', 4', 5'), 6.61 (1H, s, H-3), 6.46 (1H, d, J=2.2, H-8), 6.33 (1H, d, J=2.2, H-6), 5.48 (1H, t, J=6.7, H-2''), 4.56 (2H, d, J=6.9, H-1''), 1.81 (3H, s, H-4''), 1.76 (3H, s, H-5''); ^{13}C NMR ($CDCl_3$, 75.47 MHz) *δ*= 182.4 (C4), 164.9 (C7), 163.8 (C2), 162.0 (C5), 157.7 (C8a), 139.2 (C3''), 131.8 (C4'), 131.2 (C1'), 129.0 (C3', 5'), 126.2 (C2', 6'), 118.6 (C2''), 105.7 (C3), 105.6 (C4a), 98.8 (C6), 93.2 (C8), 65.5 (C1''), 25.8 (C4''), 18.3 (C5'').

5.2 Peak purity

Analytical HPLC-DAD analyses were performed on a SpectraSYSTEM (Thermo Fisher Scientific, Inc, USA) equipped with a P4000 pump, a AS3000 autosampler and a diode array detector UV8000. The separation was carried out on a 250 x 4.6 mm i.d. FortisBIO C18 (5 µm) (Fortis^{TM} Technologies Ltd, Cheshire, UK).

LC analysis was performed by isocratic elution using a mixture of MeOH:H_2O:$MeCO_2H$ (70:30:1 v/v/v) as mobile phase and the flow rate was set at 1 mL/ min. The injected volume was 20 µL and the eluent was monitored at 275 nm. The detector was set at a wavelength range of 190–800 nm with a spectral resolution of 1 nm. The purity parameters included a 95 % active peak region and a scan threshold of 5 mAU. ChromQuest 5.0 (version 3.2.1) software (Thermo Fisher Scientific Inc.) managed chromatographic data. Methanol (HPLC grade) was obtained from Carlo Erba Reagents (Val de Reuil, Italy), acetic acid (HPLC grade) was obtained from Romil Pure Chemistry (Cambridge, UK) and HPLC grade water obtained from a Simplicity® UV Ultrapure Water System, Millipore Corporation, USA. Prior to use, mobile phase solvents were degassed in an ultrasonic bath for 15 min.

5.3. Biological activity

5.3.1. Reagents and stock solutions of compounds

Procaspase-activating compound-1 (PAC-1) were purchased from Calbiochem. Solutions of compounds were dissolved in dimethyl sulfoxide (DMSO; Sigma-Aldrich) and stored at -20 ºC. Appropriate dilutions of the compounds were freshly prepared with culture medium prior to the assays. Glucose, galactose and glycerol were from Sigma-Aldrich (Sintra, Portugal). Yeast nitrogen base without amino acids from Difco (Quilaban, Sintra, Portugal). Sabouraud Dextrose Agar (SDA) from Liofilchem (Frilabo, Porto, Portugal).

5.3.2. Yeast procaspase-3 and -7 assay[†]

5.3.2.1. Compounds

Details concerning the synthesis of tested flavonoids **Biso1**, **Brop1** and **Bali1** are described in the **chapter III** and **V**.

5.3.2.2. Plasmids

For expression in yeast of procaspase-3 and -7 the expression vectors pGALL-(LEU2) encoding each human protein under a GAL1-10 promoter were used.

5.3.2.3. Yeast strain, transformation and growth conditions

[†] Work developed by the Master student Sofia Salazar under the supervision of Professor Lucília Saraiva (FFUP) – ongoing studies.

Saccharomyces cerevisiae (strain CG379 Mata, ade5, his2, leu2-112, trp1-289, ura3-52) was granted by Yeast Genetic Center, University of California, USA. *Saccharomyces cerevisiae* was transformed using the standard lithium acetate method [175]. For the selection of transformed yeast, cells were grown in glucose minimal selective medium with 2% (w/v) glucose, 0.67% (w/v) yeast nitrogen base without amino acids and all the amino acids required for yeast growth (50 µg/ml) except leucine, and incubated at 30 ºC, under continuous orbital shaking (170 r.p.m.). To induce the expression of human proteins, yeast cultures were diluted to 0.05 optical density at 600 nm ($_{OD600}$) in induction selective medium containing 2% (w/v) galactose and 1% glycerol and grown at 30 ºC under continuous shaking. The effects of procaspase-3 and -7 on yeast growth were analyzed as previously described for the active caspase-3 [192]. Briefly, yeast cells expressing the human protein and control yeast (transformed with the empty vector, pGALL) were grown in induction selective medium for up to 24 h for growth curves experiments. Yeast growth was analyzed by counting the number of colony-forming units per ml (CFU/ml) after 2 days incubation at 30 ºC on Sabouraud Dextrose Agar plates.

5.3.2.4. Effects of the compounds on yeast cell growth

In yeast assays with procaspase-3 and -7, the known activator of caspase-3 and -7, PAC-1 [33], was used as positive control. To analyze the effect of compounds on yeast cell growth, transformed cells were incubated in induction selective medium in the presence of 0.1–15 µM (for procaspases) compounds, 0.1-50 µM of PAC-1, or DMSO only (0.1%). Cells were incubated to approximately 0.3 OD_{600} (achieved with each transformant incubated with DMSO only), and the cell growth was analyzed as described above. For each culture, the percentage of drug-induced growth inhibition was estimated considering 100% growth the number of CFU obtained with yeast incubated with DMSO only.

5.3.2.5. Statistical analysis

For yeast-based assays results were analyzed statistically using the SigmaPlot 12.00 software and differences between means were tested for significance using the unpaired student´s *t*-test ($p < 0.01$ or $p < 0.001$).

5.4. Docking study

Structure files for each molecule were created and minimized using the chemical structure drawing tool Hyperchem 7.5 (Hypercube, FL, USA). Docking studies were performed using Autodock Vina software package (Molecular Graphics Lab, CA, USA). The molecular modeling program UCSF Chimera 1.4 was used to prepare the receptor (procaspase-3, pdb ID 4JR0; procaspase-6, pdb ID 4NBN; procaspase-7, pdb ID 1GQF).The allosteric site in the procaspases dimer interface [189] was selected for use in docking simulation by building a grid box with the dimentions 25 x 25 x 25 Å. Docking was performed by incorporating ligand flexibility, and docking scores were used for analysis. PyMol1.3 (Schrödinger , NY, USA) was used for visual inspection of results and graphical representations.

Chapter 6:

References

1. Boatright, K. M.; Salvesen, G. S., Mechanisms of caspase activation. *Current opinion in cell biology* **2003,** *15* (6), 725-731.

2. Häcker, H.-G.; Sisay, M. T.; Gütschow, M., Allosteric modulation of caspases. *Pharmacology & therapeutics* **2011,** *132* (2), 180-195.

3. McIlwain, D. R.; Berger, T.; Mak, T. W., Caspase functions in cell death and disease. *Cold Spring Harbor perspectives in biology* **2013,** *5* (4), a008656.

4. Akpan, N.; Troy, C. M., Caspase Inhibitors Prospective Therapies for Stroke. *The Neuroscientist* **2013,** *19* (2), 129-136.

5. Chowdhury, I.; Tharakan, B.; Bhat, G. K., Caspases—an update. *Comparative Biochemistry and Physiology Part B: Biochemistry and Molecular Biology* **2008,** *151* (1), 10-27.

6. Parrish, A. B.; Freel, C. D.; Kornbluth, S., Cellular mechanisms controlling caspase activation and function. *Cold Spring Harbor perspectives in biology* **2013,** *5* (6), a008672.

7. Stennicke, H. R.; Salvesen, G. S., Caspases–controlling intracellular signals by protease zymogen activation. *Biochimica et Biophysica Acta (BBA)-Protein Structure and Molecular Enzymology* **2000,** *1477* (1), 299-306.

8. Rupinder, S. K.; Gurpreet, A. K.; Manjeet, S., Cell suicide and caspases. *Vascular pharmacology* **2007,** *46* (6), 383-393.

9. Tait, S. W.; Green, D. R., Mitochondria and cell death: outer membrane permeabilization and beyond. *Nature Reviews Molecular Cell Biology* **2010,** *11* (9), 621-632.

10. Sayers, T. J., Targeting the extrinsic apoptosis signaling pathway for cancer therapy. *Cancer Immunology, Immunotherapy* **2011,** *60* (8), 1173-1180.

11. Cornelis, S.; Kersse, K.; Festjens, N.; Lamkanfi, M.; Vandenabeele, P., Inflammatory caspases: targets for novel therapies. *Current pharmaceutical design* **2007,** *13* (4), 367-385.

12. Le, G. T.; Abbenante, G.; Madala, P. K.; Hoang, H. N.; Fairlie, D. P., Organic azide inhibitors of cysteine proteases. *Journal of the American Chemical Society* **2006,** *128* (38), 12396-12397.

13. Löser, R.; Abbenante, G.; Madala, P. K.; Halili, M.; Le, G. T.; Fairlie, D. P., Noncovalent tripeptidyl benzyl-and cyclohexyl-amine inhibitors of the cysteine protease caspase-1. *Journal of medicinal chemistry* **2010,** *53* (6), 2651-2655.

14. Callus, B.; Vaux, D., Caspase inhibitors: viral, cellular and chemical. *Cell Death & Differentiation* **2007,** *14* (1), 73-78.

15. Boxer, M. B.; Quinn, A. M.; Shen, M.; Jadhav, A.; Leister, W.; Simeonov, A.; Auld, D. S.; Thomas, C. J., A Highly Potent and Selective Caspase 1 Inhibitor that Utilizes a Key 3-Cyanopropanoic Acid Moiety. *ChemMedChem* **2010,** *5* (5), 730-738.

16. Wannamaker, W.; Davies, R.; Namchuk, M.; Pollard, J.; Ford, P.; Ku, G.; Decker, C.; Charifson, P.; Weber, P.; Germann, U. A., (S)-1-((S)-2-{[1-(4-Amino-3-chloro-phenyl)-methanoyl]-amino}-3, 3-dimethyl-butanoyl)-pyrrolidine-2-carboxylic acid ((2R, 3S)-2-ethoxy-5-oxo-tetrahydro-furan-3-yl)-amide (VX-765), an Orally Available Selective Interleukin (IL)-Converting Enzyme/Caspase-1 Inhibitor, Exhibits Potent Anti-Inflammatory Activities by Inhibiting the Release of IL-1β and IL-18. *Journal of Pharmacology and Experimental Therapeutics* **2007,** *321* (2), 509-516.

17. Fuentes-Prior, P.; Salvesen, G., The protein structures that shape caspase activity, specificity, activation and inhibition. *Biochem. J* **2004,** *384*, 201-232.

18. Lee, D.; Long, S. A.; Adams, J. L.; Chan, G.; Vaidya, K. S.; Francis, T. A.; Kikly, K.; Winkler, J. D.; Sung, C.-M.; Debouck, C., Potent and selective nonpeptide inhibitors of caspases 3 and 7 inhibit apoptosis and maintain cell functionality. *Journal of Biological Chemistry* **2000,** *275* (21), 16007-16014.

19. Weber, I. T.; Fang, B.; Agniswamy, J., Caspases: structure-guided design of drugs to control cell death. *Mini reviews in medicinal chemistry* **2008,** *8* (11), 1154-1162.

20. Chu, W.; Rothfuss, J.; d'Avignon, A.; Zeng, C.; Zhou, D.; Hotchkiss, R. S.; Mach, R. H., Isatin sulfonamide analogs containing a Michael addition acceptor: a new class of caspase 3/7 inhibitors. *Journal of medicinal chemistry* **2007,** *50* (15), 3751-3755.

21. Chu, W.; Rothfuss, J.; Chu, Y.; Zhou, D.; Mach, R. H., Synthesis and in vitro evaluation of sulfonamide isatin Michael acceptors as small molecule inhibitors of caspase-6. *Journal of medicinal chemistry* **2009,** *52* (8), 2188-2191.

22. Fattorusso, R.; Jung, D.; Crowell, K. J.; Forino, M.; Pellecchia, M., Discovery of a novel class of reversible non-peptide caspase inhibitors via a structure-based approach. *Journal of medicinal chemistry* **2005,** *48* (5), 1649-1656.

23. Kravchenko, D. V.; Kysil, V. V.; Ilyn, A. P.; Tkachenko, S. E.; Maliarchouk, S.; Okun, I. M.; Ivachtchenko, A. V., 1, 3-Dioxo-4-methyl-2, 3-dihydro-1< i> H</i>-pyrrolo [3, 4-< i> c</i>] quinolines as potent caspase-3 inhibitors. *Bioorganic & medicinal chemistry letters* **2005,** *15* (7), 1841-1845.

24. Kravchenko, D. V.; Kysil, V. M.; Tkachenko, S. E.; Maliarchouk, S.; Okun, I. M.; Ivachtchenko, A. V., Synthesis and caspase-3 inhibitory activity of 8-sulfonyl-1, 3-dioxo-2, 3-dihydro-1H-pyrrolo[3, 4-c] quinolines. *Il Fármaco* **2005,** *60* (10), 804-809.

25. Hauske, P.; Ottmann, C.; Meltzer, M.; Ehrmann, M.; Kaiser, M., Allosteric regulation of proteases. *ChemBioChem* **2008,** *9* (18), 2920-2928.

26. Erlanson, D. A.; Braisted, A. C.; Raphael, D. R.; Randal, M.; Stroud, R. M.; Gordon, E. M.; Wells, J. A., Site-directed ligand discovery. *Proceedings of the National Academy of Sciences* **2000,** *97* (17), 9367-9372.

27. Scheer, J. M.; Romanowski, M. J.; Wells, J. A., A common allosteric site and mechanism in caspases. *Proceedings of the National Academy of Sciences* **2006,** *103* (20), 7595-7600.

28. Hardy, J. A.; Lam, J.; Nguyen, J. T.; O'Brien, T.; Wells, J. A., Discovery of an allosteric site in the caspases. *Proceedings of the National Academy of Sciences of the United States of America* **2004,** *101* (34), 12461-12466.

29. Murray, J.; Renslo, A. R., Modulating caspase activity: beyond the active site. *Current opinion in structural biology* **2013,** *23* (6), 812-819.

30. MacKenzie, S. H.; Clark, A. C., Targeting cell death in tumors by activating caspases. *Current cancer drug targets* **2008,** *8* (2), 98.

31. Wu, T. Y.; Wagner, K. W.; Bursulaya, B.; Schultz, P. G.; Deveraux, Q. L., Development and characterization of nonpeptidic small molecule inhibitors of the XIAP/caspase-3 interaction. *Chemistry & biology* **2003,** *10* (8), 759-767.

32. Huang, J.-W.; Zhang, Z.; Wu, B.; Cellitti, J. F.; Zhang, X.; Dahl, R.; Shiau, C.-W.; Welsh, K.; Emdadi, A.; Stebbins, J. L., Fragment-based design of small molecule X-linked inhibitor of apoptosis protein inhibitors. *Journal of medicinal chemistry* **2008,** *51* (22), 7111-7118.

33. Putt, K. S.; Chen, G. W.; Pearson, J. M.; Sandhorst, J. S.; Hoagland, M. S.; Kwon, J.-T.; Hwang, S.-K.; Jin, H.; Churchwell, M. I.; Cho, M.-H., Small-molecule activation of procaspase-3 to caspase-3 as a personalized anticancer strategy. *Nature Chemical Biology* **2006,** *2* (10), 543-550.

34. Peterson, Q. P.; Goode, D. R.; West, D. C.; Ramsey, K. N.; Lee, J. J.; Hergenrother, P. J., PAC-1 activates procaspase-3 in vitro through relief of zinc-mediated inhibition. *Journal of molecular biology* **2009,** *388* (1), 144-158.

35. Peterson, Q. P.; Hsu, D. C.; Goode, D. R.; Novotny, C. J.; Totten, R. K.; Hergenrother, P. J., Procaspase-3 activation as an anti-cancer strategy: structure− activity relationship of procaspase-activating compound 1 (PAC-1) and Its cellular co-localization with caspase-3. *Journal of medicinal chemistry* **2009,** *52* (18), 5721-5731.

36. MacKenzie, S. H.; Schipper, J. L.; Clark, A. C., The potential for caspases in drug discovery. *Current opinion in drug discovery & development* **2010,** *13* (5), 568.

37. Roth, H. S.; Botham, R. C.; Schmid, S. C.; Fan, T. M.; Dirikolu, L.; Hergenrother, P. J., Removal of Metabolic Liabilities Enables Development of Derivatives of Procaspase-Activating Compound 1 (PAC-1) with Improved Pharmacokinetics. *Journal of medicinal chemistry* **2015,** *58* (9), 4046-4065.

38. Ma, J.; Chen, D.; Lu, K.; Wang, L.; Han, X.; Zhao, Y.; Gong, P., Design, synthesis, and structure–activity relationships of novel benzothiazole derivatives bearing the ortho-hydroxy N-carbamoylhydrazone moiety as potent antitumor agents. *European journal of medicinal chemistry* **2014,** *86*, 257-269.

39. Ma, J.; Zhang, G.; Han, X.; Bao, G.; Wang, L.; Zhai, X.; Gong, P., Synthesis and Biological Evaluation of Benzothiazole Derivatives Bearing the ortho-Hydroxy-N-acylhydrazone Moiety as Potent Antitumor Agents. *Archiv der Pharmazie* **2014,** *347* (12), 936-949.

40. Wolan, D. W.; Zorn, J. A.; Gray, D. C.; Wells, J. A., Small-molecule activators of a proenzyme. *Science* **2009,** *326* (5954), 853-858.

41. Li, Y.-L.; Gan, G.-P.; Zhang, H.-Z.; Wu, H.-Z.; Li, C.-L.; Huang, Y.-P.; Liu, Y.-W.; Liu, J.-W., A flavonoid glycoside isolated from< i> Smilax china</i> L. rhizome< i> in vitro</i> anticancer effects on human cancer cell lines. *Journal of ethnopharmacology* **2007,** *113* (1), 115-124.

42. Procházková, D.; Boušová, I.; Wilhelmová, N., Antioxidant and prooxidant properties of flavonoids. *Fitoterapia* **2011,** *82* (4), 513-523.

43. Romagnolo, D. F.; Selmin, O. I., Flavonoids and cancer prevention: a review of the evidence. *Journal of nutrition in gerontology and geriatrics* **2012,** *31* (3), 206-238.

44. Cheng, A.-X.; Han, X.-J.; Wu, Y.-F.; Lou, H.-X., The function and catalysis of 2-oxoglutarate-dependent oxygenases involved in plant flavonoid biosynthesis. *International journal of molecular sciences* **2014,** *15* (1), 1080-1095.

45. Harborne, J. B.; Mabry, T. J.; Mabry, H., *The Flavonoids*. Academic Press: 1975.

46. Ma, D.; Sun, D.; Wang, C.; Li, Y.; Guo, T., Expression of flavonoid biosynthesis genes and accumulation of flavonoid in wheat leaves in response to drought stress. *Plant Physiology and Biochemistry* **2014,** *80*, 60-66.

47. Russo, G. L., Ins and outs of dietary phytochemicals in cancer chemoprevention. *Biochemical Pharmacology* **2007,** *74* (4), 533-544.

48. Sato, M.; Ramarathnam, N.; Suzuki, Y.; Ohkubo, T.; Takeuchi, M.; Ochi, H., Varietal differences in the phenolic content and superoxide radical scavenging potential of wines from different sources. *Journal of Agricultural and Food Chemistry* **1996,** *44* (1), 37-41.

49. ib Bhattacharya, S., Natural antimutagens: a review. *Research Journal of Medicinal Plant* **2011,** *5* (2), 116-126.

50. Cushnie, T.; Lamb, A. J., Recent advances in understanding the antibacterial properties of flavonoids. *International journal of antimicrobial agents* **2011,** *38* (2), 99-107.

51. Ravishankar, D.; Rajora, A. K.; Greco, F.; Osborn, H. M., Flavonoids as prospective compounds for anti-cancer therapy. *The international journal of biochemistry & cell biology* **2013,** *45* (12), 2821-2831.

52. Mojzis, J.; Varinska, L.; Mojzisova, G.; Kostova, I.; Mirossay, L., Antiangiogenic effects of flavonoids and chalcones. *Pharmacological research* **2008,** *57* (4), 259-265.

53. García-Lafuente, A.; Guillamón, E.; Villares, A.; Rostagno, M. A.; Martínez, J. A., Flavonoids as anti-inflammatory agents: implications in cancer and cardiovascular disease. *Inflammation Research* **2009,** *58* (9), 537-552.

54. Santangelo, C.; Varì, R.; Scazzocchio, B.; Di Benedetto, R.; Filesi, C.; Masella, R., Polyphenols, intracellular signalling and inflammation. *Annali-istituto superiore di sanita* **2007,** *43* (4), 394.

55. Kawai, M.; Hirano, T.; Higa, S.; Arimitsu, J.; Maruta, M.; Kuwahara, Y.; Ohkawara, T.; Hagihara, K.; Yamadori, T.; Shima, Y., Flavonoids and related compounds as anti-allergic substances. *Allergol Int* **2007,** *56* (2), 113-123.

56. Nishiumi, S.; Miyamoto, S.; Kawabata, K.; Ohnishi, K.; Mukai, R.; Murakami, A.; Ashida, H.; Terao, J., Dietary flavonoids as cancer-preventive and therapeutic biofactors. *Frontiers in bioscience (Scholar edition)* **2010,** *3*, 1332-1362.

57. Yao, H.; Xu, W.; Shi, X.; Zhang, Z., Dietary flavonoids as cancer prevention agents. *Journal of Environmental Science and Health, Part C* **2011,** *29* (1), 1-31.

58. Ribeiro, D.; Freitas, M.; Tomé, S. M.; Silva, A. M.; Porto, G.; Cabrita, E. J.; Marques, M. M. B.; Fernandes, E., Inhibition of LOX by flavonoids: a structure–activity relationship study. *European journal of medicinal chemistry* **2014,** *72*, 137-145.

59. Marzocchella, L.; Fantini, M.; Benvenuto, M.; Masuelli, L.; Tresoldi, I.; Modesti, A.; Bei, R., Dietary flavonoids: molecular mechanisms of action as anti-inflammatory agents. *Recent patents on inflammation & allergy drug discovery* **2011,** *5* (3), 200-220.

60. Cermak, R., Effect of dietary flavonoids on pathways involved in drug metabolism. **2008**.

61. Gamet-Payrastre, L.; Manenti, S.; Gratacap, M.-P.; Tulliez, J.; Chap, H.; Payrastre, B., Flavonoids and the inhibition of PKC and PI 3-kinase. *General Pharmacology: The Vascular System* **1999,** *32* (3), 279-286.

62. Bensasson, R. V.; Zoete, V.; Jossang, A.; Bodo, B.; Arimondo, P. B.; Land, E. J., Potency of inhibition of human DNA topoisomerase I by flavones assessed through

physicochemical parameters. *Free Radical Biology and Medicine* **2011,** *51* (7), 1406-1410.

63. Nguyen, N. T.; Nguyen, M. H. K.; Nguyen, H. X.; Bui, N. K. N.; Nguyen, M. T. T., Tyrosinase Inhibitors from the Wood of Artocarpus heterophyllus. *Journal of natural products* **2012,** *75* (11), 1951-1955.

64. Zheng, Z.-P.; Tan, H.-Y.; Wang, M., Tyrosinase inhibition constituents from the roots of Morus australis. *Fitoterapia* **2012,** *83* (6), 1008-1013.

65. Awasthi, M.; Singh, S.; Pandey, V. P.; Dwivedi, U. N., Molecular docking and 3D-QSAR-based virtual screening of flavonoids as potential aromatase inhibitors against estrogen-dependent breast cancer. *Journal of Biomolecular Structure and Dynamics* **2015,** *33* (4), 804-819.

66. Middleton, E.; Kandaswami, C.; Theoharides, T. C., The effects of plant flavonoids on mammalian cells: implications for inflammation, heart disease, and cancer. *Pharmacological reviews* **2000,** *52* (4), 673-751.

67. Banerjee, S.; Li, Y.; Wang, Z.; Sarkar, F. H., Multi-targeted therapy of cancer by genistein. *Cancer letters* **2008,** *269* (2), 226-242.

68. Karp, J. E.; Passaniti, A.; Gojo, I.; Kaufmann, S.; Bible, K.; Garimella, T. S.; Greer, J.; Briel, J.; Smith, B. D.; Gore, S. D., Phase I and pharmacokinetic study of flavopiridol followed by 1-β-d-arabinofuranosylcytosine and mitoxantrone in relapsed and refractory adult acute leukemias. *Clinical Cancer Research* **2005,** *11* (23), 8403-8412.

69. Smith, M. E.; Cimica, V.; Chinni, S.; Challagulla, K.; Mani, S.; Kalpana, G. V., Rhabdoid tumor growth is inhibited by flavopiridol. *Clinical Cancer Research* **2008,** *14* (2), 523-532.

70. Castelli, S.; Coletta, A.; D'Annessa, I.; Fiorani, P.; Tesauro, C.; Desideri, A., Interaction between natural compounds and human topoisomerase I. **2012**.

71. Salti, G.; Grewal, S.; Mehta, R.; Gupta, T. D.; Boddie Jr, A.; Constantinou, A., Genistein induces apoptosis and topoisomerase II-mediated DNA breakage in colon cancer cells. *European Journal of Cancer* **2000,** *36* (6), 796-802.

72. Li, A.-N.; Li, S.; Zhang, Y.-J.; Xu, X.-R.; Chen, Y.-M.; Li, H.-B., Resources and Biological Activities of Natural Polyphenols. *Nutrients* **2014,** *6* (12), 6020-6047.

73. Ren, W.; Qiao, Z.; Wang, H.; Zhu, L.; Zhang, L., Flavonoids: promising anticancer agents. *Medicinal research reviews* **2003,** *23* (4), 519-534.

74. Qiao, C.; Wei, L.; Dai, Q.; Zhou, Y.; Yin, Q.; Li, Z.; Xiao, Y.; Guo, Q.; Lu, N., UCP2-Related Mitochondrial Pathway Participates in Oroxylin A-Induced Apoptosis in Human Colon Cancer Cells. *Journal of cellular physiology* **2015,** *230* (5), 1054-1063.

75. Das, A.; Banik, N. L.; Ray, S. K., Mechanism of apoptosis with the involvement of calpain and caspase cascades in human malignant neuroblastoma

SH-SY5Y cells exposed to flavonoids. *International journal of cancer* **2006,** *119* (11), 2575-2585.

76. Shchemelinin, I.; Sefc, L.; Necas, E., Protein kinases, their function and implication in cancer and other diseases. *Folia biologica* **2005,** *52* (3), 81-100.

77. Singh, M.; Kaur, M.; Silakari, O., Flavones: an important scaffold for medicinal chemistry. *European journal of medicinal chemistry* **2014,** *84*, 206-239.

78. Lee, L.-T.; Huang, Y.-T.; Hwang, J.-J.; Lee, A. Y.-L.; Ke, F.-C.; Huang, C.-J.; Kandaswami, C.; Lee, P.-P. H.; Lee, M.-T., Transinactivation of the epidermal growth factor receptor tyrosine kinase and focal adhesion kinase phosphorylation by dietary flavonoids: effect on invasive potential of human carcinoma cells. *Biochemical pharmacology* **2004,** *67* (11), 2103-2114.

79. Kern, M.; Tjaden, Z.; Ngiewih, Y.; Puppel, N.; Will, F.; Dietrich, H.; Pahlke, G.; Marko, D., Inhibitors of the epidermal growth factor receptor in apple juice extract. *Molecular nutrition & food research* **2005,** *49* (4), 317-328.

80. Li, F.; Zhang, Y.; Qiu, D.; Kang, J., Screening of epidermal growth factor receptor inhibitors in natural products by capillary electrophoresis combined with high performance liquid chromatography–tandem mass spectrometry. *Journal of Chromatography A* **2015**.

81. Moyle, C. W.; Cerezo, A. B.; Winterbone, M. S.; Hollands, W. J.; Alexeev, Y.; Needs, P. W.; Kroon, P. A., Potent inhibition of VEGFR-2 activation by tight binding of green tea epigallocatechin gallate and apple procyanidins to VEGF: Relevance to angiogenesis. *Molecular nutrition & food research* **2015,** *59* (3), 401-412.

82. Li, F.; Bai, Y.; Zhao, M.; Huang, L.; Li, S.; Li, X.; Chen, Y., Quercetin Inhibits Vascular Endothelial Growth Factor-Induced Choroidal and Retinal Angiogenesis in vitro. *Ophthalmic research* **2015,** *53* (3), 109-116.

83. Singh, R. P.; Agarwal, R., Natural flavonoids targeting deregulated cell cycle progression in cancer cells. *Current drug targets* **2006,** *7* (3), 345-354.

84. Khoo, B. Y.; Chua, S. L.; Balaram, P., Apoptotic effects of chrysin in human cancer cell lines. *International journal of molecular sciences* **2010,** *11* (5), 2188-2199.

85. Daskiewicz, J.-B.; Depeint, F.; Viornery, L.; Bayet, C.; Comte-Sarrazin, G.; Comte, G.; Gee, J. M.; Johnson, I. T.; Ndjoko, K.; Hostettmann, K., Effects of flavonoids on cell proliferation and caspase activation in a human colonic cell line HT29: an SAR study. *Journal of medicinal chemistry* **2005,** *48* (8), 2790-2804.

86. Hsiao, P.-C.; Lee, W.-J.; Yang, S.-F.; Tan, P.; Chen, H.-Y.; Lee, L.-M.; Chang, J.-L.; Lai, G.-M.; Chow, J.-M.; Chien, M.-H., Nobiletin suppresses the proliferation

and induces apoptosis involving MAPKs and caspase-8/-9/-3 signals in human acute myeloid leukemia cells. *Tumor Biology* **2014,** *35* (12), 11903-11911.

87. Kunimasa, K.; Ikekita, M.; Sato, M.; Ohta, T.; Yamori, Y.; Ikeda, M.; Kuranuki, S.; Oikawa, T., Nobiletin, a citrus polymethoxyflavonoid, suppresses multiple angiogenesis-related endothelial cell functions and angiogenesis in vivo. *Cancer science* **2010,** *101* (11), 2462-2469.

88. Moon, J. Y.; Cho, M.; Ahn, K. S.; Cho, S. K., Nobiletin induces apoptosis and potentiates the effects of the anticancer drug 5-fluorouracil in p53-mutated SNU-16 human gastric cancer cells. *Nutrition and cancer* **2013,** *65* (2), 286-295.

89. Ma, X.; Jin, S.; Zhang, Y.; Wan, L.; Zhao, Y.; Zhou, L., Inhibitory effects of Nobiletin on hepatocellular carcinoma in vitro and in vivo. *Phytotherapy Research* **2014,** *28* (4), 560-567.

90. Pan, M.-H.; Lai, Y.-S.; Lai, C.-S.; Wang, Y.-J.; Li, S.; Lo, C.-Y.; Dushenkov, S.; Ho, C.-T., 5-Hydroxy-3, 6, 7, 8, 3', 4'-hexamethoxyflavone induces apoptosis through reactive oxygen species production, growth arrest and DNA damage-inducible gene 153 expression, and caspase activation in human leukemia cells. *Journal of agricultural and food chemistry* **2007,** *55* (13), 5081-5091.

91. Dong, Y.; Cao, A.; Shi, J.; Yin, P.; Wang, L.; Ji, G.; Xie, J.; Wu, D., Tangeretin, a citrus polymethoxyflavonoid, induces apoptosis of human gastric cancer AGS cells through extrinsic and intrinsic signaling pathways. *Oncology reports* **2014,** *31* (4), 1788-1794.

92. Lust, S.; Vanhoecke, B.; Van Gele, M.; Philippé, J.; Bracke, M.; Offner, F., The flavonoid tangeretin activates the unfolded protein response and synergizes with imatinib in the erythroleukemia cell line K562. *Molecular nutrition & food research* **2010,** *54* (6), 823-832.

93. Charoensinphon, N.; Qiu, P.; Dong, P.; Zheng, J.; Ngauv, P.; Cao, Y.; Li, S.; Ho, C. T.; Xiao, H., 5-Demethyltangeretin inhibits human nonsmall cell lung cancer cell growth by inducing G2/M cell cycle arrest and apoptosis. *Molecular nutrition & food research* **2013,** *57* (12), 2103-2111.

94. Shin, S. Y.; Hyun, J.; Yu, J.-R.; Lim, Y.; Lee, Y. H., 5-Methoxyflavanone induces cell cycle arrest at the G2/M phase, apoptosis and autophagy in HCT116 human colon cancer cells. *Toxicology and applied pharmacology* **2011,** *254* (3), 288-298.

95. Wudtiwai, B.; Sripanidkulchai, B.; Kongtawelert, P.; Banjerdpongchai, R., Methoxyflavone derivatives modulate the effect of TRAIL-induced apoptosis in human leukemic cell lines. *J. Hematol. Oncol* **2011,** *4*, 52.

96. Cheng, A.-C.; Huang, T.-C.; Lai, C.-S.; Pan, M.-H., Induction of apoptosis by luteolin through cleavage of Bcl-2 family in human leukemia HL-60 cells. *European journal of pharmacology* **2005,** *509* (1), 1-10.

97. Yang, M.-Y.; Wang, C.-J.; Chen, N.-F.; Ho, W.-H.; Lu, F.-J.; Tseng, T.-H., Luteolin enhances paclitaxel-induced apoptosis in human breast cancer MDA-MB-231 cells by blocking STAT3. *Chemico-biological interactions* **2014,** *213*, 60-68.

98. Wang, Y.; Kong, D.; Wang, X.; Dong, X.; Tao, Y.; Gong, H., Molecular Mechanisms of Luteolin Induced Growth Inhibition and Apoptosis of Human Osteosarcoma Cells. *Iranian journal of pharmaceutical research: IJPR* **2015,** *14* (2), 531.

99. Das, S.; Das, J.; Samadder, A.; Boujedaini, N.; Khuda-Bukhsh, A. R., Apigenin-induced apoptosis in A375 and A549 cells through selective action and dysfunction of mitochondria. *Experimental Biology and Medicine* **2012,** *237* (12), 1433-1448.

100. Way, T.-D.; Kao, M.-C.; Lin, J.-K., Degradation of HER2/neu by apigenin induces apoptosis through cytochrome c release and caspase-3 activation in HER2/neu-overexpressing breast cancer cells. *Febs letters* **2005,** *579* (1), 145-152.

101. Vargo, M. A.; Voss, O. H.; Poustka, F.; Cardounel, A. J.; Grotewold, E.; Doseff, A. I., Apigenin-induced-apoptosis is mediated by the activation of PKCδ and caspases in leukemia cells. *Biochemical pharmacology* **2006,** *72* (6), 681-692.

102. Shukla, S.; Gupta, S., Apigenin-induced prostate cancer cell death is initiated by reactive oxygen species and p53 activation. *Free Radical Biology and Medicine* **2008,** *44* (10), 1833-1845.

103. Chan, L.-P.; Chou, T.-H.; Ding, H.-Y.; Chen, P.-R.; Chiang, F.-Y.; Kuo, P.-L.; Liang, C.-H., Apigenin induces apoptosis via tumor necrosis factor receptor-and Bcl-2-mediated pathway and enhances susceptibility of head and neck squamous cell carcinoma to 5-fluorouracil and cisplatin. *Biochimica et Biophysica Acta (BBA)-General Subjects* **2012,** *1820* (7), 1081-1091.

104. Park, H. Y.; Kim, G.-Y.; Kwon, T. K.; Hwang, H. J.; Kim, N. D.; Yoo, Y. H.; Choi, Y. H., Apoptosis induction of human leukemia U937 cells by 7, 8-dihydroxyflavone hydrate through modulation of the Bcl-2 family of proteins and the MAPKs signaling pathway. *Mutation Research/Genetic Toxicology and Environmental Mutagenesis* **2013,** *751* (2), 101-108.

105. Park, C.; Lee, W. S.; Go, S.-I.; Nagappan, A.; Han, M. H.; Hong, S. H.; Kim, G. S.; Kim, G. Y.; Kwon, T. K.; Ryu, C. H., Morin, a Flavonoid from Moraceae, Induces Apoptosis by Induction of BAD Protein in Human Leukemic Cells. *International journal of molecular sciences* **2014,** *16* (1), 645-659.

106. Luo, H.; Rankin, G.; DePriest, L.; Chen, Y. C., Kaempferol induces apoptosis in ovarian cancer cells through intrinsic pathway. *Cancer Research* **2011,** *71* (8 Supplement), 189-189.

107. Lee, H. S.; Cho, H. J.; Yu, R.; Lee, K. W.; Chun, H. S.; Park, J. H. Y., Mechanisms underlying apoptosis-inducing effects of Kaempferol in HT-29 human colon cancer cells. *International journal of molecular sciences* **2014,** *15* (2), 2722-2737.

108. Song, H.; Bao, J.; Wei, Y.; Chen, Y.; Mao, X.; Li, J.; Yang, Z.; Xue, Y., Kaempferol inhibits gastric cancer tumor growth: An in vitro and in vivo study. *Oncology reports* **2015,** *33* (2), 868-874.

109. Chien, S.-Y.; Wu, Y.-C.; Chung, J.-G.; Yang, J.-S.; Lu, H.-F.; Tsou, M.-F.; Wood, W.; Kuo, S.-J.; Chen, D.-R., Quercetin-induced apoptosis acts through mitochondrial-and caspase-3-dependent pathways in human breast cancer MDA-MB-231 cells. *Human & experimental toxicology* **2009,** *28* (8), 493-503.

110. Granado-Serrano, A. B.; Martín, M. A.; Bravo, L.; Goya, L.; Ramos, S., Quercetin induces apoptosis via caspase activation, regulation of Bcl-2, and inhibition of PI-3-kinase/Akt and ERK pathways in a human hepatoma cell line (HepG2). *The Journal of nutrition* **2006,** *136* (11), 2715-2721.

111. Chow, J. M.; Huang, G. C.; Shen, S. C.; Wu, C. Y.; Lin, C. W.; Chen, Y. C., Differential apoptotic effect of wogonin and nor-wogonin via stimulation of ROS production in human leukemia cells. *Journal of cellular biochemistry* **2008,** *103* (5), 1394-1404.

112. Chen, Y.-C.; Shen, S.-C.; Lee, W.-R.; Lin, H.-Y.; Ko, C.-H.; Shih, C.-M.; Yang, L.-L., Wogonin and fisetin induction of apoptosis through activation of caspase 3 cascade and alternative expression of p21 protein in hepatocellular carcinoma cells SK-HEP-1. *Archives of toxicology* **2002,** *76* (5-6), 351-359.

113. Lin, C.-C.; Kuo, C.-L.; Lee, M.-H.; Lai, K.-C.; Lin, J.-P.; Yang, J.-S.; Yu, C.-S.; Lu, C.-C.; Chiang, J.-H.; Chueh, F.-S., Wogonin triggers apoptosis in human osteosarcoma U-2 OS cells through the endoplasmic reticulum stress, mitochondrial dysfunction and caspase-3-dependent signaling pathways. *International journal of oncology* **2011,** *39* (1), 217-224.

114. Ding, J.; Polier, G.; Köhler, R.; Giaisi, M.; Krammer, P. H.; Li-Weber, M., Wogonin and related natural flavones overcome tumor necrosis factor-related apoptosis-inducing ligand (TRAIL) protein resistance of tumors by down-regulation of c-FLIP protein and up-regulation of TRAIL receptor 2 expression. *Journal of Biological Chemistry* **2012,** *287* (1), 641-649.

115. Watanabe, K.; Kanno, S.-I.; Tomizawa, A.; Yomogida, S.; Ishikawa, M., Acacetin induces apoptosis in human T cell leukemia Jurkat cells via activation of a caspase cascade. *Oncology reports* **2012,** *27* (1), 204-209.

116. Shim, H.; Park, J.; Paik, H.; Nah, S.; Kim, D.; Han, Y. S., Acacetin-induced apoptosis of human breast cancer MCF-7 cells involves caspase cascade, mitochondria-mediated death signaling and SAPK/JNK1/2-c-Jun activation. *Molecules and cells* **2007,** *24* (1), 95.

117. Pan, M.-H.; Lai, C.-S.; Hsu, P.-C.; Wang, Y.-J., Acacetin induces apoptosis in human gastric carcinoma cells accompanied by activation of caspase cascades and production of reactive oxygen species. *Journal of agricultural and food chemistry* **2005,** *53* (3), 620-630.

118. Kim, M.-J.; Kim, D.-H.; Na, H.-K.; Oh, T. Y.; Shin, C.-Y.; Surh, Y.-J., Eupatilin, a pharmacologically active flavone derived from Artemisia plants, induces apoptosis in human gastric cancer (AGS) cells. *Journal of environmental pathology, toxicology and oncology* **2005,** *24* (4).

119. Park, E.-J.; Zhao, Y.-Z.; Lian, L.; Kim, Y.-C.; Sohn, D. H., Skullcapflavone I from Scutellaria baicalensis induces apoptosis in activated rat hepatic stellate cells. *Planta medica* **2005,** *71* (9), 885-887.

120. KIM, M. J.; KIM, D. H.; Lee, K. W.; YOON, D. Y.; SURH, Y. J., Jaceosidin Induces Apoptosis in ras-Transformed Human Breast Epithelial Cells through Generation of Reactive Oxygen Species. *Annals of the New York Academy of Sciences* **2007,** *1095* (1), 483-495.

121. Sheng, X.; Sun, Y.; Yin, Y.; Chen, T.; Xu, Q., Cirsilineol inhibits proliferation of cancer cells by inducing apoptosis via mitochondrial pathway. *Journal of Pharmacy and Pharmacology* **2008,** *60* (11), 1523-1529.

122. Xiao, H.; Yang, C. S.; Li, S.; Jin, H.; Ho, C. T.; Patel, T., Monodemethylated polymethoxyflavones from sweet orange (Citrus sinensis) peel inhibit growth of human lung cancer cells by apoptosis. *Molecular nutrition & food research* **2009,** *53* (3), 398-406.

123. Qiu, P.; Dong, P.; Guan, H.; Li, S.; Ho, C. T.; Pan, M. H.; McClements, D. J.; Xiao, H., Inhibitory effects of 5-hydroxy polymethoxyflavones on colon cancer cells. *Molecular nutrition & food research* **2010,** *54* (S2), S244-S252.

124. Kim, M. J.; Seo, M. J.; Park, J. U.; Kim, G. Y.; Choi, Y. H.; Jeong, Y. K., Identification of 5-hydroxy-3, 6, 7, 8, 3, 4-hexamethoxyflavone from Hizikia fusiforme involved in the induction of the apoptosis mediators in human AGS carcinoma cells. *Journal of microbiology and biotechnology* **2012,** *22* (12), 1665-1672.

125. Chung, K. S.; Choi, J. H.; Back, N. I.; Choi, M. S.; Kang, E. K.; Chung, H. G.; Jeong, T. S.; Lee, K. T., Eupafolin, a flavonoid isolated from Artemisia princeps, induced apoptosis in human cervical adenocarcinoma HeLa cells. *Molecular nutrition & food research* **2010,** *54* (9), 1318-1328.

126. Phromnoi, K.; Reuter, S.; Sung, B.; Limtrakul, P.; Aggarwal, B. B., A dihydroxy-pentamethoxyflavone from Gardenia obtusifolia suppresses proliferation and promotes apoptosis of tumor cells through modulation of multiple cell signaling pathways. *Anticancer research* **2010,** *30* (9), 3599-3610.

127. Gao, H.; Wang, H.; Peng, J., Hispidulin induces apoptosis through mitochondrial dysfunction and inhibition of P13k/Akt signalling pathway in HepG2 cancer cells. *Cell biochemistry and biophysics* **2014,** *69* (1), 27-34.

128. Yang, J.-M.; Hung, C.-M.; Fu, C.-N.; Lee, J.-C.; Huang, C.-H.; Yang, M.-H.; Lin, C.-L.; Kao, J.-Y.; Way, T.-D., Hispidulin sensitizes human ovarian cancer cells to TRAIL-induced apoptosis by AMPK activation leading to Mcl-1 block in translation. *Journal of agricultural and food chemistry* **2010,** *58* (18), 10020-10026.

129. Yue, R.; Li, B.; Shen, Y.; Zeng, H.; Yuan, H.; He, Y.; Shan, L.; Zhang, W., 6-C-methyl flavonoids isolated from Pinus densata inhibit the proliferation and promote the apoptosis of the HL-60 human promyelocytic leukaemia cell line. *Planta medica* **2013,** *79* (12), 1024-1030.

130. Wenzel, U.; Kuntz, S.; Brendel, M. D.; Daniel, H., Dietary flavone is a potent apoptosis inducer in human colon carcinoma cells. *Cancer research* **2000,** *60* (14), 3823-3831.

131. Chen, Y.-C.; Shen, S.-C.; Chow, J.-M.; Ko, C. H.; Tseng, S.-W., Flavone inhibition of tumor growth via apoptosis in vitro and in vivo. *International journal of oncology* **2004,** *25* (3), 661-670.

132. Erhart, L.; Lankat-Buttgereit, B.; Schmidt, H.; Wenzel, U.; Daniel, H.; Göke, R., Flavone initiates a hierarchical activation of the caspase-cascade in colon cancer cells. *Apoptosis* **2005,** *10* (3), 611-617.

133. Lee, C.-c.; Lin, C.-n.; Jow, G.-m., Cytotoxic and apoptotic effects of prenylflavonoid artonin B in human acute lymphoblastic leukemia cells. *Acta pharmacologica sinica* **2006,** *27* (9), 1165.

134. Chen, W.-C.; Kuo, T.-H.; Tzeng, Y.-S.; Tsai, Y.-C., Baicalin induces apoptosis in SW620 human colorectal carcinoma cells in vitro and suppresses tumor growth in vivo. *Molecules* **2012,** *17* (4), 3844-3857.

135. Huang, Y.; Hu, J.; Zheng, J.; Li, J.; Wei, T.; Zheng, Z.; Chen, Y., Down-regulation of the PI3K/Akt signaling pathway and induction of apoptosis in CA46 Burkitt lymphoma cells by baicalin. *J Exp Clin Cancer Res* **2012,** *31*, 48.

136. Chang, H.-L.; Su, J.-H.; Yeh, Y.-T.; Lee, Y.-C.; Chen, H.-M.; Wu, Y.-C.; Yuan, S.-S. F., Protoapigenone, a novel flavonoid, inhibits ovarian cancer cell growth in vitro and in vivo. *Cancer letters* **2008,** *267* (1), 85-95.

137. Chang, H.-L.; Wu, Y.-C.; Su, J.-H.; Yeh, Y.-T.; Yuan, S.-S. F., Protoapigenone, a novel flavonoid, induces apoptosis in human prostate cancer cells through activation of p38 mitogen-activated protein kinase and c-Jun NH2-terminal kinase 1/2. *Journal of Pharmacology and Experimental Therapeutics* **2008,** *325* (3), 841-849.

138. Chen, W.-Y.; Hsieh, Y.-A.; Tsai, C.-I.; Kang, Y.-F.; Chang, F.-R.; Wu, Y.-C.; Wu, C.-C., Protoapigenone, a natural derivative of apigenin, induces mitogen-activated protein kinase-dependent apoptosis in human breast cancer cells associated with induction of oxidative stress and inhibition of glutathione S-transferase π. *Investigational new drugs* **2011,** *29* (6), 1347-1359.

139. Liu, H.; Xiao, Y.; Xiong, C.; Wei, A.; Ruan, J., Apoptosis induced by a new flavonoid in human hepatoma HepG2 cells involves reactive oxygen species-mediated mitochondrial dysfunction and MAPK activation. *European journal of pharmacology* **2011,** *654* (3), 209-216.

140. Kuete, V.; Ngameni, B.; Wiench, B.; Krusche, B.; Horwedel, C.; Ngadjui, B. T.; Efferth, T., Cytotoxicity and mode of action of four naturally occuring flavonoids from the genus Dorstenia: gancaonin Q, 4-hydroxylonchocarpin, 6-prenylapigenin, and 6, 8-diprenyleriodictyol. *Planta medica* **2011,** *77* (18), 1984-1989.

141. Li, Y.; Bian, L.; Cui, F.; Li, L.; Zhang, X., TTF1-induced apoptosis of HepG-2 cells through a mitochondrial pathway. *Oncology reports* **2011,** *26* (3), 651-657.

142. Hwang, C. H.; Lin, Y. L.; Liu, Y. K.; Chen, C. H.; Wu, H. Y.; Chang, C. C.; Chang, C. Y.; Chang, Y. K.; Chiu, Y. H.; Liao, K. W., 7, 7″-Dimethoxyagastisflavone-induced Apoptotic or Autophagic Cell Death in Different Cancer Cells. *Phytotherapy Research* **2012,** *26* (4), 528-534.

143. Zhou, D.; Wei, A.; Cao, C.; Ruan, J., DICO, a novel nonaromatic B-ring flavonoid, induces G2/M cell cycle arrest and apoptosis in human hepatoma cells. *Food and Chemical Toxicology* **2013,** *57*, 322-329.

144. Zhou, Y.; Lu, N.; Zhang, H.; Wei, L.; Tao, L.; Dai, Q.; Zhao, L.; Lin, B.; Ding, Q.; Guo, Q., HQS-3, a newly synthesized flavonoid, possesses potent anti-tumor effect in vivo and in vitro. *European Journal of Pharmaceutical Sciences* **2013,** *49* (4), 649-658.

145. Zeng, S.; Liu, W.; Nie, F.-f.; Zhao, Q.; Rong, J.-j.; Wang, J.; Tao, L.; Qi, Q.; Lu, N.; Li, Z.-y., LYG-202, a new flavonoid with a piperazine substitution, shows antitumor effects in vivo and in vitro. *Biochemical and biophysical research communications* **2009,** *385* (4), 551-556.

146. Liu, W.; Dai, Q.; Lu, N.; Wei, L.; Ha, J.; Rong, J.; Mu, R.; You, Q.; Li, Z.; Guo, Q., LYG-202 inhibits the proliferation of human colorectal carcinoma HCT-116 cells through induction of G1/S cell cycle arrest and apoptosis via p53 and p21WAF1/Cip1 expression. *Biochemistry and Cell Biology* **2011,** *89* (3), 287-298.

147. Chen, F.-h.; Lu, N.; Zhang, H.-w.; Zhao, L.; He, L.-c.; Sun, H.-p.; You, Q.-d.; Li, Z.-y.; Guo, Q.-l., LYG-202 Augments Tumor Necrosis Factor-α-Induced Apoptosis via Attenuating Casein Kinase 2-Dependent Nuclear Factor-κB Pathway in HepG2 Cells. *Molecular pharmacology* **2012,** *82* (5), 958-971.

148. Zhang, L.-b.; Qiang, L.; Chen, F.-h.; Wu, T.; Rong, J.-j.; Zhao, Q.; Zou, M.-j.; Yang, Z.; You, Q.-d.; Li, Z.-y., DHF-18, a new synthetic flavonoid, induced a mitochondrial-mediated apoptosis of hepatocarcinoma cells in vivo and in vitro. *European journal of pharmacology* **2011,** *651* (1), 33-40.

149. Estévez, S.; Marrero, M. T.; Quintana, J.; Estévez, F., Eupatorin-Induced Cell Death in Human Leukemia Cells Is Dependent on Caspases and Activates the Mitogen-Activated Protein Kinase Pathway. *PloS one* **2014,** *9* (11), e112536.

150. Soner, B. C.; Aktug, H.; Acikgoz, E.; Duzagac, F.; Guven, U.; Ayla, S.; Cal, C.; Oktem, G., Induced growth inhibition, cell cycle arrest and apoptosis in CD133+/CD44+ prostate cancer stem cells by flavopiridol. *International journal of molecular medicine* **2014,** *34* (5), 1249-1256.

151. Billard, C.; Menasria, F.; Quiney, C.; Faussat, A.-M.; Kolb, J.-P., Flavopiridol-induced iNOS downregulation during apoptosis of chronic lymphocytic leukemia cells is caspase-dependent. *Leukemia research* **2008,** *32* (5), 755-760.

152. Zhang, Y.; Zhao, L.; Li, X.; Wang, Y.; Yao, J.; Wang, H.; Li, F.; Li, Z.; Guo, Q., V8, a newly synthetic flavonoid, induces apoptosis through ROS-mediated ER stress pathway in hepatocellular carcinoma. *Archives of toxicology* **2014,** *88* (1), 97-107.

153. Pan, D.; Li, W.; Miao, H.; Yao, J.; Li, Z.; Wei, L.; Zhao, L.; Guo, Q., LW-214, a newly synthesized flavonoid, induces intrinsic apoptosis pathway by down-regulating Trx-1 in MCF-7 human breast cells. *Biochemical pharmacology* **2014,** *87* (4), 598-610.

154. Piedfer, M.; Bouchet, S.; Tang, R.; Billard, C.; Dauzonne, D.; Bauvois, B., p70S6 kinase is a target of the novel proteasome inhibitor 3, 3′-diamino-4′-methoxyflavone during apoptosis in human myeloid tumor cells. *Biochimica et Biophysica Acta (BBA)-Molecular Cell Research* **2013,** *1833* (6), 1316-1328.

155. Chang, H.; Lin, H.; Yi, L.; Zhu, J.; Zhou, Y.; Mi, M.; Zhang, Q., 3, 6-Dihydroxyflavone induces apoptosis in leukemia HL-60 cell via reactive oxygen species-mediated p38 MAPK/JNK pathway. *European journal of pharmacology* **2010,** *648* (1), 31-38.

156. Torres, F.; Quintana, J.; Estévez, F., 5, 7, 3′-trihydroxy-3, 4′-dimethoxyflavone-induced cell death in human Leukemia cells is dependent on caspases and activates the MAPK pathway. *Molecular carcinogenesis* **2010,** *49* (5), 464-475.

157. Khan, M. S.; Halagowder, D.; Devaraj, S. N., Methylated chrysin induces co-ordinated attenuation of the canonical Wnt and NF-kB signaling pathway and upregulates apoptotic gene expression in the early hepatocarcinogenesis rat model. *Chemico-biological interactions* **2011,** *193* (1), 12-21.

158. Marrero, M. T.; Estévez, S.; Negrín, G.; Quintana, J.; López, M.; Pérez, F. J.; Triana, J.; León, F.; Estévez, F., Ayanin diacetate-induced cell death is amplified by TRAIL in human leukemia cells. *Biochemical and biophysical research communications* **2012,** *428* (1), 116-120.

159. Yang, X.-H.; Zheng, X.; Cao, J.-G.; Xiang, H.-L.; Liu, F.; Lv, Y., 8-Bromo-7-methoxychrysin-induced apoptosis of hepatocellular carcinoma cells involves ROS and JNK. *World journal of gastroenterology: WJG* **2010,** *16* (27), 3385.

160. Chen, H.-M.; Chang, F.-R.; Hsieh, Y.-C.; Cheng, Y.-J.; Hsieh, K.-C.; Tsai, L.-M.; Lin, A.-S.; Wu, Y.-C.; Yuan, S.-S., A novel synthetic protoapigenone analogue, WYC02-9, induces DNA damage and apoptosis in DU145 prostate cancer cells through generation of reactive oxygen species. *Free Radical Biology and Medicine* **2011,** *50* (9), 1151-1162.

161. Rubio, S.; León, F.; Quintana, J.; Cutler, S.; Estévez, F., Cell death triggered by synthetic flavonoids in human leukemia cells is amplified by the inhibition of extracellular signal-regulated kinase signaling. *European journal of medicinal chemistry* **2012,** *55*, 284-296.

162. Burmistrova, O.; Marrero, M. T.; Estévez, S.; Welsch, I.; Brouard, I.; Quintana, J.; Estévez, F., Synthesis and effects on cell viability of flavonols and 3-methyl ether derivatives on human leukemia cells. *European journal of medicinal chemistry* **2014,** *84*, 30-41.

163. Liu, H.; Dong, A.; Gao, C.; Tan, C.; Xie, Z.; Zu, X.; Qu, L.; Jiang, Y., New synthetic flavone derivatives induce apoptosis of hepatocarcinoma cells. *Bioorganic & medicinal chemistry* **2010,** *18* (17), 6322-6328.

164. Cárdenas, M. G.; Blank, V. C.; Marder, M.; Roguin, L. P., 2′-Nitroflavone induces cell cycle arrest and apoptosis in HeLa human cervical carcinoma cells. *Cancer letters* **2008,** *268* (1), 146-157.

165. Cárdenas, M. G.; Zotta, E.; Marder, M.; Roguin, L. P., In vitro induction of apoptosis and in vivo effects of a flavone nitroderivative in murine mammary adenocarcinoma cells. *International Journal of Cancer* **2009,** *125* (1), 222-228.

166. Cardenas, M. G.; Blank, V. C.; Marder, M. N.; Roguin, L. P., 2′-Nitroflavone induces apoptosis and modulates mitogen-activated protein kinase pathways in human leukaemia cells. *Anti-cancer drugs* **2012,** *23* (8), 815-826.

167. Zhang, T.; Du, J.; Liu, L.; Chen, X.; Yang, F.; Jin, Q., Inhibitory effects and underlying mechanism of 7-hydroxyflavone phosphate ester in HeLa cells. *PloS one* **2012,** *7* (5), e36652.

168. Monasterio, A.; Urdaci, M. C.; Pinchuk, I. V.; Lopez-Moratalla, N.; Martinez-Irujo, J. J., Flavonoids induce apoptosis in human leukemia U937 cells through caspase- and caspase-calpain-dependent pathways. *Nutrition and cancer* **2004,** *50* (1), 90-100.

169. Po, L. S.; Chen, Z.-y.; Tsang, D. S.; Leung, L. K., Baicalein and genistein display differential actions on estrogen receptor (ER) transactivation and apoptosis in MCF-7 cells. *Cancer letters* **2002,** *187* (1), 33-40.

170. Li-Weber, M., New therapeutic aspects of flavones: The anticancer properties of< i> Scutellaria</i> and its main active constituents Wogonin, Baicalein and Baicalin. *Cancer treatment reviews* **2009,** *35* (1), 57-68.

171. Neves, M. P.; Cidade, H.; Pinto, M.; Silva, A. M.; Gales, L.; Damas, A. M.; Lima, R. T.; Vasconcelos, M. H.; Nascimento, M. d. S. J., Prenylated derivatives of baicalein and 3, 7-dihydroxyflavone: Synthesis and study of their effects on tumor cell lines growth, cell cycle and apoptosis. *European journal of medicinal chemistry* **2011,** *46* (6), 2562-2574.

172. Hawkins, C. J.; Silke, J.; Verhagen, A.; Foster, R.; Ekert, P. G.; Ashley, D. M., Analysis of candidate antagonists of IAP-mediated caspase inhibition using yeast reconstituted with the mammalian Apaf-1-activated apoptosis mechanism. *Apoptosis* **2001,** *6* (5), 331-338.

173. Glória, P.; Coutinho, I.; Gonçalves, L. M.; Baptista, C.; Soares, J.; Newton, A. S.; Moreira, R.; Saraiva, L.; Santos, M. M., Aspartic vinyl sulfones: Inhibitors of a caspase-3-dependent pathway. *European journal of medicinal chemistry* **2011,** *46* (6), 2141-2146.

174. Pereira, C.; Lopes-Rodrigues, V.; Coutinho, I.; Neves, M. P.; Lima, R. T.; Pinto, M.; Cidade, H.; Vasconcelos, M. H.; Saraiva, L., Potential small-molecule activators of caspase-7 identified using yeast-based caspase-3 and-7 screening assays. *European Journal of Pharmaceutical Sciences* **2014**.

175. Pereira, C.; Lopes-Rodrigues, V.; Coutinho, I.; Neves, M. P.; Lima, R. T.; Pinto, M.; Cidade, H.; Vasconcelos, M. H.; Saraiva, L., Potential small-molecule activators of caspase-7 identified using yeast-based caspase-3 and-7 screening assays. *European Journal of Pharmaceutical Sciences* **2014,** *54*, 8-16.

176. Chang, W.-H.; Chen, C.-H.; Gau, R.-J.; Lin, C.-C.; Tsai, C.-L.; Tsai, K.; Lu, F.-J., Effect of baicalein on apoptosis of the human Hep G2 cell line was induced by mitochondrial dysfunction. *Planta medica* **2002,** *68* (4), 302-306.

177. Li-Weber, M., Targeting apoptosis pathways in cancer by Chinese medicine. *Cancer letters* **2013,** *332* (2), 304-312.

178. Kasala, E. R.; Bodduluru, L. N.; Madana, R. M.; Gogoi, R.; Barua, C. C., Chemopreventive and therapeutic potential of chrysin in cancer: mechanistic perspectives. *Toxicology letters* **2015,** *233* (2), 214-225.

179. Woo, K. J.; Jeong, Y.-J.; Park, J.-W.; Kwon, T. K., Chrysin-induced apoptosis is mediated through caspase activation and Akt inactivation in U937 leukemia cells. *Biochemical and biophysical research communications* **2004,** *325* (4), 1215-1222.

180. Safa, A. R.; Pollok, K. E., Targeting the anti-apoptotic protein c-FLIP for cancer therapy. *Cancers* **2011,** *3* (2), 1639-1671.

181. Fu, W.; Wang, J.; Yu, L.; Zhao, L.; Lu, N.; You, Q.; Guo, Q.; Li, Z., Synthesis and biological evaluation of 7-O-modified oroxylin A derivatives. *Bioorganic & medicinal chemistry letters* **2012,** *22* (2), 1118-1121.

182. Luo, R.; Wang, J.; Zhao, L.; Lu, N.; You, Q.; Guo, Q.; Li, Z., Synthesis and biological evaluation of baicalein derivatives as potent antitumor agents. *Bioorganic & medicinal chemistry letters* **2014,** *24* (5), 1334-1338.

183. Lee, Y.; Yeo, H.; Liu, S.-H.; Jiang, Z.; Savizky, R. M.; Austin, D. J.; Cheng, Y.-c., Increased anti-P-glycoprotein activity of baicalein by alkylation on the A ring. *Journal of medicinal chemistry* **2004,** *47* (22), 5555-5566.

184. Wang, J. F.; Ding, N.; Zhang, W.; Wang, P.; Li, Y. X., Synthesis of Ring A-Modified Baicalein Derivatives. *Helvetica Chimica Acta* **2011,** *94* (12), 2221-2230.

185. Ghani, N. A.; Ahmat, N.; Ismail, N. H.; Zakaria, I., Flavonoid constituents from the stem bark of polyalthia cauliflora var. Cauliflora. *Australian Journal of Basic and Applied Sciences* **2011,** *5* (8), 154-158.

186. Kim, H.; Lim, D.; Shin, I.; Lee, D., Gram-scale synthesis of anti-pancreatic flavonoids (±)-8-[1-(4′-hydroxy-3′-methoxyphenyl) prop-2-en-1-yl]-chrysin and-galangin. *Tetrahedron* **2014,** *70* (32), 4738-4744.

187. Cheng, N.; Yi, W.-B.; Wang, Q.-Q.; Peng, S.-M.; Zou, X.-Q., Synthesis and α-glucosidase inhibitory activity of chrysin, diosmetin, apigenin, and luteolin derivatives. *Chinese Chemical Letters* **2014,** *25* (7), 1094-1098.

188. Sutthanut, K.; Sripanidkulchai, B.; Yenjai, C.; Jay, M., Simultaneous identification and quantitation of 11 flavonoid constituents in Kaempferia parviflora by gas chromatography. *Journal of Chromatography A* **2007,** *1143* (1), 227-233.

189. Schipper, J. L.; MacKenzie, S. H.; Sharma, A.; Clark, A. C., A bifunctional allosteric site in the dimer interface of procaspase-3. *Biophysical chemistry* **2011,** *159* (1), 100-109.

190. Vickers, C. J.; González-Páez, G. E.; Umotoy, J. C.; Cayanan-Garrett, C.; Brown, S. J.; Wolan, D. W., Small-Molecule Procaspase Activators Identified Using Fluorescence Polarization. *ChemBioChem* **2013,** *14* (12), 1419-1422.

191. Perrin, D. D.; Armarego, W. F., Purification of laboratory chemicals. ed., r., Ed. Oxford: Pergamon Press: 1988.

192. Glória, P. M.; Coutinho, I.; Gonçalves, L. M.; Baptista, C.; Soares, J.; Newton, A. S.; Moreira, R.; Saraiva, L.; Santos, M. M., Aspartic vinyl sulfones: inhibitors of a caspase-3-dependent pathway. *European journal of medicinal chemistry* **2011,** *46* (6), 2141-2146.

Chapter 7:

Appendix

Table 23: Structures of the synthesized flavonoids and their precursors.

Structure	*Name*	*Code*
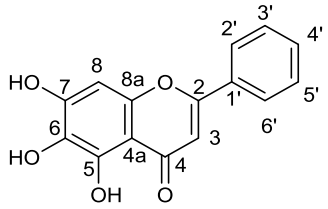	5,6,7-trihydroxy-2-phenyl-4H-chromen-4-one	**B**
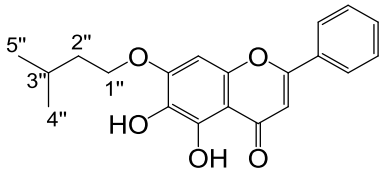	5,6-dihydroxy-7-(isopentyloxy)-2-phenyl-4H-chromen-4-one	**Biso1**
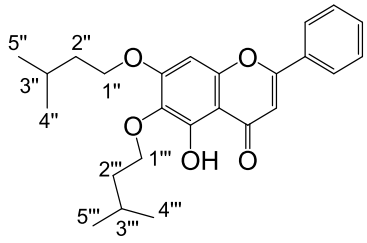	5-hydroxy-6,7-bis(isopentyloxy)-2-phenyl-4H-chromen-4-one	**Biso2**
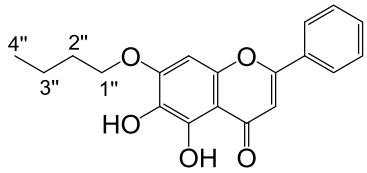	7-butoxy-5,6-dihydroxy-2-phenyl-4H-chromen-4-one	**Butil1**
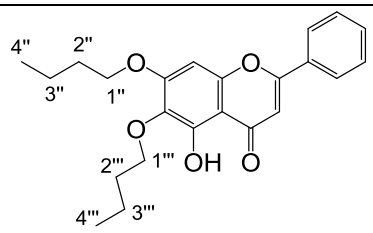	6,7-dibutoxy-5-hydroxy-2-phenyl-4H-chromen-4-one	**Butil2**
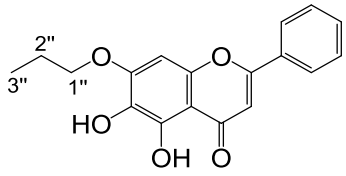	5,6-dihydroxy-2-phenyl-7-propoxy-4H-chromen-4-one	**Brop1**
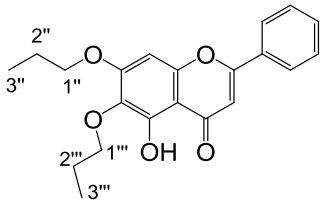	5-hydroxy-2-phenyl-6,7-dipropoxy-4H-chromen-4-one	**Brop2**

Table23 (contd): Structures of the synthesized flavonoids and their precursors.

Structure	*Name*	*Code*
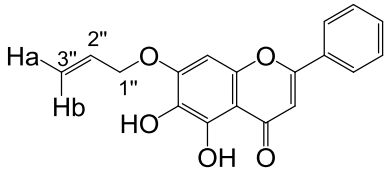	7-(allyloxy)-5,6-dihydroxy-2-phenyl-4H-chromen-4-one	**Bali1**
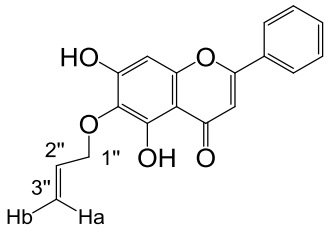	6-(allyloxy)-5,7-dihydroxy-2-phenyl-4H-chromen-4-one	**Bali1'**
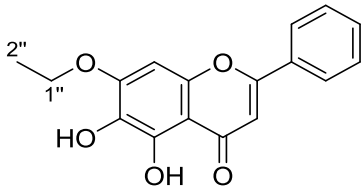	7-ethoxy-5,6-dihydroxy-2-phenyl-4H-chromen-4-one	**Betil1**
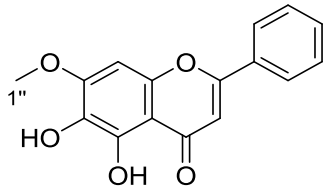	5,6-dihydroxy-7-methoxy-2-phenyl-4H-chromen-4-one	**Bemet1**
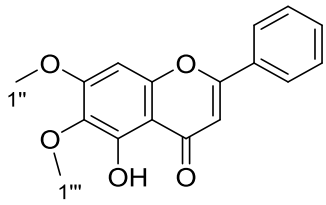	5-hydroxy-6,7-dimethoxy-2-phenyl-4H-chromen-4-one	**Bemet2**
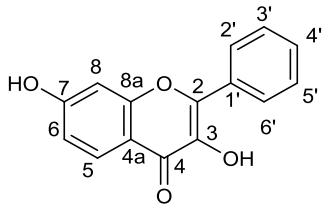	3,7-dihydroxy-2-phenyl-4H-chromen-4-one	**H**

Table23 (contd): Structures of the synthesized flavonoids and their precursors.

Structure	*Name*	*Code*
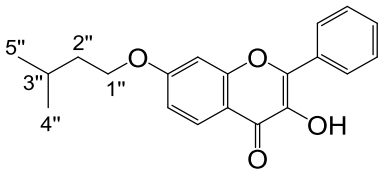	3-hydroxy-7-(isopentyloxy)-2-phenyl-4H-chromen-4-one	**Hiso**
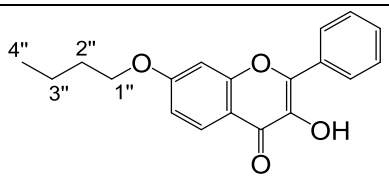	7-butoxy-3-hydroxy-2-phenyl-4H-chromen-4-one	**Hutil1**
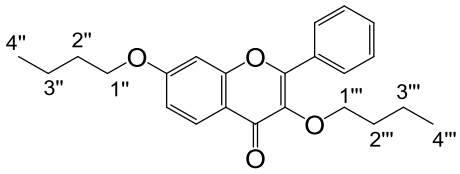	3,7-dibutoxy-2-phenyl-4H-chromen-4-one	**Hutil2**
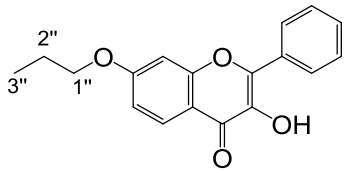	3-hydroxy-2-phenyl-7-propoxy-4H-chromen-4-one	**Hrop**
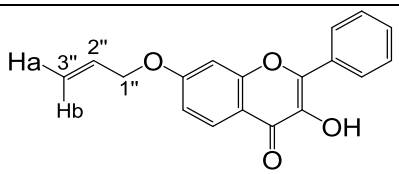	7-(allyloxy)-3-hydroxy-2-phenyl-4H-chromen-4-one	**Hali**
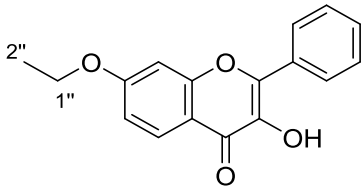	7-ethoxy-3-hydroxy-2-phenyl-4H-chromen-4-one	**Hetil**
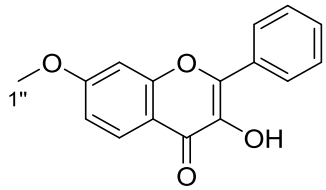	3-hydroxy-7-methoxy-2-phenyl-4H-chromen-4-one	**Hemet**
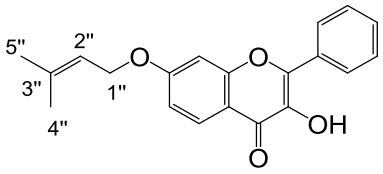	3-hydroxy-7-((3-methylbut-2-en-1-yl)oxy)-2-phenyl-4H-chromen-4-one	**Hrep**

Table23 (contd): Structures of the synthesized flavonoids and their precursors.

Structure	*Name*	*Code*
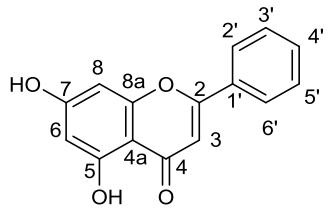	5,7-dihydroxy-2-phenyl-4H-chromen-4-one	**C**
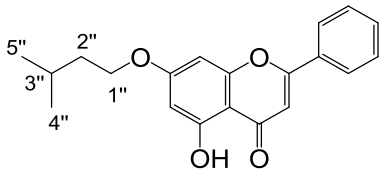	5-hydroxy-7-(isopentyloxy)-2-phenyl-4H-chromen-4-one	**Ciso**
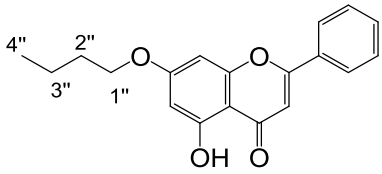	5-hydroxy-2-phenyl-7-propoxy-4H-chromen-4-one	**Cutil**
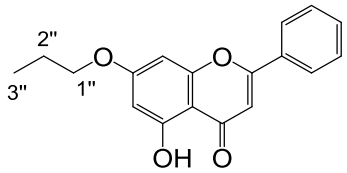	5-hydroxy-2-phenyl-7-propoxy-4H-chromen-4-one	**Crop**
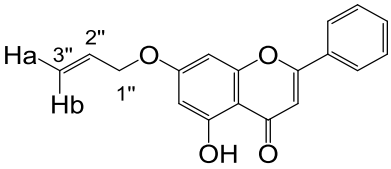	7-(allyloxy)-5-hydroxy-2-phenyl-4H-chromen-4-one	**Cali**
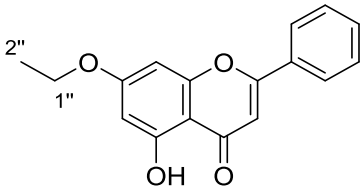	7-ethoxy-5-hydroxy-2-phenyl-4H-chromen-4-one	**Cetil**
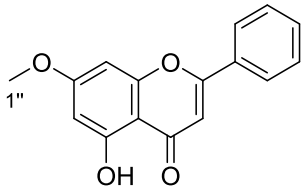	5-hydroxy-7-methoxy-2-phenyl-4H-chromen-4-one	**Cemet**
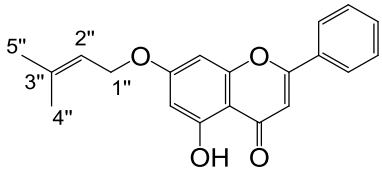	5-hydroxy-7-((3-methylbut-2-en-1-yl)oxy)-2-phenyl-4H-chromen-4-one	**Crep**